nature portfolio

Peer Review File

Programmable Control of Spatial Transcriptome in Live Cells and Neurons

Corresponding Author: Dr Lei Qi

This file contains all reviewer reports in order by version, followed by all author rebuttals in order by version.

Version 1:

Reviewer comments:

Referee #1

(Remarks to the Author)
Han et al Review Round 1

Summary
Han et al present a manuscript describing a new technique “CRISPR-TO” to manipulate mRNA subcellular localization to various organelles/subcellular structures in live cells, in a sequence specific manner. After an initial proof of concept and vector design, the authors show that this technology can be used to localize specific mRNAs to the outer mitochondrial membrane, p-bodies, stress granules, telomeres, and nuclear stress bodies. Excitingly, they were able to use this technology to recruit mRNAs to microtubules and in live cells and real time observe bidirectional movement along these microtubules. The authors then show this also recruits ribosomes and allows for local translation at neurite terminals and allow for screening for transcripts that when forced to be localized to neurites can modulate neurite outgrowth. Overall, this is a clever use of Cas13, and most of the interpretations are supported by well-controlled experiments and explained in a well written manuscript. That said, some claims and interpretations that impact the conclusions and usefulness of this technology are oversold and not backed up by the required data, and as a result some major and minor concerns need to be addressed. See below for my specific comments:

Major Comments

1. One of the main criticisms I have with how this technology is described in the abstract and throughout parts of the main text: “Real time investigation of RNA dynamics”. In my opinion, if you’re perturbing the localization of the mRNA in non-natural ways by forcing it into a specific compartment synthetically, and thus I’m not sure one can claim this technology can be used to understand native dynamics of mRNA transport given the perturbation is likely changing the native kinetics of how mRNAs are transported? One way to potentially remedy this concern is to change the emphasis on real time modulation/manipulation as opposed ‘investigation’ of RNA dynamics given you’re deliberately perturbing the system.

2. ED figure 3 it would be great to quantify in each panel the % of colocalization? Particularly as some of the mRNAs targeted aren’t localizing as effectively (by eye; e.g. SDHC, SDHD, NDUFS2?). It would be more convincing with these quantified as you did with ED3.j.

3. Relatedly, OMM localization in different cell lines is different in morphology, is this expected? For example, the morphology in HEKs is rounder and puncta like, same as with Neuro 2A, compare to HeLa cells which stain more elongated and string-like. It might be worth commenting on this phenomenon.

4. In some cases, you see colocalization between the Cas13 PYL1 fusion without ABA or with ABA and a non-target gRNA suggesting that interpretation of whether there is actually specificity in the experiment could be an issue, in particular if the smFISH doesn’t work optimally or at all for a particular target (this is sometimes the case). What alternatives do you think there are to make sure targeting is specific? Perhaps this observation needs to be suggested as a limitation?

5. In a similar observation, why don’t you see Cas13 puncta on TERRA for example given it’s likely to colocalize there without the need for the PYL1 fusion for forcing the interaction? It’s also surprising all the background disappears, likewise with Cas13 and GAPDH and stress granules? Is Cas13 non-specifically binding to stress granules with a non-targeting (and

perhaps targeting) guide given it looks like in the DMSO condition there is little GAPDH smFISH signal in SG puncta? On that note were SGs induced with Arsenite or some other stressor? As far as I can tell, it's not included in the text anywhere what stressor was used in many of these experiments.

6. I also have concerns about the interpretation of the P body and GAPDH storage vs. degradation experiment given only a single non-kinetic GAPDH mRNA expression level measurement was taken. There likely could be compensatory mechanisms to replace any GAPDH being degraded in the P body given GAPDH is an essential (housekeeping) gene (according to DepMap), so there are likely buffering mechanisms to keep its gene expression consistent. Have the author's considered this caveat when making these measurements? A better approach would be to measurement the rates of RNA decay across the time course of the experiment and see if they change pre- and post- localization to the P-body with the appropriate housekeeping controls, they may best be done by targeting a non-essential gene instead of GAPDH.

7. I object to the use of Michalis-Menten kinetics to describe the fitted curve in ED Fig 7, as MM kinetics requires the determination of initial rates (reaction velocity) which naturally contain a time component and is used to describe enzyme catalysis (which this interaction isn't). I would prefer to see the date referred to as fitting a standard 1:1 ligand binding isotherm/curve or rectangular hyperbola. Particularly, as in the next paragraph you mention a two-phase model of recruitment which wouldn't be described by MM kinetics.

8. I think the manuscripts needs a much more careful consideration of the potential for ff-target localization, and an understanding of the effects of mismatch tolerance. It is well understood that Cas13 binding is more permissive than Cas13 cleavage in terms of off-target and so it would be good to understand the gRNA design considerations for this specific type of technology as they may need to be more careful with respect to number of mismatches allowed vs. the current Cas13 cleavage-based design rules/algorithms currently available. With this in mind, perhaps a mismatch tolerance experiment or some small-scale specificity test (for example, design a guide with a perfect match to transcript x but with some probability of off-targets with 1-3 (or more) mismatches to a second transcript, and see if you get colocalization using mRNA FISH with the off-target as well (vs. the on-target as a control). Without this information it's going to be difficult to know the extent of off-targets and whether this system has the require specificity to be useful here.

Other Comments

1. The decision to use an NLS vs NES in each localization case explained? Is it clear in each case which one is used? The figures for example in ED Fig 2 don't show this level of detail?

2. As mentioned above, it appears not to be documented how stress was induced in the cell lines given SGs don't always appear under basal conditions and can be different in different cell lines? Same for cytosolic SGs vs nuclear stress bodies?

3. Figure 1g / ED Fig. 4e, have you considered trying to further increase the expression of Cas13 etc. (or gRNA?) to overcome this barrier with respect to OMM enrichment for lowly expressed mRNAs? Would be interesting to seeing if increasing the transfection amounts / ratios of Cas13:gRNA of each would help.

4. ED Fig. 4I gRNA score is introduced without any explanation in the figure legend or main text? It would make it clearer to the reader to introduce what is meant by a gRNA score here? Which algorithm is it derived from etc.?

5. Likewise, it's not super clear what the Polarization Index and Dispersion index is? One sentence to describe how these metrics work/are generated would be useful to the reader.

6. Line 373.. the authors mention that 21 mRNAs were selected but didn't provide a rationale for why these mRNAs were included? Previous evidence in the literature? Known +ve and -ve mRNA controls (i.e. b-actin vs. an RNA that is normally nuclear retained?). It would be great to see these controls?

7. What proportion of the 21 mRNAs did you expect to affect neurite outgrowth given the selection procedure? Why was it interesting that 4 were determined to be hits? Was that expected, surprising? More information in the main text here to explain the experimental design/interpretation would be helpful for the reader. Could it be explained by gRNA choice? How were they selected. Could they somehow be checked make sure they're binding your target of interest? The Cas13design algorithm was based on training data from an RfXCas13d RNA cleavage screen and not a PspCas13b binding screen. Could one argue that one reason for the low hit rate here is due to gRNA design limitations? Is this a major limitation to effectively implementing this in the field?

8. What are the natural Cues for Stmn2 localization and neurite outgrowth, given it's in the soma under basal conditions? Any guesses it might be good to include some evidence (from the literature) as to how it is normally regulated? And why it's not in the neurites already in this neuronal culture (it may help the reader further understand the process).

9. As far as I can tell there is no mention of your flow cytometry gating strategy etc. or any plots shown to highlight gating.

10. Perhaps I missed it, as far as I can tell, Supplementary Fig. 3 is not referred to anywhere in the text (main text, supplementary or methods etc.) and it is not super clear that this figure is demonstrating or clear that the caption completely matches what is shown in the figure.

11. Supplementary data file, typo: Persons should read Pearson's

Referee #2

(Remarks to the Author)
Han et al., present a well written and comprehensive study describing CRISPR-TO, a novel implementation of RNA-guided CRISPR-Cas13 to perturb RNA localization. The authors describe the design of the system and present key data supporting to support its composition and application. The authors comprehensively describe considerations for use of the technology including number of guides required per target, the effect of binding, and the expected guide RNA design issues (universal to Cas13 in cells). The authors describe the use of inducible CRISPR-TO to reversibly drive RNA around the cell. They then go on to describe its use in the study of dynamics in RNA localization including specific insights into RNA transport within human neuronal cells. Finally, the authors describe a specific use case in high throughput screens to study RNA localization. Overall, the study is comprehensive and presents a unique tool to accelerate the critical study of RNA dynamics in human cells. The methods are novel and the data robust to this reviewer. I have only a few minor comments.

Minor Comments:
The authors described testing a variety of RNA targeting systems including Cas13a, Cas13bt, Cas13d, and Cas7-11. Could the authors comment on why each Cas13 system behaves so different in the same setting in Figure 1e? Did the authors see anything in the imaging that might suggest why they performed poorly relative to PspCas13b? I noted that representative images are absent from the Supplementary Figures. It is the opinion of this reviewer that they should be included, mostly because numerous labs will likely want to implement this technology and build on what is clearly a solid foundation. But making those images available to the community would be a valuable resource and prevent wasted effort on the part of researchers trying to minimize the delivery payload.

On the issue of delivery (which the authors highlight as a limitation in their discussion) it seems misleading to suggest researchers could use smaller systems when the smaller systems tested have been unsuccessful. I think this could be elaborated on to make it clear that there is no 'one size fits all' Cas13 protein.

The large aggregates of Cas13b within the nucleus when it is NLS tagged are intriguing. Are these nucleoli or just aggregates of Cas13b as the authors suggest? It is clearly a Cas13b dependent phenomenon which then takes me back to the other enzymes – do they show the same phenotype? For researchers wanting to study or perturb RNA within the nucleus this could be problematic.

The authors make no mention of the applicability of this tool in bacterial, archaeal, or plant cells. It would be prudent to indicate if CRISPR-TO could be adapted for use in these organisms.

Referee #3

(Remarks to the Author)
In this publication Han et al fuse PspCas13b with an inducible dimerization domain driven by the plant hormone ABA. By fusing the second part of the dimerization domain to different localising proteins, Han et al recruit an mRNA of interest to a subcellular compartment, such as the mitochondrial outer membrane or the tips of developing neurites. Using the axon targeting system, they conduct functional screens of 21 mRNAs to identify new RNAs with functional roles in local translation. They identify Stmn2 as an mRNA whose localization influences neurite outgrowth.

Major Comments:
1. PspCas13b and LwaCas13a have been shown to be more neurotoxic than RfxCas13d (Wu and Kapfhammer, 2021), which has been applied in neurons in vitro and in vivo (Zeballos et al., 2023; Powell et al., 2022, Morelli 2021, Zhou 2020) and has been shown to not impair neuronal viability or increase inflammatory markers in mouse neurons (Zeballos C. et al., 2023). For the method developed here, at least in primary culture, the authors should examine whether PspCas13b and the other components of the system expressed in neurons induces stress, impairs viability or increases inflammation. The same goes for the exposure to ABA at the used concentrations for the indicated timeframes.
2. In figure 2, it appears in some cases, that the target mRNA is present at lower levels when it is targetted? have the total levels been measured and has the mRNA half-life in the different conditions been measured?
3. The presence of dCas13 + guide has been shown to reduce translation by sterically blocking the ribosome (Apostolopoulos et al nature comm 2024), the authors consider this by targeting the 3'UTR instead of the CDS and show that binding there does not influence the abundance or stability of transcripts (Ext. Fig 5). Nevertheless, some reports in neurons have observed a reduction in target mRNA levels by expressing only the guideRNA (Powell et al Science Advances 2022). Once dCas13 is localised, especially in neurons, unbound guideRNA could accumulate in the soma, if they are indeed recognized by Dicer and lead to a reduction of target mRNA in the soma this could influence any functional readout. To examine this, the authors should analyse target mRNA levels in the soma of neurons they have analyzed. This is important to convince the readers that any observed effects truly arise from the localization of the guide.
4. The authors did not show that the endogenous mRNA localised to the axon tip is actually translated there. In page 10 line 324-328 they write that mRNAs "...located to neurite tips by CRISPR-TO can be actively translated there". This has not been shown for endogenous transcripts. They further write that "mRNAs during transport may undergo translation" and that ribosomes are co-transported there with the mRNAs. These claims are not sufficiently backed by data.
5. The authors assume that any phenotypic effect observed is indeed caused by the localization of the target mRNA and not by other effects, i.e. interference with the cell's internal localization machinery. To control for this in the case of beta-actin and

Stmn2 the localized mRNA condition should have an additional control of enforced somatic localization. This could be achieved by comparing the fusion to retrograde or anterograde localization machinery.

Minor comments:
1. The authors test which CRISPR effector would be the best suited by testing localization of GAPDH to the outer mitochondrial membrane (Fig 1d,e). They should indicate if guides with the appropriate direct repeat sequence and orientation were used for each effector and if the same guide sequences were used or if the guides were optimized for the PFS requirements of each effector. Related to this, essential citations are missing. dead-PspCas13b has previously been shown to perform better than other orthologs in RNA-binding applications (Yang et al Molecular Cell 2022, Wang et al Science 2019). The authors write “These results suggest that different dCas proteins possess distinct RNA binding activities…” page 5 like 125. This has previously been shown and should be cited and discussed as such.
2. Ext. Fig 2e is denoted as a scatterplot in the figure legend but its a swarm plot
3. On page 5, line 149-160 authors switch from HEK/HeLa experiments to primary culture and then back to HEK/HeLa, why? This should be explained.
4. regarding the same passage, guide design principles for many Cas effectors have been extensively studied, also specifically for PspCas13 (among others: Hu et al Biorxive 2022, Bandaru scientific reports 2020, Cox Science 2017, Yang et al Cell insight 2022), the additional merit coming from the gRNA design factors studied here should be discussed in the light of previous studies. The connection between read coverage and targeting efficiency should be clarified. The authors write “We explore potential factors that may contibute to CRISPR-TO efficiency, including RNA fragment expression levels, …These findings underscore the importance of maximizing read coverage…” Read coverage does not necessarily equal RNA fragment expression level.A slight rephrasing may be necessary to avoid equating these terms.
5. beta-actin mRNA is well established as being localised to the growth cone of axons (XX, XX), nevertheless the authors report 0 particles per neurite tip in the control group (page 9, line 278). This seems to contradict expectations from previous studies.
6. Co-localization is sometimes reported as “% of mRNA localized to”, sometimes as “% of p-bodies enriched with” and sometimes as “XX”. Please unify how these results are reported or provide a brief reasoning for changing the reported value.
7. In the time-course experiments please discuss what is known about the stability of ABA in cells, when does it get degraded?
8. Page 8, line 259 “Taken together, combining CRISPR-TO with real-time RNA tracking provides new insights into the dynamic behaviours of RNA localization in living cells.” So far no new insights have been shown. Rephrase as “has the potential to provide”
9. The authors showed that 4h ABA treatment is sufficient for localization. In subsequent experiments they use changing time-frames from 6h (page 10, line 310), and 12h (page 12, line 400), to 24h (page11, line 359). Why the changing time frames in each experiment?
10. In line 346, page 11 authors write that “we cannot track endogenous beta-actin mRNA in live neurons”, yes these tool exist (Benita Turner-Bridger et al 2018, Donlin-Asp et al 2021), also dead-Cas13b based tools exist for this purpose (Wang et al, Yang et al)
11. page 5 line 138-148 are the several guides provided as array or separately expressed, clarify in main text or figure legend
12. in line 428, page 13 the authors use the term “zip code” to refer to the protein that drives localization. This term has been used in mRNA localization to refer to specific sequences/motifs in the mRNA that drive localization. Therefore the term “zip code” should be avoided.
13. In Figure 4 j) the “Number of Actb mRNA particles per neurite tip” goes up to >60 particles, at the same time the authors quote Wang et al 2020 that most mRNAs have fewer than one copy in axons (age 11 line 352), is a count of more than 60 beta actin mRNAs per neurite tip realistic?
14. Figure 5 h) and i) both have -/- as gT presence.
15. Figure 6 a) please indicate DIV of transfection, ABA treatment and imaging in the flow chart of the experiment or the figure legend.
16. in Figure 6 g) the same cell is imaged before and after ABA treatment and therefore the dots are connected. In 6 f) this does not seem to be possible since the cells are indicated as +/- gT (assuming these are different cells transfected with and without targeting guide) nevertheless dots are connected as in g) suggesting a before and after of the same cell.
17. How was Co-localization analyzed? especially with “% of dCas13 localized on OMM” what is the cut off here to count as co-localized, threshold for total, automatized thresholding between cells? Please provide code.

Referee #4

(Remarks to the Author)
In this manuscript, Han and colleagues develop a CRISPR-mediated approach called CRISPR-TO for the relocalization of specific transcripts to defined locations within cells. This approach works by targeting the RNA to be moved with guide RNAs, facilitating its interaction with dCas13. dCas13 can then be inducibly driven to interact with protein markers of the subcellular location of interest, thus dragging the RNA along with it. The authors benchmark this system using a variety of RNAs and subcellular locations. They then use CRISPR-TO to screen a handful of genes with a focus on identifying RNAs that, when localized to neurites via targeting with dCas13 and Kif5a, promote neurite outgrowth.

This is an exciting technology. One limitation of the RNA localization field has been the relatively small number of cases reported where the mislocalization *of a specific RNA* resulted in an observable phenotype. However, one reason for this has been the difficulty associated with making mutations that result in mislocalization. Sequences that govern trafficking are unknown for almost all RNAs, and if those sequences are unknown, then it is not clear where mutations that would disrupt trafficking should be made. CRISPR-TO circumvents this problem and allows the targeted mislocalization of any RNA, at

least in principle. This technology will then be very useful to labs studying RNA trafficking.

Overall, the manuscript was clearly written and the conclusions of the authors were generally supported by the supplied data. I do, however, have suggestions that may improve the manuscript.

MAJOR COMMENTS

1. Some of the conclusions arising from figure 5 are overstated. Specifically, the claim that the Actb RNAs are engaged by ribosomes and translated during transport is not fully supported with the resolution presented. As presented, these RNAs are colocalizing with ribosomes. This is consistent with them being engaged by the ribosomes and potentially translated, but is not in itself direct evidence that they are being translated. Further, even if the ribosomes did appear to move with the Actb RNA, that is still not evidence that the ribosomes are actually engaged on the RNA as opposed to be co-transported within the same granule. This is important as the perhaps prevailing view of localized RNAs is that they are translationally repressed during transport. Providing direct evidence to the contrary, perhaps using live cell imaging of both ribosome hitchhiking as well as translation during transport (for example using SunTag, etc.), would be necessary to fully support this statement.

2. The claim about the transported RNAs being translated *in the neurite tip* (rather than during transport) is better supported using the photoconvertible fluorescent protein experiment in figure 5a. However, this could be made even stronger by adding a control in which puromycin was added.

3. While nice images, the data regarding the simultaneous targeting of two RNAs to neurite tips in figure 4h would be stronger if quantification of the results from many cells were shown. As presented, these results rely on a single set of images made from a single cell.

4. The statement on line 155 that peaks and valleys in RNAseq read coverage across a 3' UTR are due to biological differences in expression is almost certainly not true (extended data 4k). RNAseq read coverage is by its nature uneven across a transcript, but this has nothing to do with differences in the abundances of regions within that transcript in cells. Splicing is an obvious exception to this, but in the case of splicing, changes in read coverage appear as very sharp cutoffs at splice junctions. Further, splicing in 3' UTRs is rare. Although it's not fully understood, these patterns are more likely due to the differences in the abilities of different sequences to end up in RNAseq libraries, be it through differences in GC content, secondary structure, or other features.

These features that govern the ability of a gRNA to work in CRISPR-TO may overlap with features that govern the ability of a sequence to contribute RNAseq reads, but again, this is not due to differences of the abundance of that sequence within transcripts in cells, and therefore the term "variation in expression levels" is not appropriate. Further, the correlation between read coverage gRNA score is not obvious in extended data figures 4L and 4O as it is stated in the text. In these plots, it looks like gRNAs with moderate RNAseq coverage are the best as the read coverage of the best performing gRNAs are lower than those with intermediate performance.

5. In the benchmarking experiments demonstrating the targeting of RNAs to various locations, there are two slightly different metrics used. For example, one is represented in figure 1e (and other places), which is the fraction of the RNA molecules of interest that are localized to the location of interest. The other, which is represented in extended data figure 3j (and other places) is the fraction of cells in which the RNA of interest is localized to the location of interest. The latter is not ideal as it is dependent on a thresholding to decide whether or not a cell is displaying "enough" of the RNA at the location of interest in order to call the cell as positive. Further, more highly expressed RNAs, like the GAPDH RNA tested, are more likely to show some overlap with any location, simply because there are more RNA molecules.

On the other hand, the former metric of fraction of RNA molecules localized to the location of interest does not require any calls about if "enough" of that RNA was localized and should be more robust to different expression levels. It should be the metric that is always used for benchmarking. I fear the other metric is too dependent upon specific experimental parameters and therefore may be a bit misleading.

6. In figure 3f, it is posited that there are two populations of reporter constructs, one that maintained a constant distance to centrosomes and another that showed potentially directed movement towards centrosomes. How many observed RNA molecules were in each class?

7. In figure 3f, The claim that the Type II RNAs are being actively transported to the centrosome could be supported by comparing the velocities of these RNAs to those previously observed for RNA transport to centrosomes (Safieddine et al, Nat Comm, 2021).

8. In figure 3d, what fraction of the reporter RNA ends up at centrosomes? This is important as the efficiency of CRISPR-TO likely varies widely by subcellular location.

MINOR COMMENTS

1. Line 118: I believe this refers to extended data 3h-j, not 2h-j.

2. I think, but am not sure, that the gT indications in figure 5 H and I are incorrect. I believe 5H uses gNT (in which case

minus signs for gT would be correct, although slightly confusing) while 5I uses gT (in which case the minus signs for gT should be plus signs).

3. Statistics and uncertainties were generally handled appropriately.

Version 2:

Reviewer comments:

Referee #1

(Remarks to the Author)
The authors have addressed my comments and concerns appropriately, and greatly
improved the manuscript overall in response to all reviewers. Some minor comments below.

Minor comments:
1. When referring to binding constant in the main text (Line 252-255: when referring to ED Fig 7a) you define it as 'Km', which I still consider the Michaelis constant . Please reword to remove Km and use Kd (apparent) or similar.

Referee #2

(Remarks to the Author)
Han et al., have presented a compelling response to the referee assessment. The authors now provide additional data that this reviewer believes address concerns. Specifically, the authors now include additional experiments assessing transfection efficiency, expression, and cell toxicity and include these data as a Supplementary Note. This is a really important inclusion given the inconsistencies in the field and will make the work more reproducible. The authors also now include representative images of localization for each system tested and provide evidence for localization to the nucleolus. Furthermore, the authors have contextualized the method by highlighting the context-specific applicability of CRISPR-TO and potential broader applicability in bacteria and plant cells. Examining the authors responses to the comments from other reviewers highlights that they have done substantial work to more rigorously assess CRISPR-TO, all of which greatly improve the manuscript. In summary, the manuscript has been greatly improved and still presents a novel contribution to the toolbox that is well described and will be of broad interest to the field.

Referee #3

(Remarks to the Author)
the authors have dealt with my criticisms and suggestions to my satisfaction.

Referee #4

(Remarks to the Author)
The authors have addressed my concerns.

Referees' comments:
Referee #1 (Remarks to the Author):
Han et al Review Round 1

Summary
Han et al present a manuscript describing a new technique “CRISPR-TO” to manipulate mRNA subcellular localization to various organelles/subcellular structures in live cells, in a sequence specific manner. After an initial proof of concept and vector design, the authors show that this technology can be used to localize specific mRNAs to the outer mitochondrial membrane, p-bodies, stress granules, telomeres, and nuclear stress bodies. Excitingly, they were able to use this technology to recruit mRNAs to microtubules and in live cells and real time observe bidirectional movement along these microtubules. The authors then show this also recruits ribosomes and allows for local translation at neurite terminals and allow for screening for transcripts that when forced to be localized to neurites can modulate neurite outgrowth. Overall, this is a clever use of Cas13, and most of the interpretations are supported by well-controlled experiments and explained in a well written manuscript. That said, some claims and interpretations that impact the conclusions and usefulness of this technology are oversold and not backed up by the required data, and as a result some major and minor concerns need to be addressed. See below for my specific comments:

Major Comments

1. One of the main criticisms I have with how this technology is described in the abstract and throughout parts of the main text: “Real time investigation of RNA dynamics”. In my opinion, if you’re perturbing the localization of the mRNA in non-natural ways by forcing it into a specific compartment synthetically, and thus I’m not sure one can claim this technology can be used to understand native dynamics of mRNA transport given the perturbation is likely changing the native kinetics of how mRNAs are transported? One way to potentially remedy this concern is to change the emphasis on real time modulation/manipulation as opposed ‘investigation’ of RNA dynamics given you’re deliberately perturbing the system.

Response:
We agree that the term “real-time investigation of RNA dynamics” may unintentionally suggest passive observation of native mRNA transport, whereas our approach actively perturbs RNA subcellular localization. In response, we have revised the text to emphasize that CRISPR-TO enables real-time manipulation and subsequent monitoring of RNA localization dynamics instead of saying “Real time investigation of RNA dynamics”. Specifically, we have updated the text as follows:
Line 25-28:
“It allows for inducible and reversible bidirectional RNA transport along microtubules via motor proteins, facilitating real-time manipulation and monitoring of RNA localization dynamics in living cells.”
Line 272-273:

"We leveraged the inducibility of CRISPR-TO to manipulate and monitor RNA localization dynamics in real-time."
Line 271:
"Manipulation and monitoring of RNA localization dynamics via CRISPR-TO"

2. ED figure 3 it would be great to quantify in each panel the % of colocalization? Particularly as some of the mRNAs targeted aren't localizing as effectively (by eye; e.g. SDHC, SDHD, NDUFS2?). It would be more convincing with these quantified as you did with ED3.j.

Response:
In response, we have quantified the % of localization of the mRNA and dCas13 protein on the OMM for each endogenous gene in the original **Extended Data Fig. 3b-3g**. We also updated representative images to better show the localization of *SDHC*, *SDHD*, and *NDUFS2* mRNAs on the OMM. The original **Extended Data Fig. 3b-3g** was replaced by **Extended Data Fig. 2b-g** shown below. Quantification of many cells further supports the efficiency and versatility of CRISPR-TO in manipulating different endogenous mRNA localization across diverse cell types (**Extended Data Fig. 2b-g**).

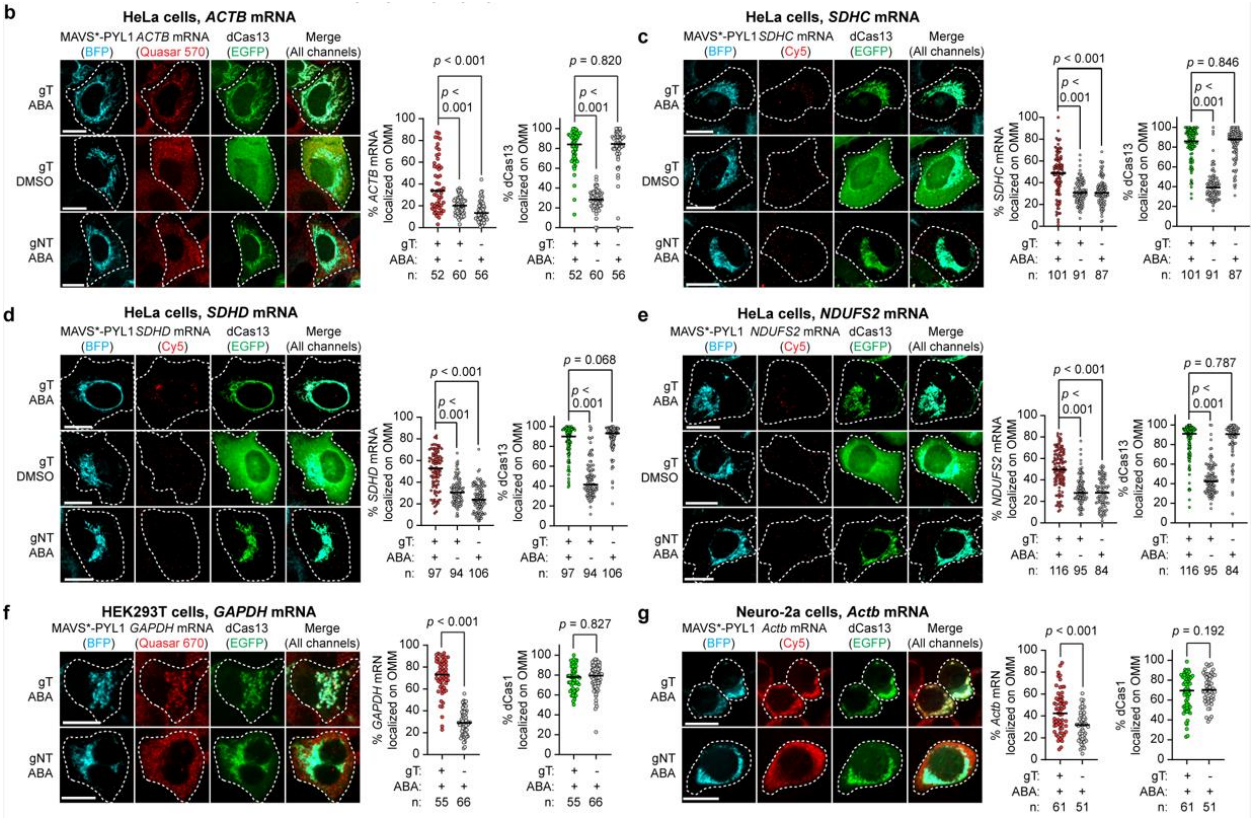

Extended Data Fig. 2 | b-e, Left: representative microscopic images showing the localization of endogenous *ACTB*, *SDHC*, *SDHD*, and *NDUFS2* mRNAs to the OMM in HeLa cells under different gRNA and ABA conditions. Scale bar, 20 μm. Right: quantification of the percentage of the target mRNA and dCas13 protein localized on the OMM in single cells. **f-g**, Left: representative microscopic images showing the localization of endogenous *GAPDH* mRNA and *Actb* mRNA to the OMM in HEK293T cells and Neuro-2a cells under different gRNA conditions, respectively.

Scale bar, 20 μm. Right: quantification of the percentage of the target mRNA and dCas13 protein localized on the OMM in single cells. In **b-g**, white dotted lines indicate the plasma membrane of the imaged cells.

3. Relatedly, OMM localization in different cell lines is different in morphology, is this expected? For example, the morphology in HEKs is rounder and puncta like, same as with Neuro 2A, compare to HeLa cells which stain more elongated and string-like. It might be worth commenting on this phenomenon.

Response:

We thank the reviewer for this interesting observation. To verify these differences, we stained wild-type HeLa, HEK293T, and Neuro-2a cells with MitoTracker Red CMXRos (Thermo, M7512), a broadly used fluorescent dye that selectively accumulates in active mitochondria based on their membrane potential. We observed that mitochondrial morphology indeed varies among these cell lines. Specifically, HeLa cells mostly display elongated and string-like mitochondria, while HEK293T and Neuro-2a cells show more round and puncta-like mitochondria (**Supplementary Fig. 3**). This is consistent with what we observed in CRISPR-TO perturbed cells in **Fig. 1b** and **Extended Data Fig. 2f-2g**. Literature search confirmed that mitochondrial morphology is known to vary widely across cell types, including small vesicles, rods, tubules, and branched reticular networks[1]. We have added a statement of this difference in the revised manuscript.

Line 117-119:

"The observed mitochondrial morphology is different across HeLa, HEK293T, and Neuro-2a cells (**Fig. 1b, Extended Data Fig. 2f-2g, Supplementary Fig. 3**) and consistent with previous reports[1]."

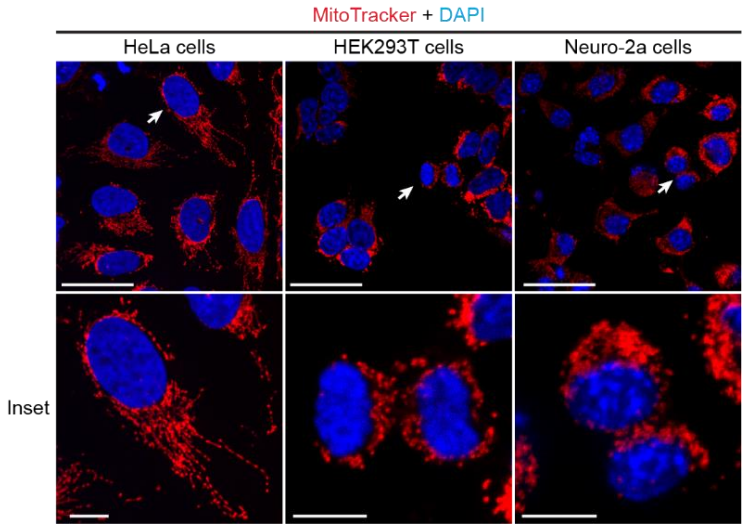

Supplementary Figure 3 | The morphological difference of mitochondria across different cell types. Representative microscopic images showing that mitochondrial morphology is different among HeLa, HEK293T, and Neuro-2a cell lines which were stained with MitoTracker Red CMXRos. Scale bar, 40 μm. Bottom: insets showing cells pointed by the white arrow. Scale bar, 10 μm.

4. In some cases, you see colocalization between the Cas13 PYL1 fusion without ABA or with ABA and a non-target gRNA suggesting that interpretation of whether there is actually specificity in the experiment could be an issue, in particular if the smFISH doesn't work optimally or at all for a particular target (this is sometimes the case). What alternatives do you think there are to make sure targeting is specific? Perhaps this observation needs to be suggested as a limitation?

Response:

We acknowledge the reviewer's comment of the specificity of smFISH staining. Regarding the observed colocalization between dCas13-ABI (hereafter referred to as dCas13) and the PYL1 fusion without ABA, we guess the reviewer is referring to the observed 20% of dCas13 protein localized to the OMM without ABA treatment (**Fig. 1c**). Since mitochondria and the cytoplasm are closely intertwined, high expression levels of dCas13 protein in the cytoplasm can make it look like dCas13 is colocalized with the mitochondria due to the close proximity under diffraction-limited confocal microscopy imaging (~250 nm). However, upon ABA treatment, the % dCas13 localized on the OMM is increased significantly to around 80% (**Fig. 1c**). Regarding the question on the colocalization between dCas13 and PYL1 fusion with ABA and a non-target gRNA, we believe this may be a misunderstanding. The colocalization between dCas13 and the PYL1 fusion is only influenced by ABA treatment and not by gRNA expression. Even when expressing a non-targeting gRNA (gNT), dCas13 should still colocalize with the PYL1 fusion upon ABA treatment.

To address the reviewer's concern regarding RNA FISH probe specificity, we performed additional validation experiments. We split the RNA FISH probes targeting *GAPDH* mRNA used in this manuscript into two sets, each labeled with a different fluorescent dye (**Supplementary Fig. 2a**). We reason that if the RNA FISH probes are specific, the staining signals of the two different sets of RNA FISH probes should colocalize perfectly. We co-stained wild-type HeLa cells with these two probe sets and found that their labeling signals colocalize almost perfectly (**Supplementary Fig. 2b**).

To further prove the RNA FISH specificity, we co-stained the two RNA FISH probe sets targeting *GAPDH* mRNA or RNA FISH probes targeting *GAPDH* mRNA and *ACTB* mRNA in HeLa cells, where *GAPDH* mRNA was recruited to the OMM by CRISPR-TO. We found that the two *GAPDH* probe sets colocalized, but *GAPDH* mRNA signals did not colocalize with *ACTB* mRNA (**Supplementary Fig. 2c**). This further supports the staining specificity of the RNA FISH probes used in our experiments. We hope this clarification and additional data address the reviewer's concerns. We also revised the manuscript to confirm the specificity of RNA FISH labeling.

Line 104-105:

"We imaged *GAPDH* mRNA using single molecule RNA FISH and confirmed the specificity of imaging (**Supplementary Fig. 2**)."

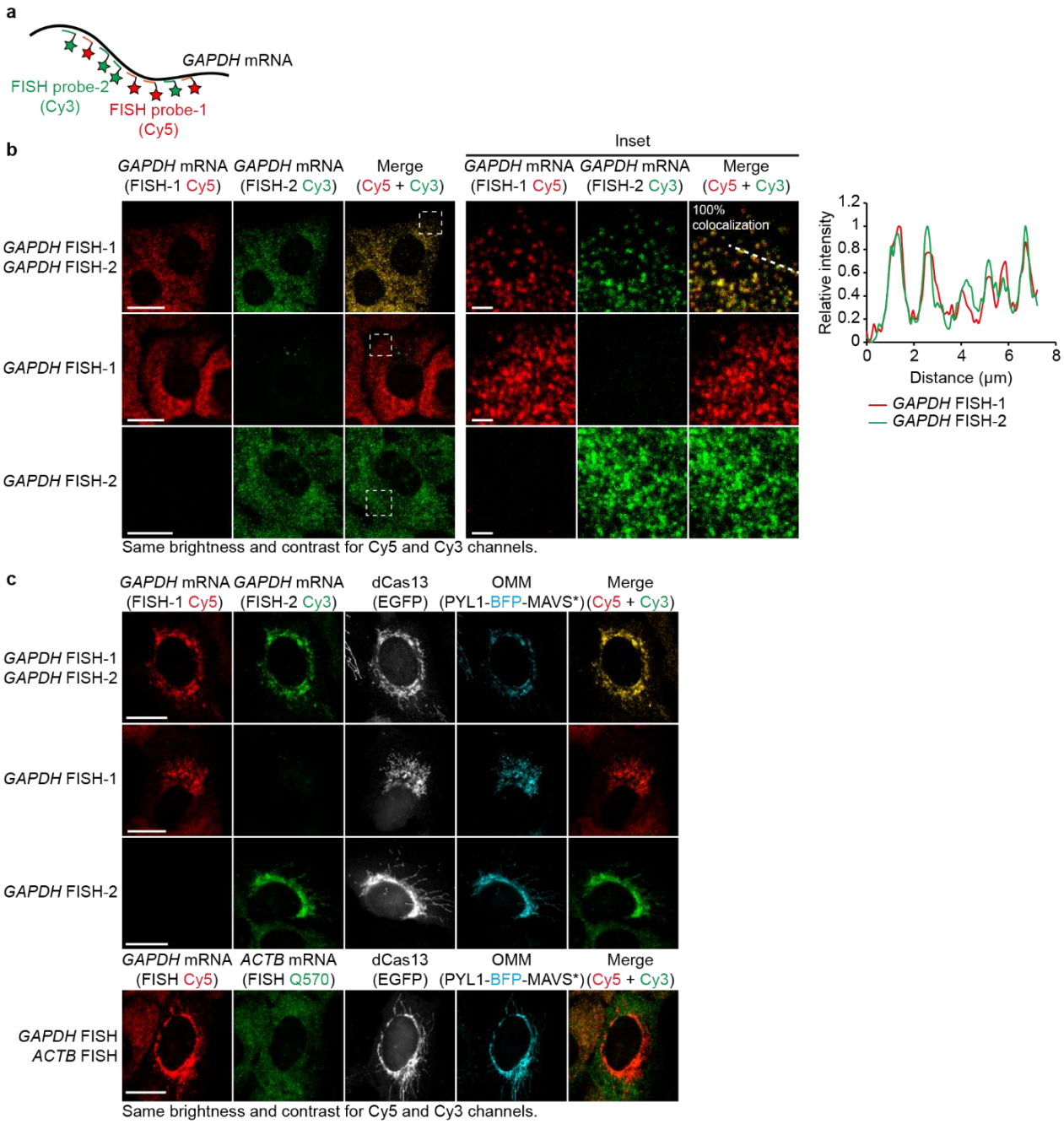

Supplementary Figure 2 | Testing the specificity of designed RNA FISH probes. a, Schematic showing the design of two RNA FISH probe sets targeting *GAPDH* mRNA. **b**, Representative microscopic images showing near-perfect colocalization of staining signals using the two RNA FISH probe sets targeting *GAPDH* mRNA in HeLa cells. Scale bar, 20 μm. Middle: insets of dotted boxes. Scale bar, 2 μm. Right: intensity plots of the dotted line in the left image. **c**, Representative microscopic images showing colocalization of the staining signals of the two RNA FISH probe sets targeting *GAPDH* mRNA. In contrast, there is no evident colocalization of staining signals for *GAPDH* mRNA and *ACTB* mRNA in HeLa cells where *GAPDH* mRNA was recruited to the OMM by CRISPR-TO. Scale bar, 20 μm.

5. In a similar observation, why don't you see Cas13 puncta on TERRA for example given it's likely to colocalize there without the need for the PYL1 fusion for forcing the interaction? It's also surprising all the background disappears, likewise with Cas13 and GAPDH and stress granules? Is Cas13 non-specifically binding to stress granules with a non-targeting (and perhaps targeting) guide given it looks like in the DMSO condition there is little GAPDH smFISH signal in SG puncta? On that note were SGs induced with Arsenite or some other stressor? As far as I can tell, it's not included in the text anywhere what stressor was used in many of these experiments.

Response:

We acknowledge the reviewer's several questions. Here are our responses to each question.

Question 1:

In a similar observation, why don't you see Cas13 puncta on TERRA for example given it's likely to colocalize there without the need for the PYL1 fusion for forcing the interaction?

Response 1:

Regarding this question, we did observe dCas13 puncta colocalized with *TERRA* lncRNA puncta in the gT+DMSO group (**Reviewer Fig. 1a**). To better demonstrate this, we plotted the intensity plots across two *TERRA* lncRNA puncta and found that dCas13 peaks overlapped with *TERRA* lncRNA peaks (**Reviewer Fig. 1b**). This suggests that dCas13 does bind to *TERRA* lncRNA when targeting gRNA is expressed in cells. However, the overall punctate pattern of dCas13 is less pronounced in this system, because dCas13 is overexpressed and not optimal for imaging *TERRA* lncRNA with excessive dCas13 proteins contributing to the background signal.

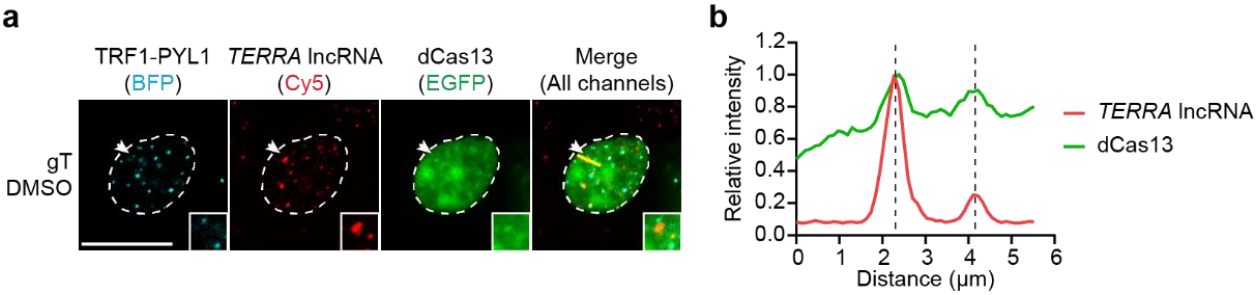

Reviewer Figure 1 | dCas13 colocalizes with *TERRA* lncRNA puncta in the presence of targeting gRNA. a, Representative microscopic images showing dCas13 enriched on *TERRA* lncRNA puncta in the gT+DMSO group. The shape of the nucleus is depicted with a white dotted line. Inset images represent magnification of the region indicated by the white arrow. Scale bar, 20 μm. **b**, Intensity plots of the yellow line in the merge image of **a**.

Question 2:

It's also surprising all the background disappears, likewise with Cas13 and GAPDH and stress granules?

Response 2:

We believe the reviewer was asking why there was diffused green signal in the whole nucleus or cytoplasm under DMSO treatment, while the diffused green signal disappeared under ABA treatment (e.g., as shown in **Fig. 2c, 2e**). The green fluorescence signal represents the expressed dCas13 protein. Under DMSO treatment, dCas13 is diffusely distributed throughout the cytoplasm

or nucleus, some binding to the target mRNA and some not, resulting in an overall green signal. After ABA treatment, dCas13 is recruited to specific subcellular compartments, such as stress granules (**Fig. 2c**) or telomeres (**Fig. 2e**), leading to its aggregation at these locations. This markedly reduces the diffused dCas13 signal in the cytoplasm or nucleus, making it looks like “all the background disappears”.

To demonstrate this clearly, we showed two representative cells with similar integrated intensity of green fluorescence (dCas13) in the nucleus (**Reviewer Fig. 2a**). In the gT+DMSO group, the green signal is diffused in the nucleus. After adding ABA, dCas13 is concentrated at the telomere (note the different values on the intensity calibration bar), as shown by an increase in localized green signal at the telomeres and a corresponding decrease in the diffuse signal (**Reviewer Fig. 2b**). We also note that due to the intrinsic transfection variation among cells, different cells may exhibit different dCas13 expression levels. But overall, the aggregation of dCas13 at specific subcellular compartments, such as stress granules, p-bodies, telomeres, nuclear stress bodies, and plus and minus ends of microtubules, makes it looks like “all the background disappears”.

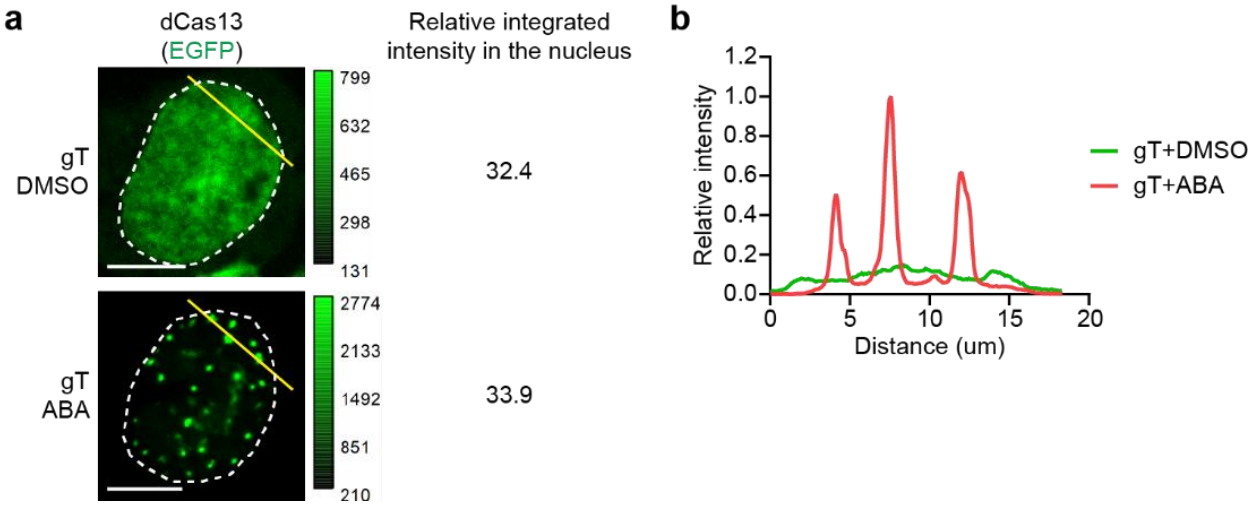

Reviewer Figure 2 | Comparison of dCas13 signals before and after ABA treatment. a, Representative microscopic images showing two cells with similar integrated intensity of green fluorescence in the nucleus from gT+DMSO and gT+ABA group, respectively. Intensity calibration bars indicate the fluorescence intensity of dCas13 proteins. Scale bar, 10 μm. **b**, Intensity plots of the yellow line in the image of **a**.

Question 3:
Is Cas13 non-specifically binding to stress granules with a non-targeting (and perhaps targeting) guide given it looks like in the DMSO condition there is little GAPDH smFISH signal in SG puncta?
Response 3:
It has been reported that under sodium arsenite-induced stress in U2OS cells, only about 4% GAPDH mRNA localizes to stress granules[2]. Therefore, it is expected to see only a minimal GAPDH smFISH signal in stress granules under the DMSO condition (**Fig. 2c**). In addition, we do find dCas13 has some non-specific recruitment to stress granules under DMSO treatment, especially in cells with very high dCas13 expression levels. However, the percentage of dCas13 and *GAPDH* mRNA in stress granules is significantly increased following ABA treatment

(**Extended Data Fig. 6b**), suggesting that CRISPR-TO effectively promotes targeted localization of dCas13 and *GAPDH* mRNA to stress granules.

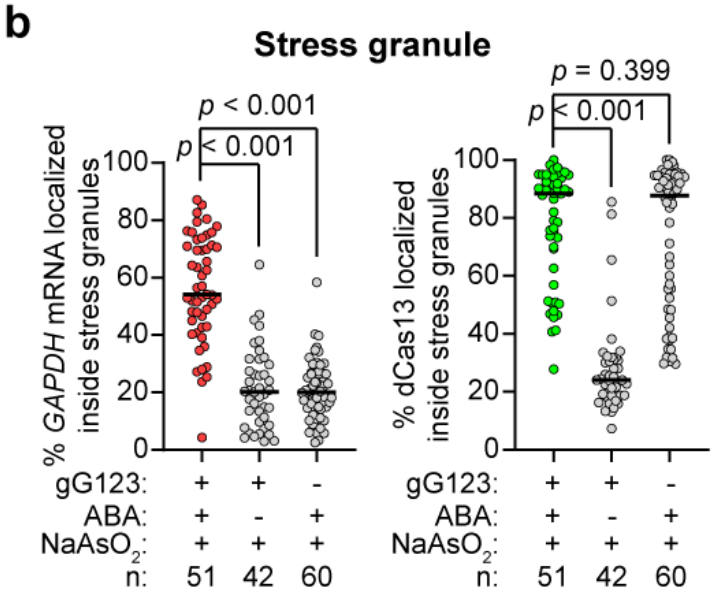

Extended Data Figure 6 | b, Quantification of the percentage of the target RNA (red) and dCas13 protein (green) localized inside stress granules related to **Fig. 2c**. The black bar indicates the median. Unpaired t-test.

Question 4:
On that note were SGs induced with Arsenite or some other stressor? As far as I can tell, it's not included in the text anywhere what stressor was used in many of these experiments.
Response 4:
We thank the reviewer for pointing this out. Although this information was previously provided in **Supplementary Table 3**, we agree that it should be more accessible to readers. We have now revised the Methods section:
Line 629-631:
"To induce the formation of stress granules, HeLa cells were treated with 50 μM $NaAsO_2$ for 6 hours. To induce the formation of nuclear stress bodies, HeLa cells were treated with 100 μM $NaAsO_2$ for 6 hours."

6. I also have concerns about the interpretation of the P body and GAPDH storage vs. degradation experiment given only a single non-kinetic GAPDH mRNA expression level measurement was taken. There likely could be compensatory mechanisms to replace any GAPDH being degraded in the P body given GAPDH is an essential (housekeeping) gene (according to DepMap), so there are likely buffering mechanisms to keep its gene expression consistent. Have the author's considered this caveat when making these measurements? A better approach would be to measurement the rates of RNA decay across the time course of the experiment and see if they change pre- and post- localization to the P-body with the appropriate housekeeping controls, they may best be done by targeting a non-essential gene instead of GAPDH.

Response:
We thank the reviewer for this great suggestion regarding kinetic measurements of RNA decay pre- and post-localization to the p-body. We also acknowledge that a single non-kinetic *GAPDH* mRNA expression level measurement is not enough to conclude that p-bodies primarily function as storage sites rather than decay centers of mRNA. To address this concern, we performed a new experiment following the reviewer's suggestion.

In this experiment, we designed a reporter plasmid (pSLQ14860, **Supplementary Table 1**) that co-expresses a BFP-7xGCN4 reporter mRNA under a doxycycline (Dox)-inducible promoter TRE3G and a rtTA (reverse tetracycline-controlled transactivator) gene under a constitutive CMV promoter (**Extended Data Fig. 6e**). We co-transfected this reporter plasmid together with CRISPR-TO components to recruit BFP-7xGCN4 reporter mRNA to p-bodies in HeLa cells. The transfected cells were first treated with Dox for 24 hours to induce reporter mRNA expression, and then treated with ABA for 2 hours to recruit reporter mRNA to p-bodies. We next removed Dox and maintained cells in fresh media with ABA but without Dox. Cells were collected at different time points (0, 4, 6, 24, and 48 hours) after removing Dox for RT-qPCR analysis (**Extended Data Fig. 6f**). We quantified three mRNA targets: 1) BFP-7xGCN4 reporter mRNA for quantifying reporter RNA decay rate; 2) rtTA mRNA as an internal control for reporter plasmid transfection; 3) *GAPDH* mRNA as a housekeeping control for RT-qPCR analysis. We designed two experimental groups for comparison: 1) gT+ABA compared with gT+DMSO; 2) gNT+ABA compared with gNT+DMSO. The expression of the reporter mRNA was normalized to rtTA mRNA, and all time points were further normalized to the initial time point (t_0). We fit the normalized data to a one-phase decay model, $Y(t) = Y_0 \times \exp(-kt) + \text{Plateau}$, using Graphpad, with Plateau set to 0 and Y_0 set to 1 (also see **Methods**).

We found that the RNA decay curves are nearly identical between gNT+DMSO and gNT+ABA groups and there is no significant difference in the decay constant *k* ($p = 0.620$), suggesting that ABA treatment does not influence the reporter mRNA decay rate. In contrast, when comparing the targeting gRNA groups, the decay curve for the gT+ABA condition where reporter mRNAs are recruited to p-bodies, is significantly shifted upward compared to the gT+DMSO condition. The reporter mRNA half-life is larger (22.7 h compared to 16.9 h), and the decay constant *k* is significantly smaller in the gT+ABA group (0.031 h^{-1} compared to 0.041 h^{-1}, $p = 0.026$), indicating that RNA decay is slower when mRNA is localized inside p-bodies (**Extended Data Fig. 6g-h**). These findings support the conclusion that p-bodies function more as storage sites rather than decay centers for mRNA. We have updated the main text with this new data to support the application of using CRISPR-TO in studying the role of p-bodies in mRNA storage versus degradation:

Line 211-220:
"To further compare RNA decay rates inside and outside p-bodies, we designed a reporter system that co-expresses BFP-7xGCN4 reporter mRNA (under a doxycycline (Dox)-inducible TRE3G promoter) and rtTA (under a constitutive CMV promoter) (**Extended Data Fig. 6e**, **Method**). Using CRISPR-TO to direct reporter mRNA localization, we found that the decay constants for the gNT+DMSO and gNT+ABA groups were similar ($p = 0.620$) (**Extended Data Fig. f-h**), suggesting

that ABA treatment does not affect mRNA stability. In contrast, when reporter mRNA was recruited to p-bodies (gT+ABA), its half-life is increased from 16.9 h to 22.7 h and the decay constant decreased significantly (from 0.041 h^{-1} to 0.031 h^{-1}, p = 0.026, **Extended Data Fig. f-h**), supporting the model that p-bodies could function more as storage sites rather than decay centers for mRNA."

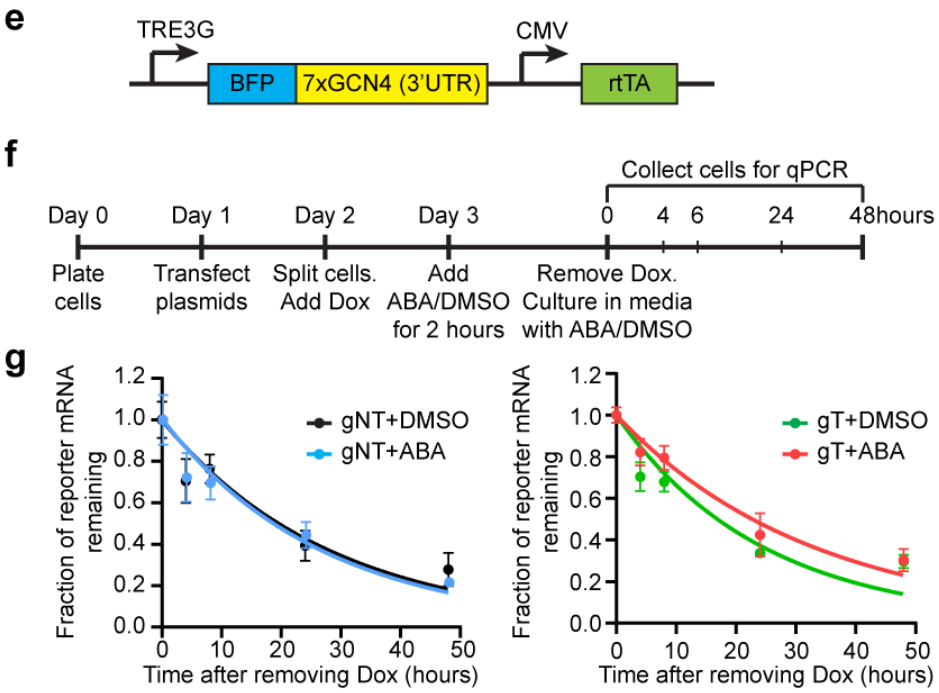

h

Group	k (hour^{-1})		Half life (hour)		R	*p* value
	Best-fit values	95% CI	Best-fit values	95% CI		
gNT+DMSO	0.036	0.027 ~ 0.047	19.5	14.7 ~ 25.9	0.913	0.620
gNT+ABA	0.037	0.029 ~ 0.049	18.5	14.3 ~ 23.9	0.930	
gT+DMSO	0.041	0.031 ~ 0.055	16.9	12.6 ~ 22.3	0.917	0.026
gT+ABA	0.031	0.025 ~ 0.037	22.7	18.9 ~ 27.3	0.961	

Extended Data Figure 6 | e, Schematics of the reporter mRNA plasmid pSLQ14860_pCAGGS-TRE3G-BFP-7xGCN4-CMV-rtta construct. **f**, Experimental procedures for measuring RNA decay rate. **g**, RNA decay curves for the BFP-7xGCN4 reporter mRNA under different conditions. Mean and standard deviation values at each time point are plotted based on multiple measurements across three biological replicates. **h**, Parameters and results for the RNA decay curves fitted by one phase decay function. p-value was calculated by Z-test of the decay constant k (**Supplementary Methods**).

7. I object to the use of Michalis-Menten kinetics to describe the fitted curve in ED Fig 7, as MM kinetics requires the determination of initial rates (reaction velocity) which naturally contain a time component and is used to describe enzyme catalysis (which this interaction isn't). I would prefer to see the date referred to as fitting a standard 1:1 ligand binding isotherm/curve or rectangular

hyperbola. Particularly, as in the next paragraph you mention a two-phase model of recruitment which wouldn't be described by MM kinetics.

Response:
We agree that the term "Michaelis-Menten kinetics" was not appropriate for describing our model used. In the model, we actually fit the data with a 1:1 ligand binding isotherm as a "saturation binding curve". In response, we have revised the text and figure legend to refer to the model as "saturation binding curve".
Line 252-255:
"The dCas13 recruitment to the OMM followed saturation binding curve (Hill coefficient ~1.6, K_m = 5.2 μM), indicating a simple, near non-cooperative interaction between ABA-induced ABI and PYL1[3]. *GAPDH* mRNA recruitment follows a similar curve with Hill coefficient at 1.1 and K_m at 8.8 μM (**Extended Data Fig. 7a**). These above suggest the binding of dCas13 onto the OMM has little to no cooperativity."

8. I think the manuscripts needs a much more careful consideration of the potential for ff-target localization, and an understanding of the effects of mismatch tolerance. It is well understood that Cas13 binding is more permissive than Cas13 cleavage in terms of off-target and so it would be good to understand the gRNA design considerations for this specific type of technology as they may need to be more careful with respect to number of mismatches allowed vs. the current Cas13 cleavage-based design rules/algorithms currently available. With this in mind, perhaps a mismatch tolerance experiment or some small-scale specificity test (for example, design a guide with a perfect match to transcript x but with some probability of off-targets with 1-3 (or more) mismatches to a second transcript, and see if you get colocalization using mRNA FISH with the off-target as well (vs. the on-target as a control). Without this information it's going to be difficult to know the extent of off-targets and whether this system has the require specificity to be useful here.

Response:
We appreciate the reviewer's suggestion on testing the mismatch tolerance of dCas13 on target binding. Cas9 is known to be more permissive for binding than for cutting[4], and comparatively, fewer studies have investigated the mismatch tolerance of PspCas13b in our system. Therefore, we performed a mismatch tolerance experiment following the reviewer's suggestion. We tested if mismatches in the gRNA spacer affect CRISPR-TO efficiency in localizing endogenous *GAPDH* mRNA to the OMM in HeLa cells. We designed a series of 30 gRNAs with different mismatches in the spacer of the targeting gRNA (gG1), including 10 gRNAs with one mismatch (gSM1-gSM10), 10 gRNAs with two mismatches (gDM1-gDM10), and 10 gRNAs with three mismatches (gTM1-gTM10). For gTM10, we added an extra 5'-g to ensure optimal transcription activity by the U6 promoter, which requires a "G" nucleotide at the transcription start site for optimal expression (**Extended Data Fig. 5a**).

We quantified the % of *GAPDH* mRNA localized on the OMM for each gRNA group and subtracted the background % of *GAPDH* mRNA localization observed with the gNT to obtain the RNA relocalization efficiency for each group. Compared to the perfectly matched gG1 group, around

75% of the mismatched gRNAs exhibited a significant decrease in relocalization efficiency (**Extended Data Fig. 5b**), suggesting that dCas13-medidated CRISPR-TO is highly sensitive to mismatches. Interestingly, we found several "hot spots" on the gRNA spacer that are particularly intolerant to mismatches. For example, locations 1-2 (1-6 nt), 4-7 (10-21 nt), and 9-10 (25-30 nt) showed lower mismatch tolerance, whereas locations such as 3 (7-9 nt) and 8 (22-24 nt) were more tolerant (**Extended Data Fig. 5c**). Although this mismatch tolerance pattern might be unique for this specific gRNA (considering slightly different mismatch tolerance patterns characterized by different methods[5-7]), our results and published literatures[5-7] consistently suggest that the 5'-end of the spacer is less tolerant to mismatches and that dPspCas13b binding overall is highly sensitive to target mismatches.

Regarding the reviewer's concern about potential off-target localization, the observed low mismatch tolerance of dPspCas13b binding inherently reduces the chance of off-target interactions. Moreover, we have found that while a single gRNA is usually not efficient for RNA relocalization, the use of two gRNAs significantly enhances CRISPR-TO efficiency (**Extended Data Fig. 3h, Extended Data Fig. 5d**). Although we do not yet know the exact mechanism underlying this synergistic effect, this multivalent effect where multiple dCas13 binding sites cooperate on the target RNA further reduces the likelihood of off-target localization, since the chance of both gRNAs simultaneously binding to the same off-target RNA is extremely low.

We have revised the manuscript to talk about the low off-target potential of the CRISPR-TO system:
Line 177-189:
"Finally, we characterized the off-target potential of CRISPR-TO using a mismatch tolerance assay by designing 30 gRNAs containing various mismatches in the gG1 spacer targeting endogenous *GAPDH* mRNA (**Extended Data Fig. 5a**). About 75% of the mismatched gRNAs exhibited significantly reduced RNA localization efficiency compared to gG1 (**Extended Data Fig. 5b**), suggesting that CRISPR-TO is sensitive to mismatches. Notably, specific regions within the gRNA spacer (locations 1-2, 4-7, and 9-10) were particularly intolerant (**Extended Data Fig. 5c**). Although this pattern may be unique to this specific gRNA, our results and prior studies[5-7] consistently suggest that the 5'-end of the gRNA spacer is less tolerant to mismatches. Moreover, using two gRNAs significantly enhanced CRISPR-TO efficiency (**Extended Data Fig. 3h, 5d**). This multivalent effect, where multiple dCas13 binding sites cooperate on the target RNA, further reduces off-target localization, since the likelihood of both gRNAs simultaneously binding to the same off-target RNA is extremely low. Overall, these results suggest that CRISPR-TO has low off-target potential for RNA localization."

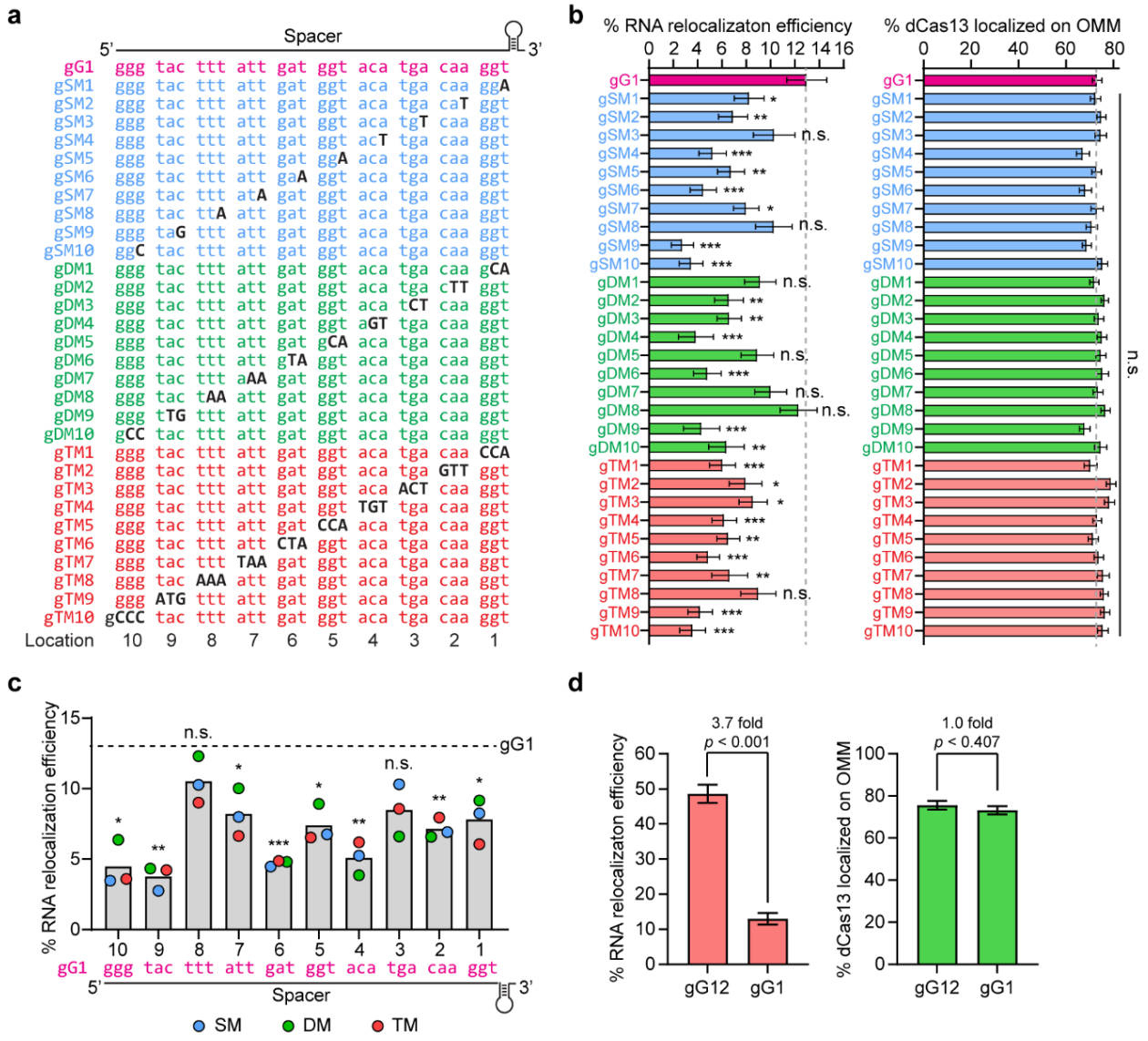

Extended Data Figure 5 | Characterization of mismatch tolerance of gRNA for dCas13 binding efficiency in the CRISPR-TO system. a, Schematic showing the design of 30 gRNAs with different mismatches from gG1 which targets the endogenous GAPDH mRNA. The mutated nucleotides are shown in black. **b**, Quantification of percentage of RNA relocalization efficiency and percentage of dCas13 localized on the OMM in single cells for different gRNAs (n = 44-80 cells per group). % RNA relocalization efficiency was calculated by subtracting the background % of GAPDH mRNA localized on the OMM using the non-targeting gRNA (gNT) from the % of GAPDH mRNA localized on the OMM for each gRNA. Only cells co-expressing dCas13 and MAVS*-PYL1 were analyzed. Data was presented as means ± SEM. n.s., not significant ($p > 0.05$); *, $p < 0.05$; **, $p < 0.01$; ***, $p < 0.001$; unpaired t-test between gG1 and individual groups. **c**, Comparison of % RNA relocalization efficiency of gRNAs with single mutation (SM), double mutations (DM), and triple mutations (TM) on different location of the gRNA spacer. n.s., not significant ($p > 0.05$); *, $p < 0.05$; **, $p < 0.01$; ***, $p < 0.001$; one sample t test with a hypothetical value 0.1298 which is the mean % RNA relocalization efficiency of the gG1 group. **d**, Comparison

of % RNA relocalization efficiency and % dCas13 localized on the OMM between gG1 group and gG12 group that co-expresses gG1 and gG2 together. Data was presented as means ± SEM. The number above each plot is the fold change between the two groups. Unpaired t-test.

Other Comments

1. The decision to use an NLS vs NES in each localization case explained? Is it clear in each case which one is used? The figures for example in ED Fig 2 don't show this level of detail?

Response:
To clarify the use of NLS vs NES, we have updated the original **Extended Data Fig. 2b** to indicate the use of NLS-dCas13 and NES-dCas13 in each case. The updated figure is now **Extended Data Fig. 1f** and is shown below. We have also revised the text to make it clear that we used NLS-dCas13 for RNA relocalization inside the nucleus:
Line 221-223:
"For nuclear RNA localization, we used NLS-dCas13 and fused PYL1 with TRF1, a core component of the telomere nucleoprotein complex[8], or HSF1, a marker protein of nuclear stress body upon stress conditions[9] (**Fig. 2d, Extended Data Fig. 1f**)."

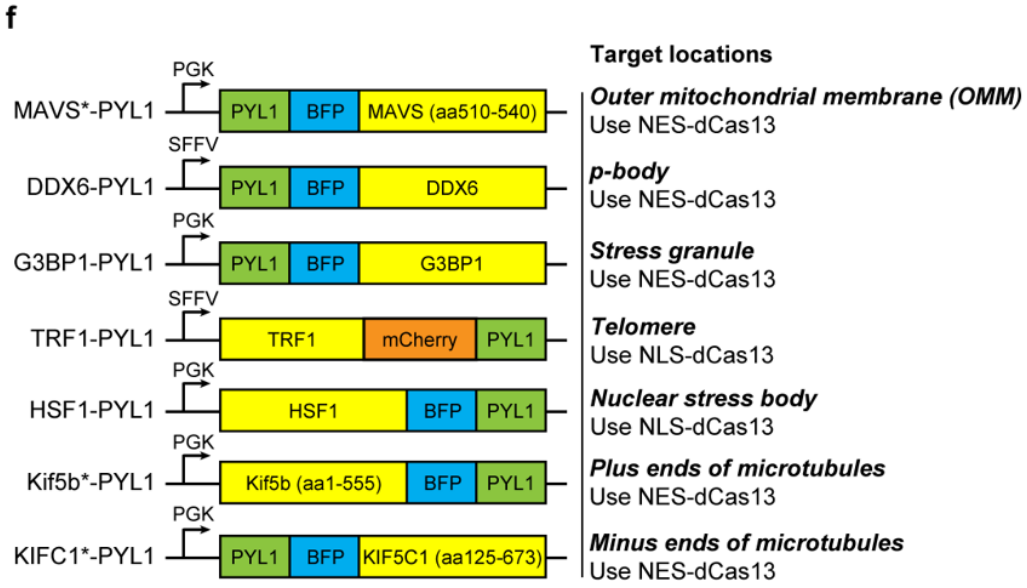

Extended Data Figure 1 | f, Schematic of plasmids expressing different PYL1-fusion proteins for localizing mRNA to various subcellular compartments. The use of NES-dCas13 or NLS-dCas13 was indicated under each target compartment.

2. As mentioned above, it appears not to be documented how stress was induced in the cell lines given SGs don't always appear under basal conditions and can be different in different cell lines? Same for cytosolic SGs vs nuclear stress bodies?

Response:

This information was previously included in **Supplementary Table 3**, but we agree with the reviewer that it should be more readily accessible. Accordingly, we have revised the Methods section:
Lines 630-632:
"To induce the formation of stress granules, HeLa cells were treated with 50 μM $NaAsO_2$ for 6 hours. To induce the formation of nuclear stress bodies, HeLa cells were treated with 100 μM $NaAsO_2$ for 6 hours."

3. Figure 1g / ED Fig. 4e, have you considered trying to further increase the expression of Cas13 etc. (or gRNA?) to overcome this barrier with respect to OMM enrichment for lowly expressed mRNAs? Would be interesting to seeing if increasing the transfection amounts / ratios of Cas13:gRNA of each would help.

Response:
In response, we performed new experiments to test if changing the transfection amounts and ratios of the dCas13 and gRNA plasmids could increase RNA localization efficiency on the OMM. We chose the reporter mRNA with 2xGCN4 repeats as our target (**Fig. 1g, Extended Data Fig. 3f**). Under our original conditions, cells were transfected with 0.125 μg dCas13 plasmid, 0.125 μg PYL1-MAVS* plasmid, 0.1 μg reporter mRNA plasmid, and 0.15 μg gRNA plasmid. We varied the amounts of transfected dCas13 plasmid (using 0.05, 0.125, 0.25, and 0.5 μg) while maintaining the other components constant, and measured the RNA localization efficiency. Surprisingly, we found that increasing the expression level of dCas13 decreased RNA localization efficiency (**Supplementary Fig. 8a**). This decrease is likely due to competition between mRNA-bound dCas13 and excessive unbound dCas13 for binding to the PYL1 fusion on the OMM.

In a separate experiment, we varied the transfected gRNA plasmid amount (0.05, 0.1, 0.15, 0.25, and 0.5 μg), and measured the RNA localization efficiency to the OMM. We found that increasing gRNA levels moderately improved mRNA localization but did not affect dCas13 localized on the OMM (**Supplementary Fig. 8b**), suggesting gRNA is a limiting factor. Although we didn't observe a clear trend of how dCas13:gRNA transfection ratios influence RNA localization efficiency, we identified conditions that enhanced RNA localization efficiency compared to our original transfection condition. As the reviewer suggested, these results confirm that fine-tuning transfection conditions can indeed increase RNA localization efficiency, which can be helpful for lowly expressed mRNAs.

We have included this part in the **Supplementary Notes**.

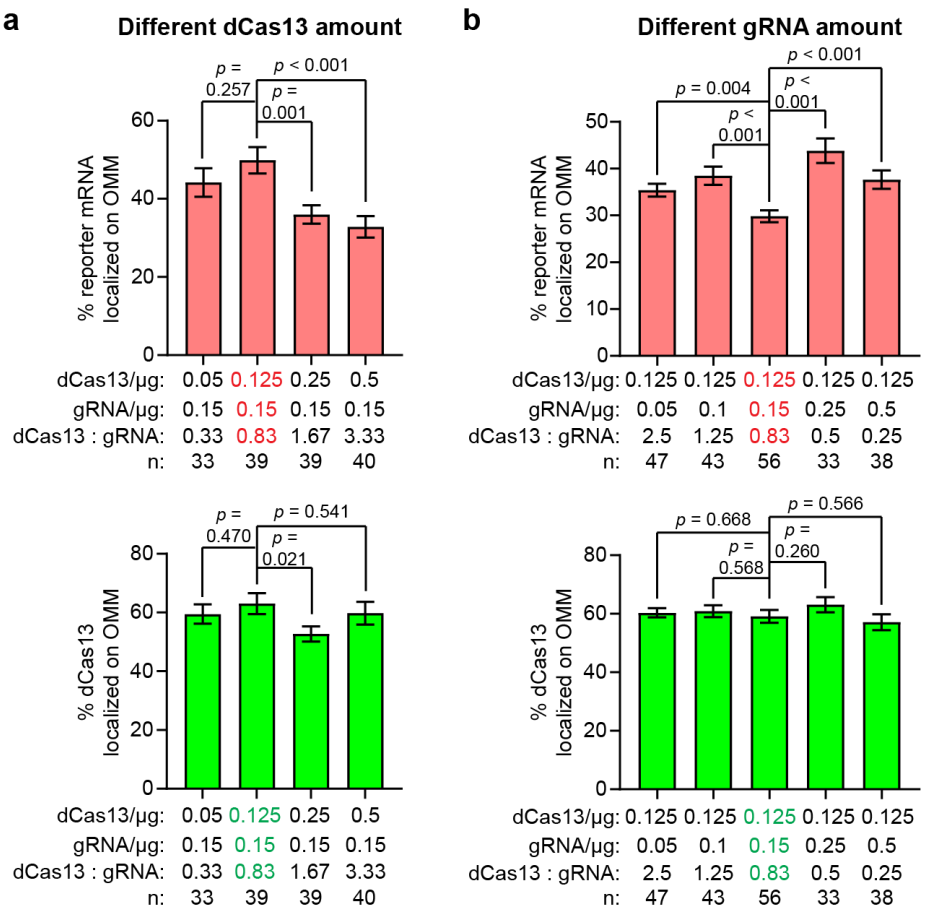

Supplementary Figure 8 | Quantification of the effect of transfection amounts/ratios of dCas13:gRNA plasmids on RNA localization efficiency. a-b, Quantification of % reporter mRNA (red bars) and % dCas13 (green bars) localized on the OMM in single cells with different transfection amounts of dCas13 plasmid (**a**) or gRNA plasmid (**b**). Only cells co-expressing dCas13 and MAVS*-PYL1 were analyzed. n indicates the number of quantified cells for each group. Data was presented as means ± SEM. Unpaired t-test.

4. ED Fig. 4l gRNA score is introduced without any explanation in the figure legend or main text? It would make it clearer to the reader to introduce what is meant by a gRNA score here? Which algorithm is it derived from etc.?

Response:

To clarify, the gRNA score (described in **Supplementary Table 5**) is a numerical rating from 0 to 4 that reflects the efficiency of target mRNA relocalization using CRISPR - TO. In our experiments, various gRNA combinations were tested in Neuro - 2a cells to recruit *Actb* or *Gap43* mRNA to the OMM. Each set of gRNAs were then scored based on the observed relocalization efficiency: 0 (not working), 1 (probably working), 2 (working), 3 (working well), and 4 (working very well). These scores were assigned based on the observed RNA relocalization efficiency and were derived arbitrarily to provide a semi-quantitative metric for training our model on gRNA design. Without

using numeric scores, it will be hard to train the model on gRNA performance. We have now revised the figure legend for **ED Fig. 4l-n** to include this explanation:
"**Extended Data Figure 4** | **l-n**, The distribution of read coverage over gRNAs (**l**), off-target genome hits (**m**), and Minimum Free Energy (MFE, **n**) for gRNAs with different scores (**Supplementary Table 5**). Each set of gRNAs targeting *Actb* or *Gap43* mRNA were arbitrarily scored from 0 to 4 based on the observed efficiency of the target mRNA relocalized to the OMM via CRISPR-TO in Neuro-2a cells: 0 (not working), 1 (probably working), 2 (working), 3 (working well), and 4 (working very well). Unpaired t-test."

5. Likewise, it's not super clear what the Polarization Index and Dispersion index is? One sentence to describe how these metrics work/are generated would be useful to the reader.

Response:
The Polarization Index quantifies the extent to which RNA molecules are concentrated in a specific region of the cell (for example, near the membrane or a targeted subcellular compartment), while the Dispersion Index measures how uniformly or clustered the RNA is distributed within the cell. We have revised the text to describe this more clearly:
Line 170-173:
"RNA distribution was quantified using the Polarization Index, which measures the degree of asymmetry or directional bias in mRNA distribution, and the Dispersion Index, which indicates how clustered or dispersed the mRNA molecules are within the cell[10] (**Supplementary Methods**). "

6. Line 373.. the authors mention that 21 mRNAs were selected but didn't provide a rationale for why these mRNAs were included? Previous evidence in the literature? Known +ve and -ve mRNA controls (i.e. b-actin vs. an RNA that is normally nuclear retained?). It would be great to see these controls?

Response:
In our primary neuron CRISPR-TO screen (**Fig. 6a**), we selected 21 mRNAs based on literature search for potential involvement of their protein function in neurite outgrowth and regeneration in human or mouse neurons (protein function details in **Supplementary Table 7**). However, the functional influence of their mRNA localization of these genes inside neurites has been understudied. This screen incorporated three negative controls (three different non-targeting gRNAs). Given this is one of the first screens of perturbing endogenous mRNA localization in primary neuronal outgrowth, we didn't have suitable positive controls. The detailed information for each selected mRNA, along with supporting references, is provided in **Supplementary Table 7**.

7. What proportion of the 21 mRNAs did you expect to affect neurite outgrowth given the selection procedure? Why was it interesting that 4 were determined to be hits? Was that expected, surprising? More information in the main text here to explain the experimental design/interpretation would be helpful for the reader. Could it be explained by gRNA choice? How were they selected. Could they somehow be checked make sure they're binding your target of interest? The Cas13design algorithm was based on training data from an RfXCas13d RNA

cleavage screen and not a PspCas13b binding screen. Could one argue that one reason for the low hit rate here is due to gRNA design limitations? Is this a major limitation to effectively implementing this in the field?

Response:
In our study, we selected 21 mRNAs based on literature implicating their protein function is related to neurite outgrowth (**Supplementary Table 7**). However, the functional influence of their mRNA localization inside neurites has been understudied. Considering the possible role of local translation of mRNA at neurite tips, we therefore expected that a subset would have a measurable functional impact when perturbed in our system. The fact that 4 out of 21 (~19%) were identified as hits was both encouraging and informative, which validates our hypothesis that localized RNA regulation can influence neurite outgrowth, while also underscoring that not all candidates have a functional contribution or sensitivity to perturbation to affect this complex process.

Regarding gRNA design, we acknowledge that our current algorithm was developed using training data from an RfxCas13d RNA cleavage screen[11] rather than dPspCas13b binding data, which may contribute to a lower hit rate due to design limitations. To our knowledge, while a comprehensive library screening dataset exists for RfxCas13d[11], a similarly large complete dataset for PspCas13b was not available. Since our experiment was performed in brain-derived mouse cortical neurons which are challenging cells to culture, we didn't perform prior gRNA validation before the screening. While these design constraints might partly explain the modest hit rate (4 out of 21), we do not view them as a fundamental limitation of the CRISPR-TO approach. Rather, they highlight an area for further optimization that could enhance targeting specificity and efficiency in future applications. For example, with accumulating gRNA datasets, it will be feasible to design a predictive algorithm specifically for dPspCas13b, which can further improve overall gRNA performance in CRISPR-TO applications. To address this comment, we have revised the text in the Discussion:
Line 445-450:
"The mRNA candidates were selected because their protein function is related to neurite outgrowth or regeneration, yet the functional influence of their mRNA localization has been understudied (**Supplementary Table 7**). Considering the possible role of local mRNA translation at neurite tips, we expected that a subset of these mRNAs would have measurable effects on neurite outgrowth upon perturbation via CRISPR-TO."

And in the Discussion (Line 522-524):
"As more gRNA data accumulates, it will be possible to develop a computational algorithm to optimize gRNA efficiency and specificity for CRISPR-TO, further increasing hit rates in large-scale screens."

8. What are the natural Cues for Stmn2 localization and neurite outgrowth, given it's in the soma under basal conditions? Any guesses it might be good to include some evidence (from the literature) as to how it is normally regulated? And why it's not in the neurites already in this neuronal culture (it may help the reader further understand the process).

Response:

Under basal conditions, *Stmn2* (also known as *SCG10* or superior cervical ganglion-10) mRNA is found in both soma and neurites[12,13], which is consistent with our observations that *Stmn2* mRNA is distributed inside somas and proximal neurites (**Reviewer Figure 3, Fig. 6d**). The Stmn2 protein is known to play a key role in microtubule destabilization and dynamics, which balances between microtubule polymerization (growth) and depolymerization (shrinkage) that is important for neurite growth[14-16]. Thus, we expect that artificially recruiting *Stmn2* mRNA to neurite tips using CRISPR - TO could potentially enhance neurite outgrowth by increasing local Stmn2 protein synthesis, thereby supporting the cytoskeletal dynamics necessary for neurite extension and outgrowth.

We have revised the manuscript to include this additional information on Stmn2:
Line 467-472:
"One hit mRNA, *Stmn2*, encodes Stathmin-2, a tubulin-binding protein involved in microtubule dynamics[14], axonal regeneration[15,16], and ALS pathology as a promising therapeutic target[17]. *Stmn2* mRNA has been identified in axons and growth cones via microarrays[12,13], but the functional relevance of its mRNA localization was unclear. It is possible that localized *Stmn2* mRNA at neurite tips can exhibit local translation to facilitate stabilizing microtubules and promoting axonal regeneration[18]."

Stmn2 mRNA in primary mouse cortical enruons

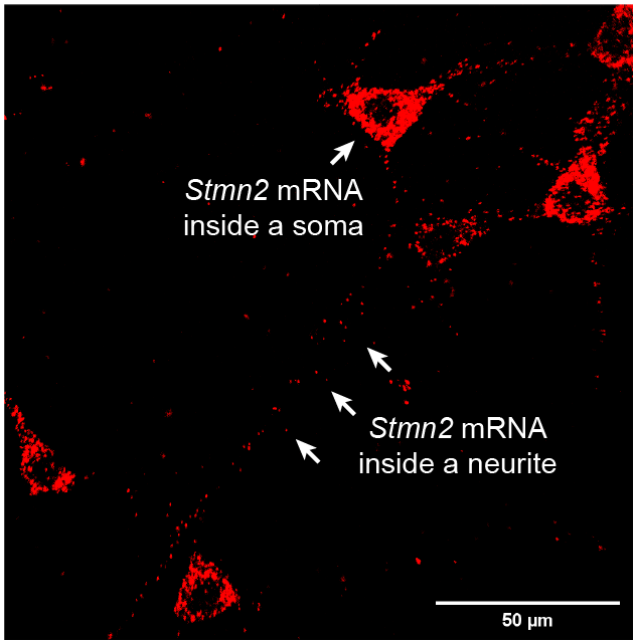

Reviewer Figure 3 | RNA FISH staining of *Stmn2* mRNA in primary mouse cortical neurons showing *Stmn2* mRNA localizing inside both somas and neurites.

9. As far as I can tell there is no mention of your flow cytometry gating strategy etc. or any plots shown to highlight gating.

Response:

We have now included gating strategies for all flow cytometry of this manuscript in **Supplementary Fig. 1**.

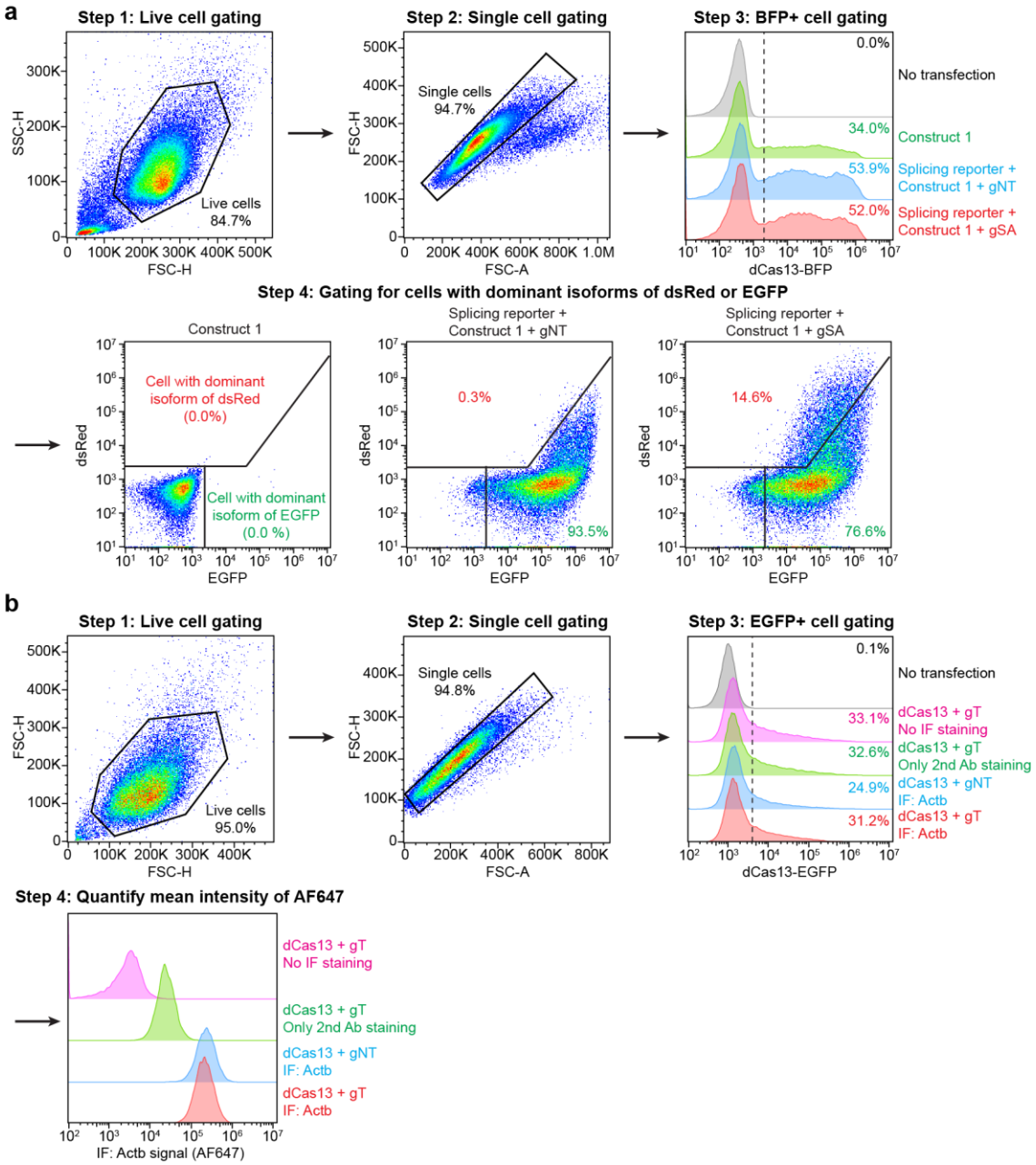

Supplementary Figure 1 | Representative gating strategies for all flow cytometry analyses in this manuscript. a, Representative gating strategies for **Extended Data Fig. 1b-c**. Step 1: live cells were gated from all cell populations. Step 2: single cells were gated from live cells. Step 3: cells expressing BFP (i.e., BFP+ cells) were gated from single cells based on cells without transfection (BFP- cells). Step 4: transfected cells (BFP+) were first gated to select cells expressing splicing reporter based on background EGFP and dsRed signals of cells only transfected with Construct 1. Then cells were further gated to calculate the percentage of cells with dominant isoform of EGFP or dsRed based on the gNT group where cells mainly expressed

the EGFP isoform. Ratio of cells with dominant isoforms of dsRed to EGFP was calculated as % cells with dominant isoform of dsRed divided by % cells with dominant isoform of EGFP to make the column plots in **Extended Data Fig. 1b-c**. **b**, Representative gating strategies for **Extended Data Fig. 4t-u**. Step 1: live cells were gated from all cell populations. Step 2: single cells were gated from live cells. Step 3: cells expressing EGFP (i.e., EGFP+ cells) were gated from single cells based on background EGFP level of cells without transfection. Step 4: the mean fluorescence intensity of Actb protein immunofluorescence (IF) staining signals were quantified for EGFP+ cells to make the column plots in **Extended Data Fig. 4t-u**. Two control groups (no IF staining and only secondary antibody staining) were included here to show the specificity of IF: Actb staining.

10. Perhaps I missed it, as far as I can tell, Supplementary Fig. 3 is not referred to anywhere in the text (main text, supplementary or methods etc.) and it is not super clear that this figure is demonstrating or clear that the caption completely matches what is shown in the figure.

Response:
Since **Supplementary Fig. 3** was not referenced in the manuscript and it was not essential to our conclusions, we have removed it from the revised manuscript.

11. Supplementary data file, typo: Persons should read Pearson's

Response:
We thank the reviewer for pointing out this mistake. Since we replaced the original **Extended Data Fig. 6e** with another figure (**Extended Data Fig. 6i**) using a better and more unified quantification strategy, this mistake has been corrected.

Referee #2 (Remarks to the Author):

Han et al., present a well written and comprehensive study describing CRISPR-TO, a novel implementation of RNA-guided CRISPR-Cas13 to perturb RNA localization. The authors describe the design of the system and present key data supporting to support its composition and application. The authors comprehensively describe considerations for use of the technology including number of guides required per target, the effect of binding, and the expected guide RNA design issues (universal to Cas13 in cells). The authors describe the use of inducible CRISPR-TO to reversibly drive RNA around the cell. They then go on to describe its use in the study of dynamics in RNA localization including specific insights into RNA transport within human neuronal cells. Finally, the authors describe a specific use case in high throughput screens to study RNA localization. Overall, the study is comprehensive and presents a unique tool to accelerate the critical study of RNA dynamics in human cells. The methods are novel and the data robust to this reviewer. I have only a few minor comments.

We thank the reviewer for the feedback and encouraging words regarding our study.

Minor Comments:
The authors described testing a variety of RNA targeting systems including Cas13a, Cas13bt, Cas13d, and Cas7-11. Could the authors comment on why each Cas13 system behaves so different in the same setting in Figure 1e? Did the authors see anything in the imaging that might suggest why they performed poorly relative to PspCas13b? I noted that representative images are absent from the Supplementary Figures. It is the opinion of this reviewer that they should be included, mostly because numerous labs will likely want to implement this technology and build on what is clearly a solid foundation. But making those images available to the community would be a valuable resource and prevent wasted effort on the part of researchers trying to minimize the delivery payload.

Response:
We acknowledge the reviewer's thoughtful questions. We observed that different Cas13 effectors or Cas7-11 perform differently in the same experimental setting (**Fig. 1e**), and we have considered several possible explanations.

Firstly, we used the same spacer sequence to design gRNAs for all Cas systems. While this spacer sequence works well for PspCas13b, it may not be optimal for the other Cas systems. This is not caused by the protospacer flanking site (PFS) requirements of each Cas effector because PFS is not required for RNA interference with PspCas13b[5,19], RfxCas13d[20], LwaCas13a[21], Cas13bt1[22], and DiCas7-11[23] in mammalian cells. However, differences in protein size, structure, and the orientation of the spacer in the gRNA (i.e., 5' or 3'), may influence binding efficiency of different dCas effectors at the same target. For example, DiCas7-11 (1,601 aa) is substantially larger than PspCas13b (1,089 aa) and uses a different orientation of the spacer in its gRNA (**Fig. 1d**). It is possible that the target region that works optimally for dPspCas13b may not provide enough space for dDiCas7-11 binding.

Secondly, efficient RNA relocalization via CRISPR-TO requires high binding affinity of dCas to the target RNA. Reported dissociation constant (K_d) varies among effectors. For example, dLwaCas13a has a reported K_d of ~46 nM[24], dDiCas7-11 K_d ~ 161 nM[23], and dBzCas13b K_d ~ 33 nM[25]. While the exact K_d for dPspCas13b is not known, live-cell RNA imaging using different dCas13 proteins (e.g., dCas13a, dCas13b, dCas13d) consistently showed that dPspCas13b exhibited the better RNA labeling efficiency[7]. This suggests that PspCas13b likely has a very strong binding affinity among Cas13 effectors, thereby facilitating efficient RNA localization.

Finally, the ABA-induced ABI/PYL1 heterodimerization system used to recruit dCas protein may influence the binding function differently across effectors. For each dCas, optimizing the linker between ABI and dCas, considering different N or C-terminal fusions, and exploring alternative heterodimerization systems might be necessary.

To further characterize the difference among different dCas effectors, we performed additional experiments. We measured the transfection efficiency, expression levels, and cell toxicity of each dCas effector in HeLa cells. We found that dPspCas13b exhibits higher transfection efficiency and expression levels compared with other dCas effectors, whereas dLwaCas13a, dCas13bt1, and dDiCas7-11 show lower expression (**Supplementary Fig. 9a-b**). Additionally, dLwaCas13a shows increased cell toxicity (**Supplementary Fig. 9c**). These results suggest that dLwaCas13a, dCas13bt1, and dDiCas7-11 would require further optimization for CRISPR-TO applications.

We have included this part of discussion in **Supplementary Note**.

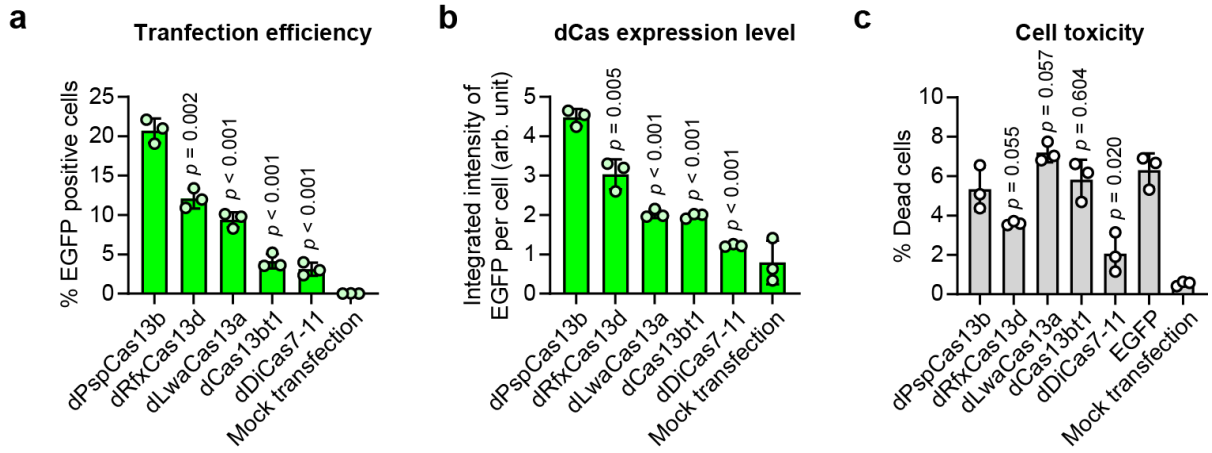

Supplementary Fig. 9 | Quantification of transfection efficiency, expression level, and cell toxicity of each dCas effector in HeLa cells. a-b, HeLa cells were transfected with different NES-dCas effector plasmids for two days and imaged using an IXM microscope to measure the transfection efficiency (**a**) and dCas expression level (**b**) (**Supplementary Methods**). **c**, HeLa were transfected with different NES-dCas effector plasmids for two days and stained with SYTOX Red Dead Cell Stain to measure % dead cells using an IXM microscope (**Supplementary Methods**). EGFP is the control group where cells were transfected with the NES-EGFP plasmid. Data is presented as means ± standard deviation. Each dot represents one biological replicate. n = 3 wells per group. Unpaired t-test.

Following the reviewer's suggestion, we have added representative images in **Supplementary Fig. 4b** for each dCas effectors shown in **Fig. 1e**. Consistent with the quantitative data, these images did not reveal obvious RNA localization that might explain the poorer performance of these dCas effectors relative to dPspCas13b.

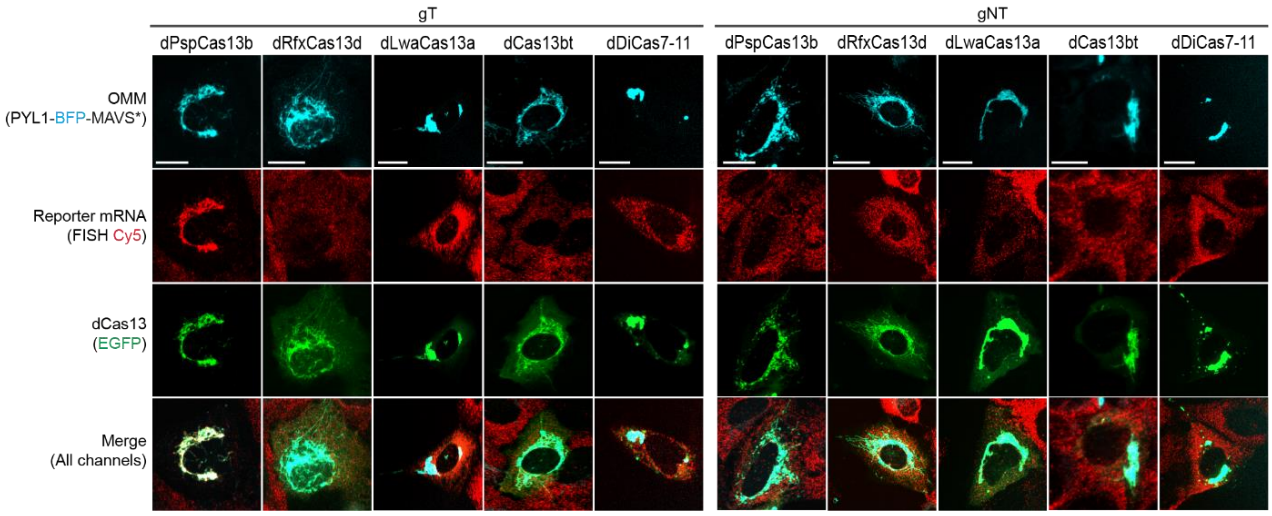

Supplementary Figure 4 | b, Representative microscopic images related to **Fig. 1e**. HeLa cells were transfected with CRISPR-TO components containing different dCas systems to recruit endogenous GAPDH mRNA to the OMM. Scale bar, 20 μm.

On the issue of delivery (which the authors highlight as a limitation in their discussion) it seems misleading to suggest researchers could use smaller systems when the smaller systems tested have been unsuccessful. I think this could be elaborated on to make it clear that there is no 'one size fits all' Cas13 protein.

Response:

We agree that the statement in the discussion could be clarified to better reflect the current limitations of the CRISPR-TO system. To address this, we have revised the relevant section in the **Discussion** to emphasize that there is no one-size-fits-all dCas13 protein and highlight the need for context-specific optimization. We believe these clarifications will provide a more accurate discussion of the current limitations and future directions associated with Cas13 delivery and CRISPR-TO:

Line 518-522:

"A current limitation of CRISPR-TO is the requirement for multiple components, making in vivo applications challenging due to delivery efficiency issues. Future improvements could address this issue by combining all components into a single vector and using more compact dCas13 variants. Since there is no one-size-fits-all dCas13 protein, further optimization of the RNA-targeting CRISPR-Cas systems are needed for context-specific applications of CRISPR-TO."

The large aggregates of Cas13b within the nucleus when it is NLS tagged are intriguing. Are these nucleoli or just aggregates of Cas13b as the authors suggest? It is clearly a Cas13b dependent

phenomenon which then takes me back to the other enzymes – do they show the same phenotype? For researchers wanting to study or perturb RNA within the nucleus this could be problematic.

Response:

To test if the aggregates of dPspCas13b within the nucleus are in nucleoli or not, we stained HeLa cells expressing NLS-dPspCas13b (without gRNA) with the antibody of Fibrillarin, an established marker for the nucleolus[26]. We found that the aggregates of NSL-dPspCas13b colocalize with Fibrillarin, confirming that NLS-dPspCas13b accumulates in the nucleoli (**Supplementary Fig. 6a**). We further tested the other four CRISPR-Cas systems including dRfxCas13d, dLwaCas13a, dCas13bt1, and dDiCas7-11 and found that all four NLS-dCas proteins also aggregate inside nucleoli (**Supplementary Fig. 6a**). This finding is consistent with previous reports for NLS-SpyCas9, which was also found to aggregate in nucleoli[27].

Importantly, this phenomenon depends on the presence of gRNA and its cognate target. In the presence of non-targeting gRNA (gNT), we observed dPspCas13b, dRfxCas13d, and dLwaCas13a still aggregate inside the nucleoli, while dCas13bt1 distributes evenly in the nucleus and dDiCas7-11 depletes from the nucleoli (**Supplementary Fig. 6a**). However, in the presence of both targeting gRNA and RNA target, we observed significantly fewer nucleoli aggregates of NLS-dCas13b with more even distribution inside the nucleus (**Supplementary Fig. 6b**). This suggests that, while 'unused' dCas13b effectors accumulate in the nucleoli, its binding to gRNA and the target RNA greatly reduces this nucleoli aggregation. This is consistent with the behavior of dCas9 which also shows fewer aggregation inside nucleoli in the presence of targeting gRNA and the target loci[28]. We have revised the manuscript to mention this phenomenon:

Line 231-234:

"One interesting observation is that NLS-dCas13 aggregates in the nucleoli without a targeting gRNA (or with a non-targeting gRNA), while the presence of both a targeting gRNA and RNA target significantly reduces this aggregation, resulting in a more even nuclear distribution (**Supplementary Fig. 6a-b**)."

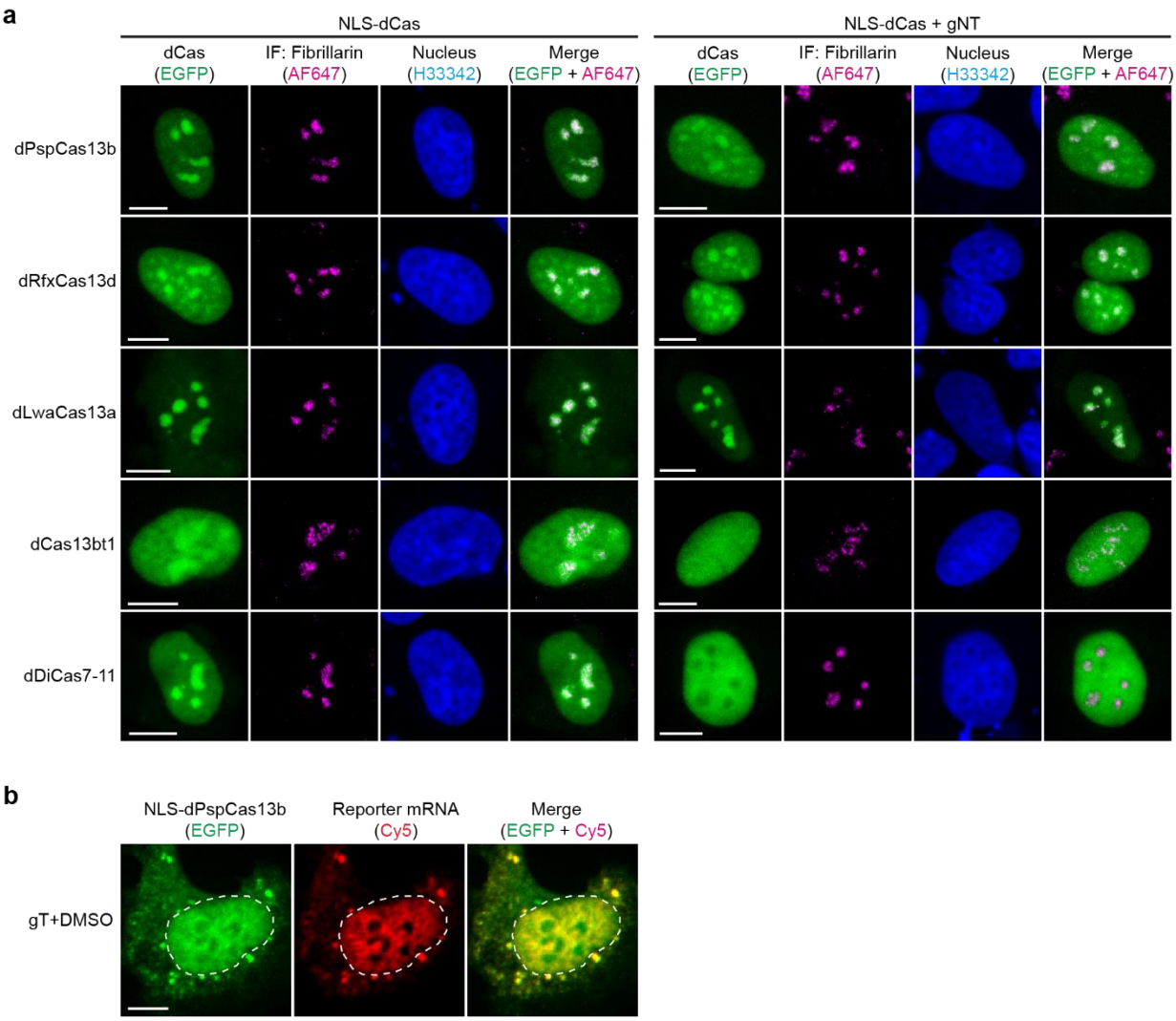

Supplementary Figure 6 | Representative microscopic images showing NLS-dCas protein aggregates in nucleoli. a, HeLa cells expressing different NLS-dCas proteins with gNT or without gRNA were stained with the antibody of Fibrillarin to image the nucleolus. Scale bar, 10 μm. **b**, HeLa cells expressing NLS-dPspCas13b, reporter mRNA, and gRNA targeting the reporter mRNA did not have aggregation of NLS-dPspCas13b in nucleoli. Some NLS-dPspCas13b signals are outside of the nucleus because they bind to the target reporter mRNAs that exist in the cytoplasm.

The authors make no mention of the applicability of this tool in bacterial, archaeal, or plant cells. It would be prudent to indicate if CRISPR-TO could be adapted for use in these organisms.

Response:

In the current study, we focused on demonstrating the utility of CRISPR-TO in mammalian cells with a particular focus on neurons. However, we agree that the underlying principles could potentially be adapted for use in other organisms. Notably, CRISPR-Cas13 systems have been

successfully used in bacterial and plant cells[21], leading us to believe that CRISPR-TO can be customized for use in these cells (e.g., using appropriate promoters, expression systems, and subcellular compartment-specific signals). To our knowledge, there are no reported applications of CRISPR-Cas13 in archaea, suggesting applying CRISPR-TO in archaea would need more careful optimization and validation. We have added several sentences in the Discussion to highlight the potential of applying CRISPR-TO in other organisms:

Line 524-527:

“While our study focused on mammalian cells, the underlying design of CRISPR-TO could be adapted for use in other organisms. Given that CRISPR-Cas13 systems have been employed in bacterial and plant cells[21], we anticipate that CRISPR-TO may also be applicable in these systems.”

Referee #3 (Remarks to the Author):

In this publication Han et al fuse PspCas13b with an inducible dimerization domain driven by the plant hormone ABA. By fusing the second part of the dimerization domain to different localising proteins, Han et al recruit an mRNA of interest to a subcellular compartment, such as the mitochondrial outer membrane or the tips of developing neurites. Using the axon targeting system, they conduct functional screens of 21 mRNAs to identify new RNAs with functional roles in local translation. They identify Stmn2 as an mRNA whose localization influences neurite outgrowth.

Major Comments:

1. PspCas13b and LwaCas13a have been shown to be more neurotoxic than RfxCas13d (Wu and Kapfhammer, 2021), which has been applied in neurons in vitro and in vivo (Zeballos et al., 2023; Powell et al., 2022, Morelli 2021, Zhou 2020) and has been shown to not impair neuronal viability or increase inflammatory markers in mouse neurons (Zeballos C. et al., 2023). For the method developed here, at least in primary culture, the authors should examine whether PspCas13b and the other components of the system expressed in neurons induces stress, impairs viability or increases inflammation. The same goes for the exposure to ABA at the used concentrations for the indicated timeframes.

Response:

We thank the reviewer for this important concern regarding the potential neurotoxicity of CRISPR-TO components and ABA treatment in primary neuron cultures. We appreciate the references provided by the reviewer and agree that assessing the potential neurotoxicity is critical, especially given the reported less neurotoxicity of RfxCas13d than PspCas13b. In response, we have performed additional experiments to evaluate the influence of CRISPR-TO components and ABA treatment on neuronal viability, inflammation, and ER stress for in vitro cultured primary mouse cortical neurons.

For cell viability, we designed two groups. In group 1, primary mouse cortical neurons were treated with 250 μM ABA or DMSO for 24 hours, with untreated neurons as controls. In group 2, primary mouse cortical neurons were transfected with plasmids expressing CRISPR-TO components (dCas13, Kif5a*-PYL1, and gT or gNT) and mScarlet3-CAAX (for imaging the neurite morphology) for two days, with the control transfected only with mScarlet3-CAAX. To measure cell viability, we stained neurons with SYTOX Red Dead Cell Stain. We found that there is no significant difference in viability between ABA- or CRISPR-TO-treated neurons and controls (**Extended Data Figure 8a**).

For neuroinflammation, the paper (Zeballos C. et al., 2023) provided by the reviewer examined neuroinflammation by measuring the number of GFAP+ and IBA1+ cells in the brain slice[29]. GFAP is a biomarker for astrocytes and its expression level increases when the brain experiences inflammation. Similarly, IBA1 is a biomarker for microglial cells and its expression level also increases when there is inflammatory response in the brain[30]. Unlike the brain, the in vitro mouse cortical neuron culture system used in our project has very few astrocytes (~2%) and microglial

cells (~0.5%) because our protocol was optimized to deplete glial cells with FUDR (Fluorodeoxyuridine) to avoid their influence on imaging (**Extended Data Figure 8c-d**). Depletion of glial cells intrinsically inhibits neuroinflammation in our culture system because neuroinflammation is regulated mainly by glial cells including astrocytes and microglial cells[31]. Therefore, examining neuroinflammation by measuring the number of glial cells in our culture system may not be a meaningful evaluation of inflammatory responses.

To examine ER stress, we stained neurons with an antibody targeting ATF4, a key marker of ER stress[32]. When cells experience ER stress, ATF4 expression significantly increases and translocates into the nucleus[32]. We quantified the ratio of ATF4 fluorescent intensity between the nucleus and cytoplasm (ATF4 nuc/cyto average fluorescence ratio) to examine ER stress. Our results showed no significant differences in the ATF4 nuc/cyto ratio between ABA-treated and control neurons, nor between neurons expressing dCas13 and those without dCas13 expression (**Extended Data Figure 8b**).

We have revised the manuscript to discuss about the potential neurotoxicity of CRISPR-TO components and ABA treatment in primary neuron cultures:
Line 307-311:
“We first tested the potential neurotoxicity of CRISPR-TO components and ABA treatment in primary mouse neuron cultures and found no significant impact on neuron viability and ER stress (**Extended Data Fig. 8a-b**). Furthermore, the inherent depletion of glial cells in our in vitro system minimizes neuroinflammation responses[31] (**Extended Data Fig. 8c-d**). Therefore, the CRISPR-TO system does not have significant neurotoxicity in our system.”

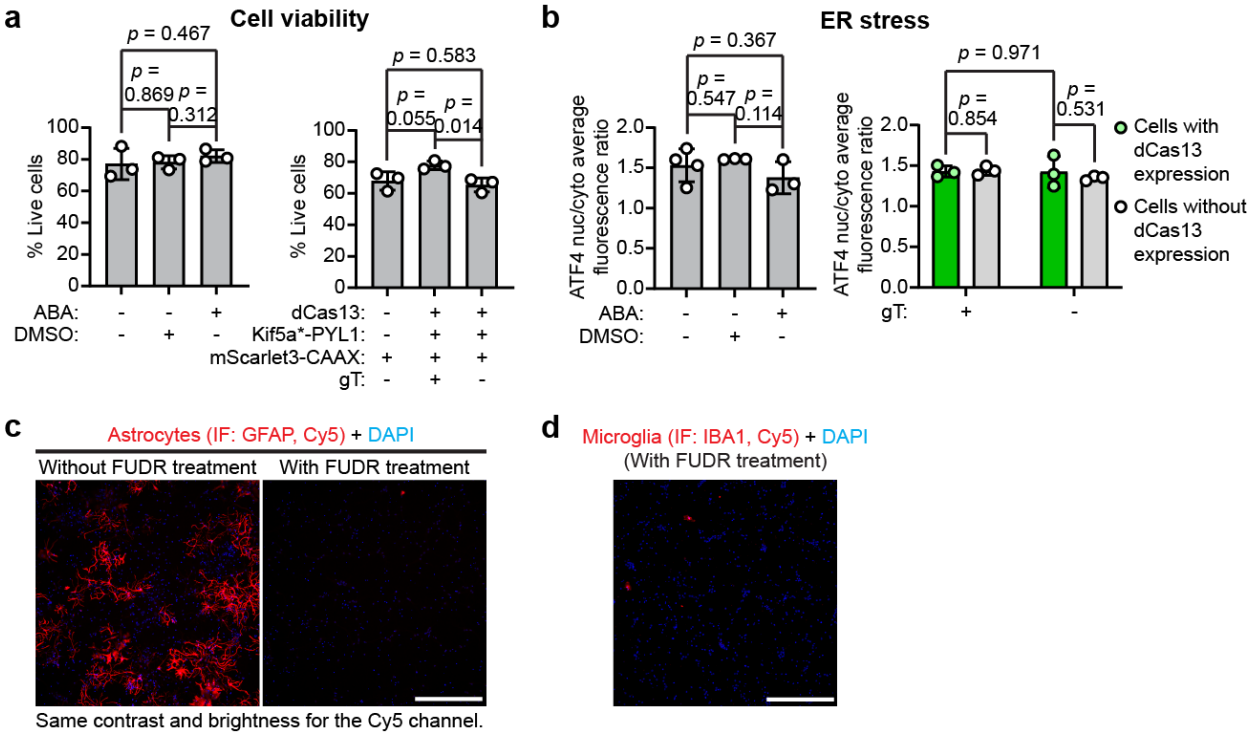

Extended Data Figure 8 | a, Quantification of cell viability for neurons under different treatments. **b**, Quantification of the ratio of ATF4 average fluorescent intensity between the nucleus and

cytoplasm for neurons under different treatments to examine ER stress[32]. In the right diagram, neurons were transfected with CRISPR-TO components with dCas13, Kif5a*-PYL1, different gRNA conditions, and mScarlet3-CAAX. Cell populations with and without dCas13 expression were analyzed. Data was presented as means ± standard deviation. Each dot represents one biological replicate. n = 3 or 4 wells per group. Unpaired t-test. **c**, Representative microscopic images showing the dramatic decrease of astrocytes after fluorodeoxyuridine (FUDR) treatment in the in vitro mouse cortical neuron culture system. Scale bar, 400 μm. **d**, Representative microscopic images showing very few microglial cells in the in vitro mouse cortical neuron culture system after FUDR treatment. Scale bar, 400 μm.

2. In figure 2, it appears in some cases, that the target mRNA is present at lower levels when it is targetted? have the total levels been measured and has the mRNA half-life in the different conditions been measured?

Response:
We have systematically measured total mRNA levels comparing targeting and non-targeting gRNAs using dCas13b. Across six endogenous mRNAs (human *GAPDH*, human *ACTB*, human *NDUFS2*, human *SDHC*, human *SDHC*, and mouse *Actb*), we found that the total mRNA levels remain similar with and without targeting gRNA (**Extended Data Fig. 4**, **Fig. 1j**). This suggests that dCas13b-targeting itself (with properly chosen gRNA) doesn't change mRNA abundance. In the CRISPR-TO case, we expect the influence on total mRNA abundance may exhibit a similar trend if recruiting that mRNA to the subcellular compartment that doesn't cause mRNA degradation or half-life change. We note that there are some visual differences in target mRNA abundance in **Fig. 2** due to different contrasts used among images to better show localization. For example, if we were to use the same contrast (e.g., **Fig. 2b**) across images, when we keep the aggregated signal clear in the ABA group, the diffused signal in the DMSO group will be largely invisible.

3. The presence of dCas13 + guide has been shown to reduce translation by sterically blocking the ribosome (Apostolopoulos et al nature comm 2024), the authors consider this by targeting the 3'UTR instead of the CDS and show that binding there does not influence the abundance or stability of transcripts (Ext. Fig 5). Nevertheless, some reports in neurons have observed a reduction in target mRNA levels by expressing only the guideRNA (Powell et al Science Advances 2022). Once dCas13 is localised, especially in neurons, unbound guideRNA could accumulate in the soma, if they are indeed recognized by Dicer and lead to a reduction of target mRNA in the soma this could influence any functional readout. To examine this, the authors should analyse target mRNA levels in the soma of neurons they have analyzed. This is important to convince the readers that any observed effects truly arise from the localization of the guide.

Response:
The reference (Powell et al Science Advances 2022)[33] provided by the reviewer highlights the need for careful examination of the influence of unbound gRNA on the target mRNA level. To address this concern, we performed experiments to measure the target *Actb* mRNA level in the soma of neurons under different treatments.

We first compared neurons transfected with gRNA targeting *Actb* mRNA (gT) or gNT and found that only expressing gT indeed decreases the target mRNA level (17% decrease, **Extended Data Fig. 8i**), which is consistent with the reference[33] provided by the reviewer. We then compared neurons transfected with dCas13+gT or dCas13+gNT and found that the target mRNA level does not have significant difference (**Extended Data Fig. 8j**). This is consistent with what we observed in Neuro-2a cells where the *Actb* mRNA level was not influenced by expressing dCas13+gT compared with dCas13+gNT (**Extended Data Fig. 4c, 4i**). These two results suggest that, for our designed gRNAs, while the binding of naked gRNAs led to the degradation of the target mRNA, the binding of dCas13-gRNA ribonucleoprotein (RNP) complex does not lead to target mRNA degradation. As mentioned by the reviewer, naked gRNA binding on the mRNA might be recognized by Dicer and processed into miRNA to degrade the target mRNA. We hypothesized that dCas13 binding on the gRNA might block Dicer from recognizing the gRNA-mRNA duplex, thus reducing the degradation of the target mRNA.

We further examined whether *Actb* mRNA inside the soma was degraded after dCas13 was transported to neurite tips via CRISPR-TO manipulation in primary mouse cortical neurons. We transfected neurons with CRISPR-TO components (gT or gNT) and treated neurons with ABA or DMSO for 24 hours. Again, we didn't observe significant difference of *Actb* mRNA levels in the somas between gT+DMSO and gNT+DMSO groups (**Extended Data Fig. 8k**), further supporting the binding of dCas13-gRNA RNPs did not degrade the target RNA. In contrast, the gT+ABA group exhibited a 10% decrease in *Actb* mRNA levels in the soma compared to the gT+DMSO group, which we attribute primarily to the transport of a portion of Actb mRNAs into neurites rather than degradation (**Extended Data Fig. 8k-l**). Supporting this, we also observed a significant amount of dCas13 proteins remains in the soma after CRISPR-TO perturbation and ABA treatment (**Extended Data Fig. 8k-l)**. Therefore, we conclude that, while there is a modest reduction in target mRNA in the soma, it is primarily due to RNA transport, with minimal degradation caused by naked gRNA (**Extended Data Fig. 85-l)**.

We have revised the manuscript to talk about the potential influence of gRNA and dCas13 binding on mRNA stability in primary neurons under CRISPR-TO perturbation:
Line 342-351:
"Finally, we examined the effect of the CRISPR-TO system on *Actb* mRNA stability in neurons. Expressing the target gRNA alone reduced soma *Actb* mRNA levels (17% reduction, **Extended Data Fig. 8i**), consistent with previously reports[33]. In contrast, the dCas13-gRNA ribonucleoprotein complex did not lead to target mRNA degradation in the soma (**Extended Data Fig. 8j**), which aligns with our observations in other cell types (**Extended Data Fig. 4c, 4i**). After CRISPR-TO-mediated transport of dCas13 to neurite tips, only a modest reduction (10% decrease) in *Actb* mRNA was observed in somas, which we attribute primarily to mRNA transport rather than degradation (**Extended Data Fig. 8k**). These results support that degradation by naked gRNA is limited, likely because residual dCas13 proteins in the soma sequester the gRNA and protect the target mRNA (**Extended Data Fig. 8k-l**)."

We want to point out that there are some important regulatory elements inside 3'UTR and the binding of these elements by either naked gRNA or dCas13-gRNA RNP could potentially influence the target mRNA level. Therefore, we should be careful when designing gRNAs and try to avoid these important regulatory elements. We have revised the text in the **Discussion** to highlight this point:

Line 505-507:

"It is important to choose gRNA target sites in the 3'UTR that do not overlap with functional regulatory elements to avoid unintended effects on mRNA expression."

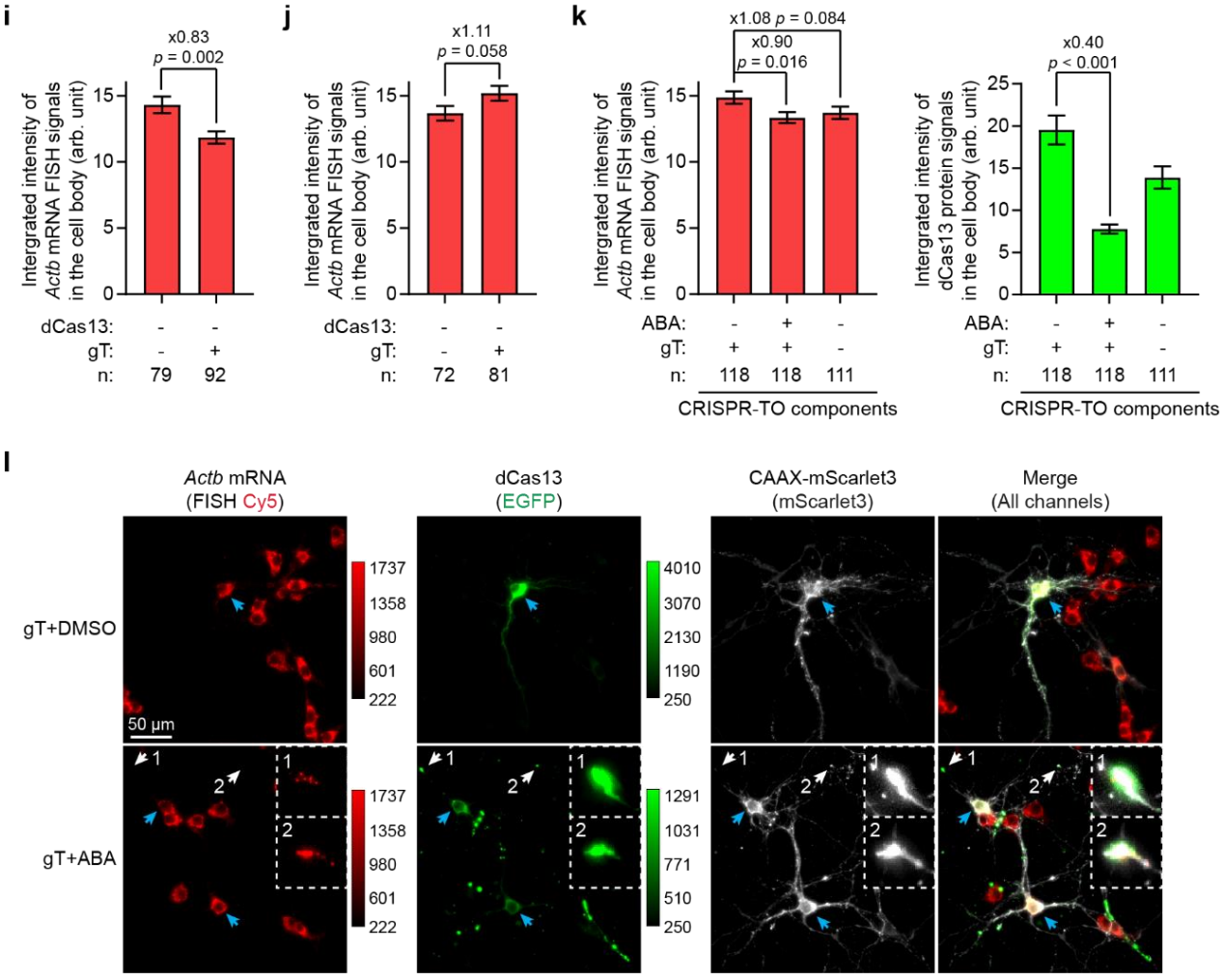

Extended Data Figure 8 | i-j, Quantification of the integrated fluorescence intensity of *Actb* mRNA FISH signals in the cell body of primary mouse cortical neurons expressing gT/gNT only (**i**) or dCas13+gT/gNT (**j**). **k**, Quantification of the integrated fluorescence intensity of *Actb* mRNA FISH signals and dCas13 protein signals in the cell body of primary mouse cortical neurons expressing CRISPR-TO components and treated with ABA or DMSO. Data presented as means ± SEM. Unpaired t-test. The number above each group is the fold change between two groups. **l**, Representative microscopic images showing similar *Actb* mRNA level inside somas (blue arrows) of neurons in gT+DMSO and gT+ABA group, and dCas13 proteins remaining inside somas after ABA treatment in the gT+ABA group. Scale bar, 50 μm. Calibration bar indicates the fluorescence

intensity of Actb mRNA FISH signals and dCas13 proteins. Inset images surrounded by the dotted line represent magnification of the region indicated by the white arrow, showing *Actb* mRNA enriched at neurite tips in the gT+ABA group via CRISPR-TO perturbation.

4. The authors did not show that the endogenous mRNA localised to the axon tip is actually translated there. In page 10 line 324-328 they write that mRNAs "...located to neurite tips by CRISPR-TO can be actively translated there". This has not been shown for endogenous transcripts. They further write that "mRNAs during transport may undergo translation" and that ribosomes are co-transported there with the mRNAs. These claims are not sufficiently backed by data.

Response:
We thank the reviewer for pointing out this limitation. We agree that our original manuscript did not directly demonstrate active translation of endogenous mRNA at neurite tips, nor did it provide sufficient evidence for ribosome co-transport and mRNA undergoing translation during transport. To address these concerns, we performed three-color super-resolution imaging using Stochastic Optical Reconstruction Microscopy (STORM)[34] to simultaneously visualize endogenous *Actb* mRNA, ribosome, and active translation site inside neurites and at neurite tips for the gT+ABA group after CRISPR-TO perturbation.

In these experiments, *Actb* mRNA was visualized via RNA FISH, ribosomes were visualized via RNA FISH staining of *Rn28s1* rRNA, and active translation sites were visualized using the ribopuromycylation method (RPM)[35]. RPM labels nascent peptides with puromycin and immobilizes the puromycylated nascent peptides on ribosomes by translation elongation inhibitor cycloheximide (CHX). By immunofluorescence staining of puromycylated nascent peptides using the anti-puromycin antibody, the active translation sites were *in situ* visualized inside neurites. We assume that under a high localization precision (~10 nm) using STORM[34], the detected colocalization of *Actb* mRNA with ribosome and active translation site could better support the actual binding of ribosomes with *Actb* mRNA particles and the active translation of *Actb* mRNA (**Fig. 5d**).

We first focused on imaging *Actb* mRNAs inside neurites in the gT+ABA group with CRISPR-TO perturbation. We have demonstrated that CRISPR-TO significantly increases the localization of *Actb* mRNA particles along the neurites, while the gT+DMSO group showed very few *Actb* mRNA particles along the neurites (**Fig. 4f**). Therefore, we assumed that most *Actb* mRNA particles detected inside neurites are transported via CRISPR-TO. Our super-resolution images, with localization precision between 7.9 nm to 22.1 nm for the three imaging channels (**Extended Data Figure 9g**), revealed clear colocalization of some *Actb* mRNA particles with both ribosome and puromycin signals within neurites, indicating active translation during transport (**Fig. 5e,** inset 1, more representative images are shown in **Extended Data Figure 9h-i**). As a control, some *Actb* mRNA particles did not colocalize with ribosomes or puromycin signals, confirming the specificity of multi-color labeling (**Fig. 5e**, inset 2). Notably, the number of puromycin-labeled active translation sites was lower than the number of *Actb* mRNA particles and ribosomes, suggesting that only a subset of transported mRNA particles undergo active translation. These results provide

additional evidence that ribosomes are co-transported with mRNA and that at least some mRNAs are actively translated during CRISPR-TO-mediated transport along neurites.

We next imaged *Actb* mRNA located at neurite tips in the gT+ABA group using STORM. From super-resolution images, we observed aggregated *Actb* mRNA clusters that colocalize with both ribosomes and active translation sites at neurite tips (**Figure 5g**), indicating active local translation of endogenous *Actb* mRNA at neurite tips. In contrast, we detected very few *Actb* mRNA particles inside neurite tips in the gNT+ABA group (**Extended Data Figure 9j**), which is consistent with our diffraction-limited microscopy data (**Fig. 4d-e**). The presence of very few *Actb* mRNA inside neurite tips at baseline condition largely precludes analysis of their local translation, highlighting the utility of CRISPR-TO for studying this question. This control group also suggests that most *Actb* mRNA molecules detected at neurite tips are transported via CRISPR-TO.

We have revised the manuscript to include these new data:
Line 378-390:
"To confirm ribosome co-transport and local translation of endogenous mRNA along neurites and at neurite tips, we performed three-color STORM super-resolution imaging[34] to visualize endogenous *Actb* mRNA, ribosomes, and active translation sites (via ribopuromycylation[35]) in the gT+ABA group (**Fig. 5d**, **Methods**). Our super-resolution images (localization precision 7.9-22.1 nm, **Extended Data Fig. 9g**) revealed colocalization of *Actb* mRNA with both ribosome and puromycin signals in neurites, indicating active translation during transport (**Fig. 5e**, inset 1, **Extended Data Fig. 9h-i**), whereas controls showed no such colocalization (**Fig. 5e**, inset 2). Notably, fewer puromycin-labeled sites compared to *Actb* mRNA particles and ribosomes suggest that only a subset of transported mRNAs is actively translated. Similarly, aggregated *Actb* mRNA clusters colocalized with ribosomes and active translation sites at neurite tips (**Fig. 5g**), indicating local translation. In contrast, the gNT+ABA group showed very few *Actb* mRNA particles at neurite tips (**Extended Data Fig. 9j**), consistent with our diffraction-limited microscopy data (**Fig. 4d-e**)."

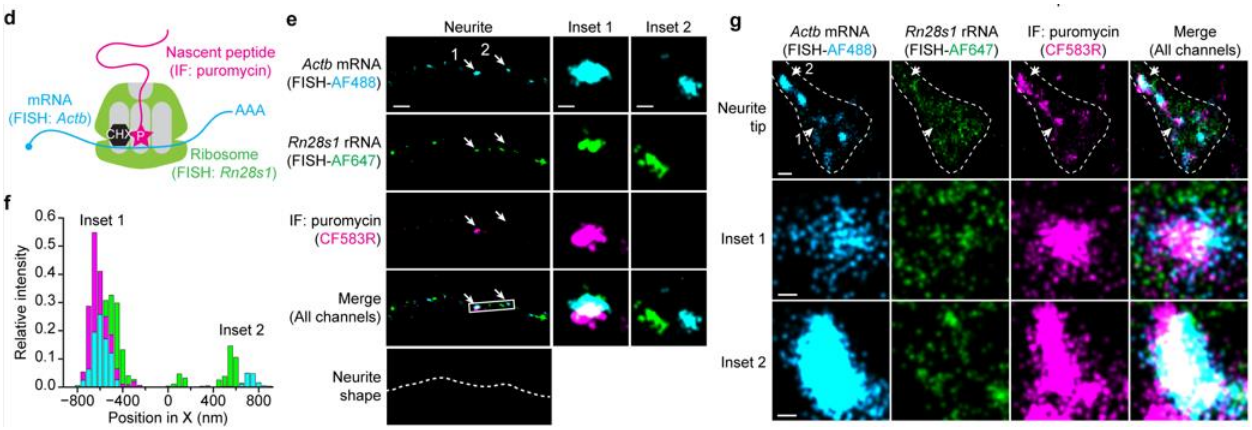

Figure 5 | d, Schematic showing the labeling of *Actb* mRNA via RNA FISH, ribosome via RNA FISH staining of *Rn28s1* rRNA, and translation site via ribopuromycylation. CHX: cycloheximide. P: puromycin. **e**, Representative super-resolution images showing the three-color staining of *Actb* mRNA, ribosome, and translation site inside neurites for the gT+ABA group after CRISPR-TO perturbation. Scale bar, 1 μm. Inset images represent magnification of the region pointed by the

white arrow. Scale bar, 200 nm. **f**, Histogram of the relative intensity of the white box region. **g**, Representative super-resolution images showing the three-color staining of *Actb* mRNA, ribosome, and translation site inside neurite tips for the gT+ABA group after CRISPR-TO perturbation. Scale bar, 500 nm. Inset images represent magnification of the region pointed by the white arrow. Scale bar, 100 nm. The shape of neurite tips is depicted with a white dotted line.

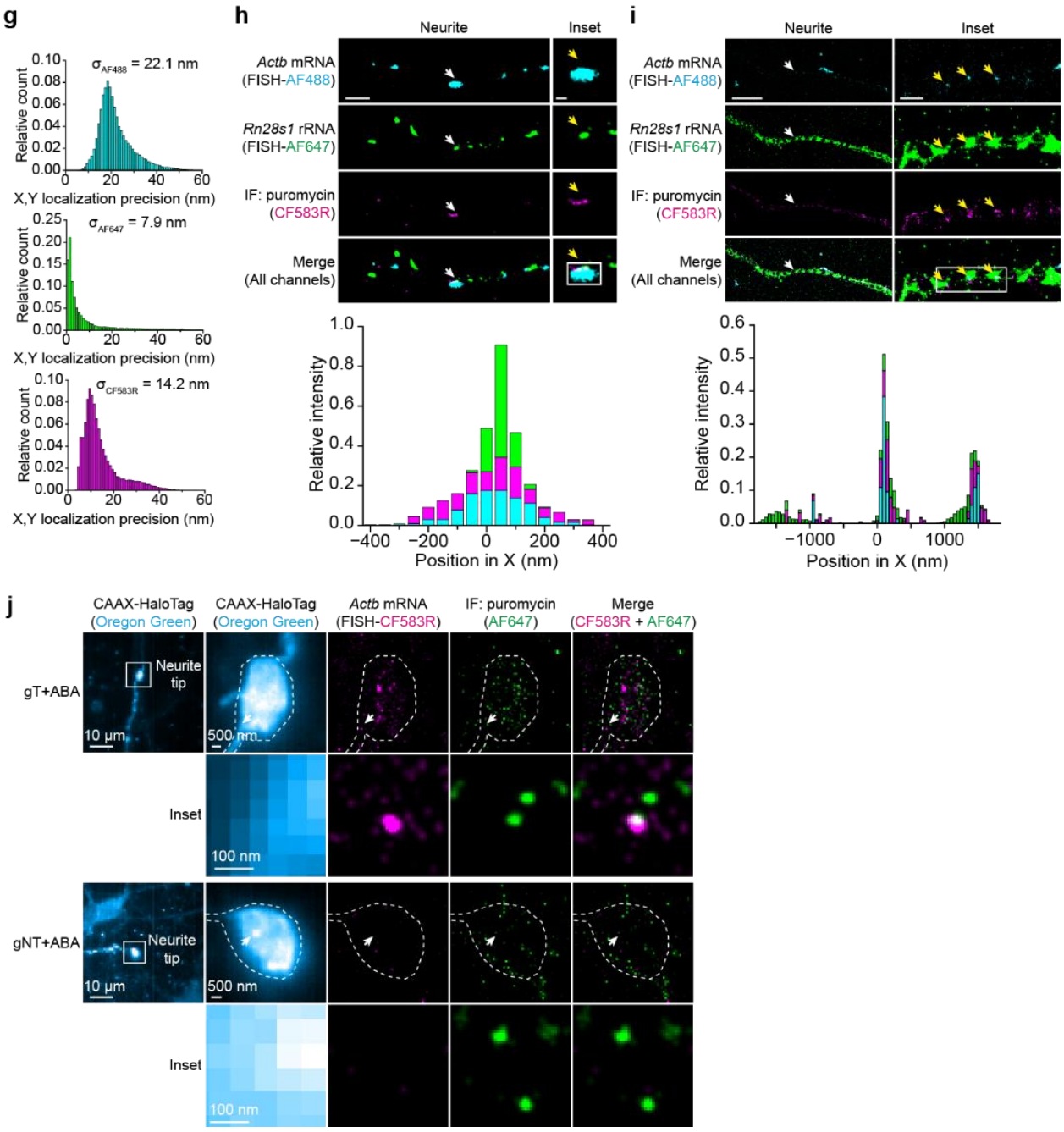

Extended Data Figure 9 | g, Histogram showing the X, Y localization precision of AF488-labeled *Actb* mRNA, AF647-labeled *Rn28s1* rRNA, and CF583R-labeled translation sites measured using STORM microscopy in fixed neurons. **h-i**, Top: representative super-resolution images showing the three-color staining of *Actb* mRNA, ribosome, and translation site inside neurites for the

gT+ABA group after CRISPR-TO perturbation. Scale bar, 1 μm (**h**) and 5 μm (**i**). Inset images represent magnification of the region pointed by the white arrow. Scale bar, 200 nm (**h**) and 1 μm (**i**). Representative *Actb* mRNA particles were pointed by yellow arrows. Bottom: histogram of the relative intensity of the white box region. **j**, Representative images for the super-resolution imaging of *Actb* mRNA, ribosome, and translation sites at neurite tips for the gT+ABA group and gNT+ABA control group after CRISPR-TO perturbation. The shape of neurite tips is depicted with a white dotted line. Inset: zoom-in images of the region pointed by the white arrow.

5. The authors assume that any phenotypic effect observed is indeed caused by the localization of the target mRNA and not by other effects, i.e. interference with the cell's internal localization machinery. To control for this in the case of beta-actin and Stmn2 the localized mRNA condition should have an additional control of enforced somatic localization. This could be achieved by comparing the fusion to retrograde or anterograde localization machinery.

Response:
In response, we have performed an experiment for *Stmn2* mRNA by manipulating its localization into soma using the retrograde transport motor protein KIFC1* (**Fig. 6h**). Our results showed that retrograde transport of *Stmn2* mRNA did not significantly affect neurite outgrowth (**Fig. 6h**) and anterograde localization significantly promoted neurite outgrowth (**Fig. 6f**), possibly because most Stmn2 mRNAs are naturally localized in the soma of in vitro cultured primary mouse cortical neurons. We also compared conditions of targeting and non-targeting gRNA conditions for both retrograde and anterograde transport, as well as ABA and DMSO conditions for anterograde transport, and only targeting gRNA in the presence of ABA with anterograde transport promoted neurite growth, while all other conditions showed no effect on neurite outgrowth (**Fig. 6f-h**). If there was indeed interference on cellular internal localization machinery that had led to the observed phenotype, we would expect to see no difference between targeting and non-targeting gRNAs conditions or between ABA and DMSO treatments. This further supports the observed neurite growth is due to the localization of the target *Stmn2* mRNA instead of interference with the cell's internal localization machinery. We didn't perform the retrograde localization for *Actb* mRNA because it is highly abundant in the soma and very few *Actb* mRNAs are localized in the spindly shaped neurite tips that predominate in our in vitro neuronal culture system (see also the response below and **Supplementary Figure 10**).

Minor comments:

1. The authors test which CRISPR effector would be the best suited by testing localization of GAPDH to the outer mitochondrial membrane (Fig 1d,e). They should indicate if guides with the appropriate direct repeat sequence and orientation were used for each effector and if the same guide sequences were used or if the guides were optimized for the PFS requirements of each effector. Related to this, essential citations are missing. dead-PspCas13b has previously been shown to perform better than other orthologs in RNA-binding applications (Yang et al Molecular Cell 2022, Wang et al Science 2019). The authors write "These results suggest that different dCas proteins possess distinct RNA binding activities…" page 5 like 125. This has previously been shown and should be cited and discussed as such.

Response:

For each CRISPR-Cas system, we designed gRNAs using the appropriate direct repeat sequence and orientation, as illustrated in **Supplementary Figure 4a**. Based on our literature search, the protospacer flanking site (PFS) requirements of each Cas effector do not affect RNA interference for PspCas13b[5,19], RfxCas13d[20], LwaCas13a[21], Cas13bt1[22], and DiCas7-11[23] in mammalian cells. Therefore, we used the same spacer sequence for all dCas effectors. As suggested by the reviewer, we have revised our text and cited the reference (Yang et al Molecular Cell 2022; Apostolopoulos et al Nat Commun 2024) that demonstrate similar observations that dPspCas13b exhibits better performance for RNA-binding applications, such as RNA imaging:

Line 129-132:

"This is consistent with previous reports that dPspCas13b performs better for RNA-binding applications such as RNA imaging[7,36]. These results suggest that the intrinsic properties of different dCas proteins can significantly impact CRISPR-TO efficiency (**Supplementary Notes**)."

GAPDH mRNA	3'-accaactcgtgtcccatgaaataactaccatgtactgttccacgccgagggatc-5'
PspCas13b gRNA	5'-gggtactttattgatggtacatgacaaggtGTTGTGGAAGGTCCAGTTTTGAGGGGCTATTACAAC-3'
RfxCas13d gRNA	5'-gAACCCCTACCAACTGGTCGGGGTTTGAAACgggtactttattgatggtacatgacaaggt-3'
LwaCas13a gRNA	5'-GATTTAGACTACCCCAAAAACGAAGGGGACTAAAACgggtactttattgatggtacatgacaaggt-3'
Cas13bt1 gRNA	3'-gggtactttattgatggtacatgacaaggtGCTGAAGAAGCCTCCGATTTGTGGGGTGATTACAGC-5'
DiCas7-11 gRNA	5'-GTTGATGTCACGGAACgggtactttattgatggtacatgacaaggt-3'
	Direct repeat (DR) Spacer Direct repeat (DR)

Supplementary Figure 4 | a, Schematic showing the spacer and direct repeat sequences of different gRNAs used for different CRISPR-Cas systems. These gRNAs use the same spacer sequence of gG1 targeting the same region of endogenous human *GAPDH* mRNA. The target sequence of GAPDH mRNA is in red, the spacer sequence of gRNA is in blue, and the direct repeat sequence is in orange. An extra 5'-g was added to RfxCas13d gRNA considering the U6 promoter requires a "G" nucleotide at the transcription start site for optimal expression.

2. Ext. Fig 2e is denoted as a scatterplot in the figure legend but its a swarm plot

Response:

In response, we have revised the figure legend:

"**Extended Data Figure 2** | **e**, Swarm plots depicting the percentage of 24xGCN4 reporter mRNA and dCas13 protein localized on the OMM in single cells (n = 51-57 cells per group)."

3. On page 5, line 149-160 authors switch from HEK/HeLa experiments to primary culture and then back to HEK/HeLa, why? This should be explained.

Response:

We chose primary neuronal cells and used their RNA-seq data to analyze gRNA design rules because our planned CRISPR-TO screening was in these neurons (as shown in **Fig. 6**), where gRNA design is more challenging in these cells. In subsequent experiments (pages 6-7), we used HEK/HeLa cells, which allowed us to leverage a large number of constructs and demonstrate the versatility of CRISPR-TO for targeting diverse subcellular compartments and dynamic behaviors.

4. regarding the same passage, guide design principles for many Cas effectors have been extensively studied, also specifically for PspCas13 (among others: Hu et al Biorxive 2022, Bandaru scientific reports 2020, Cox Science 2017, Yang et al Cell insight 2022), the additional merit coming from the gRNA design factors studied here should be discussed in the light of previous studies. The connection between read coverage and targeting efficiency should be clarified. The authors write “We explore potential factors that may contibute to CRISPR-TO efficiency, including RNA fragment expression levels, …These findings underscore the importance of maximizing read coverage…” Read coverage does not necessarily equal RNA fragment expression level.A slight rephrasing may be necessary to avoid equating these terms.

Response:

We thank the reviewer for the references and comments on gRNA design principles. Among these references, several studies explored PspCas13b gRNA design from different aspects. For example, our observation that gRNA secondary structure has only a marginal effect on dPspCas13b binding efficiency (**Fig. 1h-i, Extended Data Fig. 3n**) is consistent with Hu et al. (2022), which reported that gRNA folding has a moderate effect on target RNA silencing[5]. In addition, while Cox et al. (2017) reported that a central region (12-26 nt) of PspCas13b is relatively intolerant to mismatches for RNA cleavage[19], Yang et al. (2022) found that mismatches in the 5’ region are less tolerant than those in the 3’ region when using dead PspCas13b for RNA imaging[6,7]. Although our study focuses on RNA localization manipulation rather than cleavage or imaging, our new results reveal an interesting mismatch tolerance pattern using CRISPR-TO (**Extended Data Fig. 5**). Specifically, we found multiple “hot spots” on the gRNA spacer that are intolerant to mismatches. For example, mismatches at locations 1-2 (1-6 nt), 4-7 (10-21 nt), and 9-10 (25-30 nt) significantly impair CRISPR-TO efficiency, whereas locations 3 (7-9 nt) and 8 (22-24 nt) are more tolerant (**Extended Data Fig. 5c**). This pattern supports that the 5’-end of the spacer is less tolerant to mismatches and that dCas13b binding overall is highly sensitive to target mismatches, which is consistent with Yang et al. (2022) that studied mismatch tolerance for RNA imaging[6].

We have revised the manuscript to discuss these studies of gRNA design principles for PspCas13b:

Line 165-167:

“The effect of gRNA secondary structure was marginal, consistent with previous studies that gRNA folding has a moderate effect on PspCas13b-mediated RNA silencing[5].”

Line 183-184:

“Although this pattern may be unique to this specific gRNA, our results and prior studies[5-7] consistently suggest that the 5’-end of the gRNA spacer is less tolerant to mismatches.”

Additionally, unlike RNA cleavage that typically targets the protein coding sequence (CDS), we focused on targeting the 3’UTR of mRNA, which promoted us to explore factors that influence CRISPR-TO efficiency. We explored several factors that might contribute to CRISPR-TO efficiency, including read coverage over the target RNA fragment, off-target hits, and secondary structure (quantified by Minimum Free Energy, MFE). Among all factors, we found that read coverage had the strongest positive correlation with CRISPR-TO efficiency (permutation mean = 0.30, coefficient = 0.49) (**Fig. 1h-i, ED Fig. 3l**). We agree with the reviewer that “read coverage

does not necessarily equal RNA fragment expression level" and thank the reviewer for pointing this out. We have revised the text to avoid equating the two terms:
Line 157-165:
"We explored potential factors that may contribute to CRISPR-TO efficiency, including read coverage over the target RNA fragment, off-target hits, and gRNA secondary structure. Our RNA-seq data from primary mouse cortical neurons showed significant variation in read coverage across 3' UTR of many mRNAs (e.g., *Actb*) (**Extended Data Fig. 3k**). Using linear regression and permutation feature importance analyses, we determined that read coverage had the strongest positive influence on CRISPR-TO efficiency (permutation mean = 0.30, coefficient = 0.49), while off-target hits exerted the most significant negative impact (permutation mean = 0.23, coefficient = -0.44) (**Fig. 1h-i, Extended Data Fig. 3l-n**)"

5. beta-actin mRNA is well established as being localised to the growth cone of axons (XX, XX), nevertheless the authors report 0 particles per neurite tip in the control group (page 9, line 278). This seems to contradict expectations from previous studies.

Response:
We were also confused when we detected nearly zero *Actb* mRNA particles in neurite tips in the control group because *Actb* mRNA has been reported to localize to the axonal growth cones[37]. However, after carefully reviewing the original study on *Actb* mRNA localization in cortical neurons[38], we noted that strong *Actb* mRNA signals were observed only in growth cones with a flattened lamellar morphology, whereas spindly growth cones that predominate in our in vitro primary mouse cortical neuron culture system exhibited very weak signals. The original text of the paper states: "The amount of hybridization signal for b-actin varied among growth cones, and the morphology of the growth cone correlated with the extent of actin mRNA signal. A weak hybridization signal was observed in spindly growth cones that lacked a lamellar morphology (data not shown). In contrast, growth cones with a flattened lamellar morphology and defined central and peripheral regions had a strong signal. Large axonal growth cones with well spread lamella contained the strongest hybridization signal, showing even greater intensity than the cell body."[38]

To further confirm this observation, we performed *Actb* mRNA FISH on non-transfected wild-type mouse cortical neurons and imaged the morphology of growth cones using immunofluorescence staining of beta-actin protein and Tau (**Supplementary Figure 10a**) or differential interference contrast (DIC) microscopy (**Supplementary Figure 10b**). Consistent with the original report[38], *Actb* mRNA was abundant in the few growth cones with flattened lamellar morphology but largely absent from spindly growth cones, which explains our observations without contradicting previous studies (**Supplementary Figure 10a-b**).

We have included this part of discussion in **Supplementary Notes** which was also cited in the main text:
Line 312-313:
"Without ABA treatment, dCas13 predominantly localized to the soma and minimal *Actb* mRNA was detected at neurite tips (**Extended Data Fig. 8e, Supplementary Notes**)."

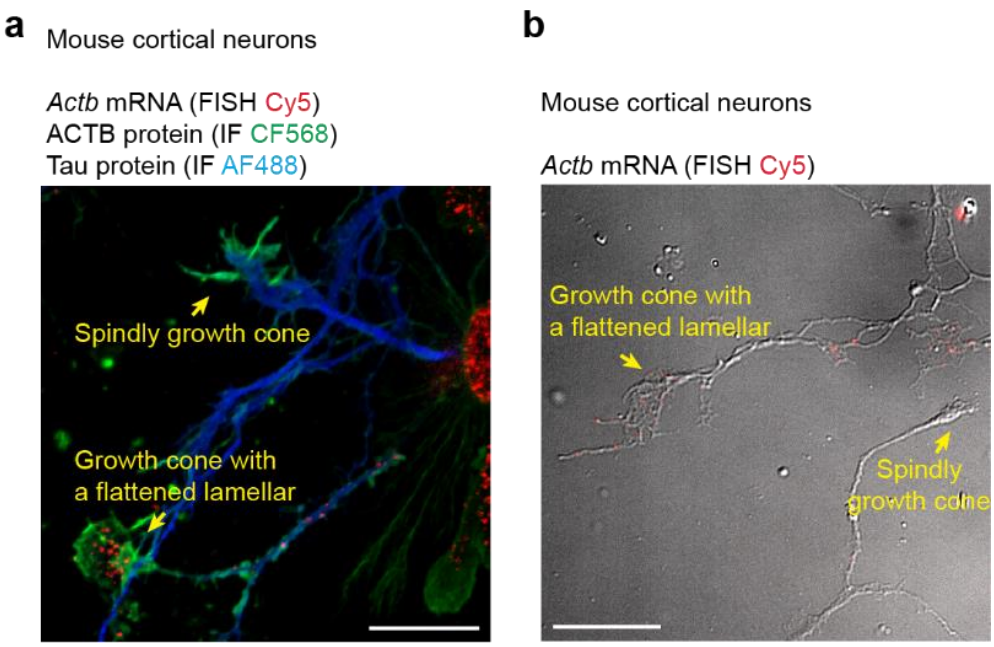

Supplementary Figure 10 | Monitoring *Actb* mRNA localization inside growth cones of mouse cortical neurons. a-b, Representative microscopic images showing the different localization of *Actb* mRNA particles inside two distinct types of growth cones, one with a spindly morphology and one with a flattened lamellar morphology. The growth cone morphology was monitored using immunofluorescence staining of beta-actin protein and Tau (**a**) or differential interference contrast (DIC) microscopy (**b**). Scale bar, 20 μm.

6. Co-localization is sometimes reported as "% of mRNA localized to", sometimes as "% of p-bodies enriched with" and sometimes as "XX". Please unify how these results are reported or provide a brief reasoning for changing the reported value.

Response:

To ensure consistency, we have unified our co-localization metrics ("% of mRNA localized to") throughout the manuscript (**Fig. 1c, 1e, 1f-g, 3a-b,** and **Extended Data Fig. 1i, 2b-g, 2j, 3d, 3g-h, 5b-d, 6a-b, 6i-j, 6l, 7a**). We note that in some images, especially for the plus end of microtubule (anterograde) group (**Fig. 2h**), it is challenging to quantify the percentage of RNA and dCas13 localized around the plus end of microtubules, because it's difficult to generate an accurate mask for the localized compartment in this case. This is because truncated Kif5b (Kif5b*) has a reported interesting property that its anterograde transport is dependent on cargo loading[39]. Both our results (**Fig. 2h**) and reported studies[39] showed Kif5b* does not localize to the plus end of microtubules without cargo loading. Therefore, in our image analysis, we cannot use the signal of Kif5b* protein from the DMSO group (which does not have a cargo loaded to Kif5b*) to generate the mask for quantifying the % of RNA and dCas13 localized to the plus ends of microtubules in cells. Therefore, for these images, we only quantified the percentage of cells with endogenous

mRNA and dCas13 protein enriched at the leading edge of cells for this group (**Extended Data Fig. 6k**).

7. In the time-course experiments please discuss what is known about the stability of ABA in cells, when does it get degraded?

Response:
In our study, we performed two time-course experiments. Experiment 1 investigated various ABA treatment durations (**Fig. 3a**), and Experiment 2 characterized the reversibility of CRISPR-TO by removing ABA for different periods (**Fig. 3b**). We agree with the reviewer that it is important to know the stability of ABA in cells for interpreting these results. Our literature search found one study reporting that about 60% of ABA activity was retained in culture media after 24 hours of incubation with 100 μM ABA in CHO cells[3], suggesting that ABA is sufficiently stable in mammalian cell culture while still being actively consumed or degraded by mammalian cells. In Experiment 2, we assumed that ABA is rapidly depleted from cells after removal from the culture media through both degradation and rapid diffusion. The protonated form of ABA, which is a weak acid (pKa = 4.7), is uncharged and more hydrophobic and can readily dissolve within the lipid bilayer to permeate the cell membrane[40]. Therefore, we assumed that ABA inside cells can more rapidly diffuse into the media across cell membrane after removal from the media. We have included this discussion in **Supplementary Notes**.

8. Page 8, line 259 “Taken together, combining CRISPR-TO with real-time RNA tracking provides new insights into the dynamic behaviours of RNA localization in living cells.” So far no new insights have been shown. Rephrase as “has the potential to provide”

Response:
We have revised the manuscript based on this suggestion: Line 295-297:
“Taken together, combining CRISPR-TO with real-time RNA tracking has the potential to provide new insights into the dynamic behaviors of RNA localization in living cells.”

9. The authors showed that 4h ABA treatment is sufficient for localization. In subsequent experiments they use changing time-frames from 6h (page 10, line 310), and 12h (page 12, line 400), to 24h (page11, line 359). Why the changing time frames in each experiment?

Response:
For cell lines, we mostly used a 4-hour ABA treatment, whereas for primary neurons we employed a 24-hour treatment. We increased the ABA treatment time for neurons because the greater distance between the soma and neurite tips might require longer transport times. In live-cell time-course experiments (e.g., lines 363 and line 478), practical constraints due to limited availability of time-lapse microscopy required some flexibility in ABA treatment duration in these long time-course experiments. Nevertheless, our data shows that target mRNA localization at neurite tips via CRISPR-TO increases significantly after just 1 hour of ABA treatment and continues to rise over time (**Extended Data Fig. 9m**), suggesting that we can be relatively flexible on the ABA treatment time between 1 to 24 hours to start imaging measurements.

10. In line 346, page 11 authors write that “we cannot track endogenous beta-actin mRNA in live neurons”, yes these tool exist (Benita Turner-Bridger et al 2018, Donlin-Asp et al 2021), also dead-Cas13b based tools exist for this purpose (Wang et al, Yang et al)

Response:
The reviewer is correct that endogenous beta-actin mRNA can be tracked in live neurons using molecular beacons[41,42]. In response, we have revised the statement:
Line 419-420:
“We next performed RNA FISH to verify the successful transport of endogenous β-actin mRNA to neurite tips via CRISPR-TO.”

11. page 5 line 138-148 are the several guides provided as array or separately expressed, clarify in main text or figure legend

Response:
The gRNAs were expressed separately and not as an array. We revised the figure legend for clarification (**Extended Data Figure 3h**):
“**Extended Data Figure 3 | h**, Box-and-whisker plots depicting the percentage of endogenous GAPDH mRNA and dCas13 protein localized on the OMM in single cells after ABA treatment for cells transfected with dCas13, MAVS*-PYL1, and gNT or combinations of one to three targeting gRNAs, each expressed from a separate plasmid.”

12. in line 428, page 13 the authors use the term “zip code” to refer to the protein that drives localization. This term has been used in mRNA localization to refer to specific sequences/motifs in the mRNA that drive localization. Therefore the term “zip code” should be avoided.

Response:
We have revised the text to remove the term “zip code”:
Line 507-509:
“Secondly, it enables RNA localization to various subcellular compartments by modifying the localization signal fused with PYL1 (**Fig. 2**, **Extended Data Fig. 6**).”

13. In Figure 4 j) the “Number of Actb mRNA particles per neurite tip” goes up to >60 particles, at the same time the authors quote Wang et al 2020 that most mRNAs have fewer than one copy in axons (age 11 line 352), is a count of more than 60 beta actin mRNAs per neurite tip realistic?

Response:
In **Fig. 4j**, we applied CRISPR-TO to actively transport *Actb* mRNA to neurite tips, which leads to a dramatic increase of *Actb* mRNA particles per tip. In contrast, Wang et al. (2020) quantified the natural, unmanipulated distribution of mRNA in axons[43], where most axons have fewer than one copy of *Actb* mRNA. Therefore, our finding of some neurite tips with >60 particles does not contradict their observations. Indeed, while a few neurite tips show very high counts (>60), the median number of *Actb* mRNA particles is 13 (**Fig. 4j**).

14. Figure 5 h) and i) both have -/- as gT presence.

Response:
We have now edited **Fig. 5i** to correct this.

15. Figure 6 a) please indicate DIV of transfection, ABA treatment and imaging in the flow chart of the experiment or the figure legend.

Response:
Following the suggestion, we have now edited **Fig. 6a** to indicate DIV of transfection, ABA treatment, and imaging in the flow chart of the experiment.

16. in Figure 6 g) the same cell is imaged before and after ABA treatment and therefore the dots are connected. In 6 f) this does not seem to be possible since the cells are indicated as +/- gT (assuming these are different cells transfected with and without targeting guide) nevertheless dots are connected as in g) suggesting a before and after of the same cell.

Response:
To clarify, in **Fig. 6g**, each dot represents neurite lengths quantified from a specific well and each line represents the same batch of primary neurons placed on the imaging plate. We did this because the primary neurons can have different growth rates from different litters of mouse used for neuron dissection. Similarly, in **Fig. 6f**, each dot also represents neurite lengths quantified from a specific well and each line represents the same batch of primary neurons placed on the imaging plate. While we are open to suggestions on better presenting this data, we have revised the legend of **Figure 6**:
"Figure 6 | For **f-h**, each dot represents neurite lengths quantified from an imaging well and each line represents the same batch of primary neurons cultured on the same imaging plate."

17. How was Co-localization analyzed? especially with "% of dCas13 localized on OMM" what is the cut off here to count as co-localized, threshold for total, automatized thresholding between cells? Please provide code.

Response:
In our original submission, we manually adjusted the threshold for quantifying % of RNA or dCas13 localized on the OMM in most figures (except **Fig. 1e)**. To standardize and automate this localization analysis, we developed a new code (calculate_%_RNA_dCas13_colocalization.m) to calculate % of RNA or dCas13 localized on the OMM (or other subcellular compartments) via automatized thresholding and reanalyzed all the images related to endogenous mRNA localization on the OMM (**Fig. 1c, Fig. 3a-b, Extended Data Fig. 3h, 7a**). The code was uploaded to Github (https://github.com/ym3141/Han2023).

In this automated method, the cut-off value for the colocalization factor is calculated based on the statistics of the pixel values in the image. For the RNA and dCas13 channel, pixels with intensity

values greater than the median + 1×STD are considered positive. For the OMM (or other subcellular compartments) channel, we tested factors of 1, 1.5, and 2 (applied as median + factor×STD) and selected the factor that best reflected the OMM (or other subcellular compartments) distribution for each batch (detailed in **Supplementary Table 10**). We noted that this automated approach does not perform well for reporter mRNA quantification due to the high variability in expression levels from plasmid transfection (**Fig. 1f**). Therefore, we still manually adjusted thresholds to quantify % of RNA or dCas13 localized on the OMM for the images related to reporter mRNA localization on the OMM (**Fig. 1f-g, Extended Data Fig. 3d, 3g**).

We have revised the **Supplementary Methods** to describe this new code:
"To quantify the percentage of target RNA and dCas13 protein localized at the specific subcellular location (OMM, p-bodies, stress granules, telomeres, nuclear stress bodies, and centrosomes) (**Fig. 1c, 1e, 3a-b,** and **Extended Data Fig. 2b-g, 2j, 3h, 5b-d, 6a-b, 6i-j, 6l, 7a**), we developed a new matlab code (calculate_%_RNA_dCas13_colocalization.m) which enables automatized thresholding of each channel for calculation. In this code, the cut-off value for the colocalization factor is calculated based on the statistics of the pixel values in the image. For the RNA and dCas13 channel, pixels with intensity values greater than the median + 1×STD are considered positive. For the subcellular location channel, we tested factors of 1, 1.5, and 2 (applied as median + factor×STD) and selected the factor that best reflected the subcellular location distribution to generate a mask for each batch (detailed in **Supplementary Table 10**). The percentage of target RNA or dCas13 protein localized at the subcellular location was determined by calculating the percentage of the integrated intensity of RNA or dCas13 channel within the mask to that within the cell. This code was uploaded to Github (https://github.com/ym3141/Han2023)."

Referee #4 (Remarks to the Author):

In this manuscript, Han and colleagues develop a CRISPR-mediated approach called CRISPR-TO for the relocalization of specific transcripts to defined locations within cells. This approach works by targeting the RNA to be moved with guide RNAs, facilitating its interaction with dCas13. dCas13 can then be inducibly driven to interact with protein markers of the subcellular location of interest, thus dragging the RNA along with it. The authors benchmark this system using a variety of RNAs and subcellular locations. They then use CRISPR-TO to screen a handful of genes with a focus on identifying RNAs that, when localized to neurites via targeting with dCas13 and Kif5a, promote neurite outgrowth.

This is an exciting technology. One limitation of the RNA localization field has been the relatively small number of cases reported where the mislocalization *of a specific RNA* resulted in an observable phenotype. However, one reason for this has been the difficulty associated with making mutations that result in mislocalization. Sequences that govern trafficking are unknown for almost all RNAs, and if those sequences are unknown, then it is not clear where mutations that would disrupt trafficking should be made. CRISPR-TO circumvents this problem and allows the targeted mislocalization of any RNA, at least in principle. This technology will then be very useful to labs studying RNA trafficking.

Overall, the manuscript was clearly written and the conclusions of the authors were generally supported by the supplied data. I do, however, have suggestions that may improve the manuscript.

We thank the reviewer for the feedback and encouraging words regarding our study.

MAJOR COMMENTS

1. Some of the conclusions arising from figure 5 are overstated. Specifically, the claim that the Actb RNAs are engaged by ribosomes and translated during transport is not fully supported with the resolution presented. As presented, these RNAs are colocalizing with ribosomes. This is consistent with them being engaged by the ribosomes and potentially translated, but is not in itself direct evidence that they are being translated. Further, even if the ribosomes did appear to move with the Actb RNA, that is still not evidence that the ribosomes are actually engaged on the RNA as opposed to be co-transported within the same granule. This is important as the perhaps prevailing view of localized RNAs is that they are translationally repressed during transport. Providing direct evidence to the contrary, perhaps using live cell imaging of both ribosome hitchhiking as well as translation during transport (for example using SunTag, etc.), would be necessary to fully support this statement.

Response:
We agree with the reviewer that our current diffraction-limited confocal microscopy images of *Actb* mRNAs and ribosomes do not fully support the claim that the *Actb* mRNAs are engaged by ribosomes during transport. Ribosomes may be co-transported with the *Actb* mRNAs in the same granules or hitchhiking[44], instead of being actually engaged on the *Actb* mRNA, and this cannot

be resolved with the diffraction-limited (~250 nm) images. In addition, we didn't provide direct evidence supporting that the *Actb* mRNAs are being translated during transport. To address these concerns, we performed two additional experiments and revised the text to avoid overclaim (line 378-397).

In Experiment 1, we applied super-resolution microscopy to increase the imaging resolution (around 10 nm), aiming to resolve whether ribosomes directly bind on the *Actb* mRNA during transport. To assess whether *Actb* mRNA is under translation during transport, we also visualized the translation sites along neurites using the ribopuromycylation method (RPM)[35]. RPM labels nascent peptides with puromycin and immobilizes the puromycylated nascent peptides on ribosomes by translation elongation inhibitor cycloheximide (CHX). By immunofluorescence staining of puromycylated nascent peptides using the anti-puromycin antibody, the translation sites were *in situ* visualized inside neurites. In our experiment, we labeled *Actb* mRNA and ribosomes (*Rn28s1* rRNA) using RNA FISH staining, and co-stained translation sites using RPM, for three-color super-resolution imaging using Stochastic Optical Reconstruction Microscopy (STORM)[34] (**Fig. 5d**).

We focused on imaging *Actb* mRNAs located inside neurites in the gT+ABA group with CRISPR-TO perturbation. We demonstrated that CRISPR-TO significantly increases the localization of *Actb* mRNA particles along the neurites compared to the gT+DMSO control (**Fig. 4f**), indiciating that many *Actb* mRNA particles detected inside neurites are transported via CRISPR-TO. Our super-resolution images, with localization precision between 7.9 nm to 22.1 nm for the three imaging channels (**Extended Data Fig. 9g**), revealed colocalization of some *Actb* mRNA particles with ribosomes and puromycin signals, indicating active translation during transport (**Fig. 5e-f**, inset 1**, Extended Data Fig. 9h-i**). As a control, some *Actb* mRNA particles did not colocalize with ribosomes or puromycin signals, confirming the specificity of multi-color labeling (**Fig. 5e-f**, inset 2). Notably, the number of puromycin-labeled active translation sites was lower than the number of *Actb* mRNA particles and ribosomes, suggesting that only a subset of transported mRNA particles undergo active translation. These results provide additional evidence that ribosomes are co-transported with mRNA and that at least some mRNAs are translated during transport along neurites.

We have revised the manuscript to include the new data:
Line 378-390:
"To confirm ribosome co-transport and local translation of endogenous mRNA along neurites and at neurite tips, we performed three-color STORM super-resolution imaging[34] to visualize endogenous *Actb* mRNA, ribosomes, and active translation sites (via ribopuromycylation[35]) in the gT+ABA group (**Fig. 5d**, **Methods**). Our super-resolution images (localization precision 7.9-22.1 nm, **Extended Data Fig. 9g**) revealed colocalization of *Actb* mRNA with both ribosome and puromycin signals in neurites, indicating active translation during transport (**Fig. 5e**, inset 1, **Extended Data Fig. 9h-i**), whereas controls showed no such colocalization (**Fig. 5e**, inset 2). Notably, fewer puromycin-labeled sites compared to *Actb* mRNA particles and ribosomes suggest that only a subset of transported mRNAs is actively translated. Similarly, aggregated *Actb* mRNA clusters colocalized with ribosomes and active translation sites at neurite tips (**Fig. 5g**), indicating

local translation. In contrast, the gNT+ABA group showed very few *Actb* mRNA particles at neurite tips (**Extended Data Fig. 9j**), consistent with our diffraction-limited microscopy data (**Fig. 4d-e**)."

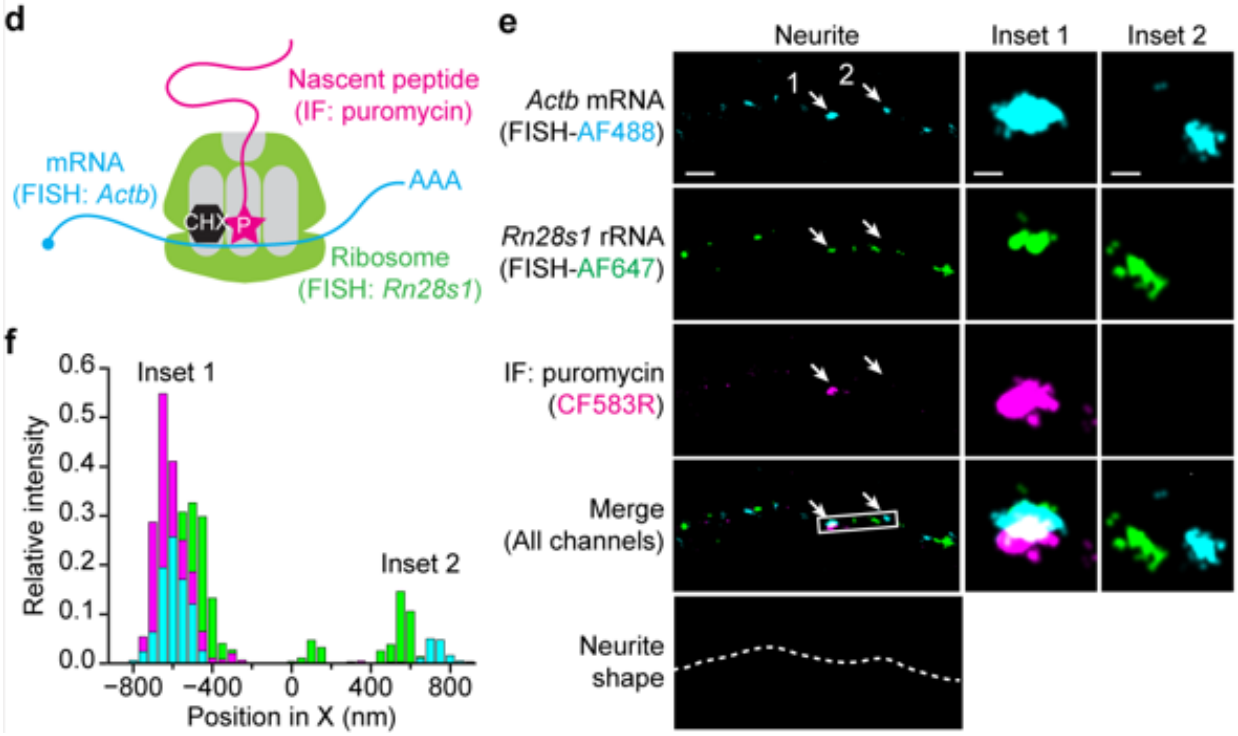

Figure 5 | d, Schematic showing the labeling of *Actb* mRNA via RNA FISH, ribosome via RNA FISH staining of *Rn28s1* rRNA, and translation site via ribopuromycylation. CHX: cycloheximide. P: puromycin. **e**, Representative super-resolution images showing the three-color staining of *Actb* mRNA, ribosome, and translation site inside neurites for the gT+ABA group after CRISPR-TO perturbation. Scale bar, 1 μm. Inset images represent magnification of the region pointed by the white arrow. Scale bar, 200 nm. **f**, Histogram of the relative intensity of the white box region.

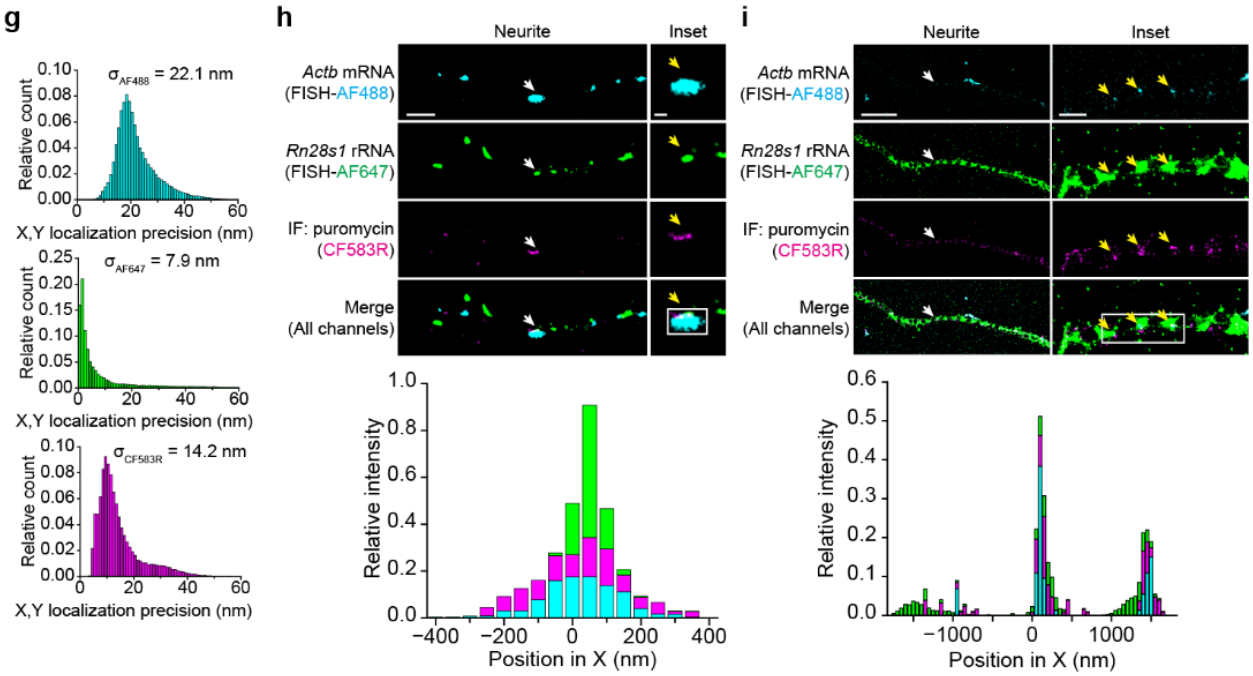

Extended Data Figure 9 |g, Histogram showing the X, Y localization precision of AF488-labeled *Actb* mRNA, AF647-labeled *Rn28s1* rRNA, and CF583R-labeled translation sites measured using STORM microscopy in fixed neurons. **h-i**, Top: representative super-resolution images showing the three-color staining of *Actb* mRNA, ribosome, and translation site inside neurites for the gT+ABA group after CRISPR-TO perturbation. Scale bar, 1 μm (**h**) and 5 μm (**i**). Inset images represent magnification of the region pointed by the white arrow. Scale bar, 200 nm (**h**) and 1 μm (**i**). Representative *Actb* mRNA particles were pointed by yellow arrows. Bottom: histogram of the relative intensity of the white box region.

In Experiment 2, as suggested by the reviewer, we performed live-cell imaging of a MS2-tagged reporter mRNA and its local translation using a SunTag-based labeling strategy (SINAPS) in neurites[45]. We co-transfected mouse primary cortical neurons with CRISPR-TO components, a SINAPS reporter mRNA plasmid, stdMCP-tdTomato for reporter RNA imaging, and scFv-EGFP for SunTag protein imaging. One day after transfection, we treated neurons with ABA for 24 hours to induce reporter mRNA transport toward neurite tips. We formed TIRF (total internal reflection fluorescence) microscopy to image both reporter mRNA and SunTag protein signals at 0.6 second intervals. Our results revealed two distinct populations of reporter mRNAs: while many mRNA particles do not colocalize with SunTag signals (untranslated), a small subset showed colocalization (**Extended Data Fig. 9k-l**). Interestingly, the colocalized mRNA particles exhibited significantly slower movement compared to non-translated mRNA (**Supplementary Video 5**). These findings imply that actively translating mRNAs are co-transported and that active translation slows mRNA movement.

We note that the SINAPS system produces two population of SunTag protein signals. One population, which does not colocalize with the reporter mRNA, exhibits faster movement than the population that does colocalize with the reporter mRNA (**Supplementary Video 5, Extended**

Data Fig. 9k-l). This observation is consistent with the previous report that the SINAPS system typically yields signals from both local translation sites and fully translated, diffused proteins[45].

While live-cell imaging offers unique insights into the temporal dynamics of local translation, this experiment has two major limitations. First, the SINAPS system's scFV-EGFP is rapidly photobleached under TIRF conditions, limiting tracking to about ~30 seconds (0.6 s interval), during which the actively translating mRNA particle showed minimal movement. Longer tracking may reveal more detailed trafficking dynamics but requires engineering of the SINAPS system such as replacing EGFP with a less-photobleachable fluorescent protein. Second, future studies should incorporate a dCas13 channel in addition to the mRNA, protein, and neurite morphology channels, necessitating 4-color simultaneous imaging. Nonetheless, our data indicates that mRNAs transported along neurites can undergo co-transport translation, with the actively translated mRNA moving more slowly than non-translated mRNA. We have revised the manuscript to include these findings and expanded the discussion accordingly.

Line 391-397:

"We also performed live-cell total internal reflection fluorescence (TIRF) imaging in primary mouse cortical neurons using a SINAPS system[45]. Neurons were co-transfected with CRISPR-TO components, a SINAPS reporter mRNA[45], stdMCP-tdTomato to visualize reporter mRNA, and scFv-EGFP to visualize active translation. Live-cell tracking (0.6 s interval) revealed two reporter mRNA populations. While many mRNA particles did not colocalize with SunTag signals (indicating they were untranslated), a small subset did colocalize (**Extended Data Fig. 9k-l**) and exhibited slower movement (**Supplementary Video 5**)."

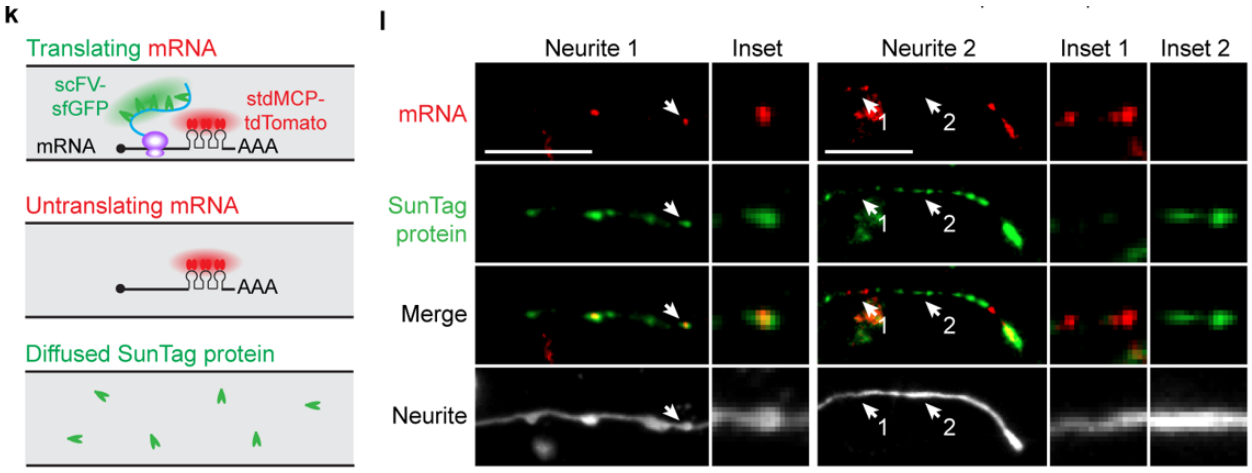

Extended Data Figure 9 | k, Schematics showing SINAPS reporter mRNA and translated proteins observed in live primary mouse cortical neurons along neurites. Reporter mRNA was visualized using stdMCP-tdTomato (green), and translated SunTag protein (red) was visualized using scFV-sfGFP. From top to bottom: translating mRNA (particles with colocalized green and red signals); untranslating mRNA (particles only with red signal); and diffused SunTag protein (particles only with green signal). **l**, Representative microscopic images of the SINAPS reporter mRNA and SunTag protein inside two neurites. Scale bar, 20 μm. Inset images represent magnification of the region pointed by white arrows.

2. The claim about the transported RNAs being translated *in the neurite tip* (rather than during transport) is better supported using the photoconvertible fluorescent protein experiment in figure 5a. However, this could be made even stronger by adding a control in which puromycin was added.

Response:

In response, in addition to the control in which puromycin was added, we also included another control using Anisomycin[46], a translation inhibitor. We repeated the photoconvertible fluorescent protein experiment (**Fig. 5a-c**) by including the two control groups. After UV conversion, we monitored Dendra2 fluorescence recovery at neurite tips for 70 minutes. We found that the fluorescence recovery in the gT+ABA group is significantly larger than the gT+DMSO group, which is consistent with **Fig. 5c**. In contrast, both translation inhibitor-treated gT+ABA groups exhibited negligible (i.e., negative fluorescence) recovery (**Extended Data Fig. 9c**). These results further support the transported mRNAs are locally translated at neurite tips. We have revised the manuscript to include this data:

Line 367-369:

"This was further supported by the control groups where gT+ABA group was treated with translation inhibitor puromycin or Anisomycin, leading to negligible recovery (**Extended Data Fig. 9c**)."

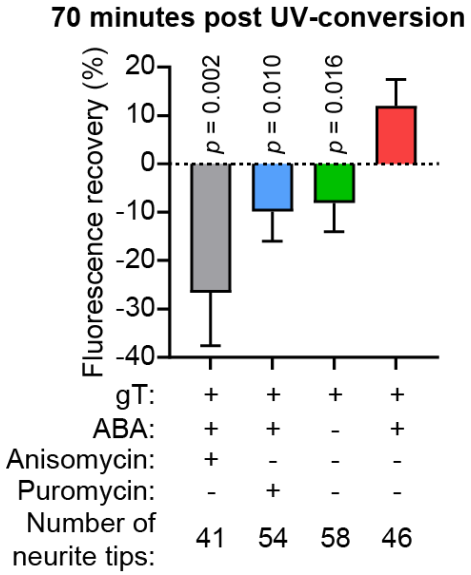

Extended Data Figure 9 | c, Quantification of the green florescence recovery of Dendra2 at 70 minutes post UV-conversion under different conditions. Data was presented as means ± SEM. Unpaired t-test.

3. While nice images, the data regarding the simultaneous targeting of two RNAs to neurite tips in figure 4h would be stronger if quantification of the results from many cells were shown. As presented, these results rely on a single set of images made from a single cell.

Response:

We quantified the fluorescence intensity of endogenous *Actb* mRNA and *Gap43* mRNA inside

neurite tips after CRISPR-TO perturbation with different gRNAs. We found that both *Actb* mRNA and *Gap43* mRNA were significantly enriched at neurite tips co-expressing both targeting gRNAs (gActb and gGap43) in neurons. In contrast, neurons expressing only gActb showed significant enrichment of *Actb* mRNA (but not *Gap43* mRNA), and those expressing only gGap43 exhibited significant enrichment of *Gap43* mRNA (but not *Actb* mRNA) (**Extended Data Fig. 8h**). This quantification further supports that CRISPR-TO can simultaneously manipulate the localization of multiple RNAs in primary neurons. We have included the quantification in the manuscript.

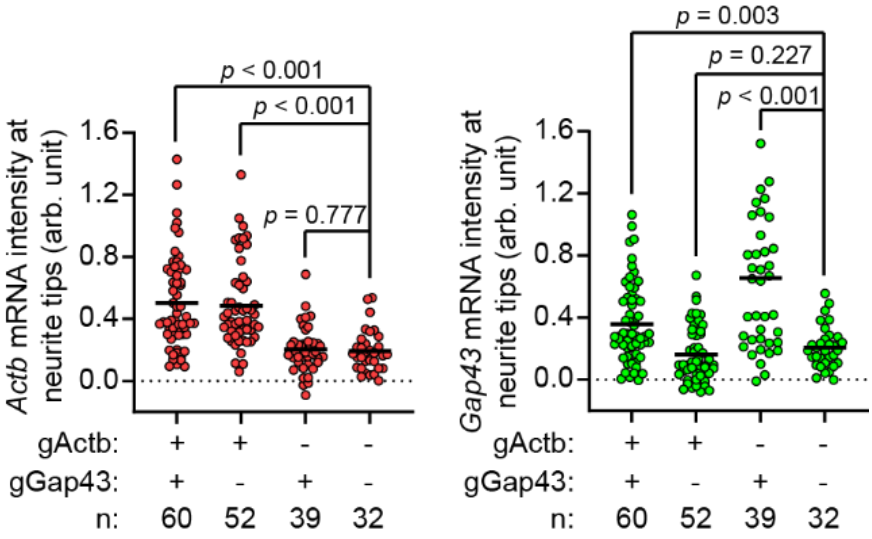

Extended Data Figure 8 | h, Quantification of the fluorescence intensity of endogenous *Actb* mRNA (red) and *Gap43* mRNA (green) at neurite tips after CRISPR-TO perturbation with different gRNAs, related to **Fig. 4h**. n indicates the number of quantified neurite tips for each group. The black bar indicates the mean value. Unpaired t-test.

4. The statement on line 155 that peaks and valleys in RNAseq read coverage across a 3' UTR are due to biological differences in expression is almost certainly not true (extended data 4k). RNAseq read coverage is by its nature uneven across a transcript, but this has nothing to do with differences in the abundances of regions within that transcript in cells. Splicing is an obvious exception to this, but in the case of splicing, changes in read coverage appear as very sharp cutoffs at splice junctions. Further, splicing in 3' UTRs is rare. Although it's not fully understood, these patterns are more likely due to the differences in the abilities of different sequences to end up in RNAseq libraries, be it through differences in GC content, secondary structure, or other features.

These features that govern the ability of a gRNA to work in CRISPR-TO may overlap with features that govern the ability of a sequence to contribute RNAseq reads, but again, this is not due to differences of the abundance of that sequence within transcripts in cells, and therefore the term "variation in expression levels" is not appropriate. Further, the correlation between read coverage gRNA score is not obvious in extended data figures 4L and 4O as it is stated in the text. In these plots, it looks like gRNAs with moderate RNAseq coverage are the best as the read coverage of the best performing gRNAs are lower than those with intermediate performance.

Response:
We thank the reviewer for this important insight. We agree with the reviewer that RNA-seq read coverage by its nature is uneven across the transcript, which is often attributed to a technical artifact of the library generation process or difference of GC content, secondary structure, or other features of the RNA fragment. The peaks and valleys in RNA-seq read coverage across the 3'UTR region of *Actb* mRNA likely have nothing to do with differences in RNA fragment expression level. We have revised the text to avoid equating read coverage with RNA fragment expression level.
Line 157-165:
"We explored potential factors that may contribute to CRISPR-TO efficiency, including read coverage over the target RNA fragment, off-target hits, and gRNA secondary structure. Our RNA-seq data from primary mouse cortical neurons showed significant variation in read coverage across 3' UTR of many mRNAs (e.g., *Actb*) (**Extended Data Fig. 3k**). Using linear regression and permutation feature importance analyses, we determined that read coverage had the strongest positive influence on CRISPR-TO efficiency (permutation mean = 0.30, coefficient = 0.49), while off-target hits exerted the most significant negative impact (permutation mean = 0.23, coefficient = -0.44) (**Fig. 1h-i, Extended Data Fig. 3l-n**)."

We also agree with the reviewer that **Extended Data Fig. 4l** shows "gRNAs with moderate RNAseq coverage are the best as the read coverage of the best performing gRNAs are lower than those with intermediate performance". The RNA fragment with low read coverage reflects inaccessibility (e.g., due to secondary structure) and high read coverage may indicate unfavorable sequence composition (e.g., high TA content). Both types of RNA fragments might not be good targeting regions for gRNAs, while the RNA fragment with moderate read coverage might provide the highest potency. Since both linear regression and permutation feature importance analysis suggest read coverage had the strongest positive influence on CRISPR-TO efficiency (permutation mean = 0.30, coefficient = 0.49) (**Fig. 1h-i**). we have revised the text to highlight the importance of read coverage while deemphasizing "the importance of maximizing read coverage" for optimal CRISPR-TO efficiency:
Line 167-168:
"These findings suggest that selecting gRNA target sites with moderate read coverage on 3' UTR while minimizing off-target hits could achieve better CRISPR-TO efficiency."

5. In the benchmarking experiments demonstrating the targeting of RNAs to various locations, there are two slightly different metrics used. For example, one is represented in figure 1e (and other places), which is the fraction of the RNA molecules of interest that are localized to the location of interest. The other, which is represented in extended data figure 3j (and other places) is the fraction of cells in which the RNA of interest is localized to the location of interest. The latter is not ideal as it is dependent on a thresholding to decide whether or not a cell is displaying "enough" of the RNA at the location of interest in order to call the cell as positive. Further, more highly expressed RNAs, like the GAPDH RNA tested, are more likely to show some overlap with any location, simply because there are more RNA molecules.

On the other hand, the former metric of fraction of RNA molecules localized to the location of interest does not require any calls about if "enough" of that RNA was localized and should be

more robust to different expression levels. It should be the metric that is always used for benchmarking. I fear the other metric is too dependent upon specific experimental parameters and therefore may be a bit misleading.

Response:

To ensure clarity and consistency, we have standardized our co-localization metrics ("% of mRNA localized to") throughout the manuscript. We reanalyzed images for p-body, stress granule, telomere, nuclear stress body, and minus end of microtubule (retrograde) groups to calculate the percentage of RNA and dCas13 localized at the target subcellular compartments (**Extended Data Fig. 6a-b, 6i-j, 6l**). This unified metrics robustly quantify CRISPR-TO efficiency without relying on subjective judgments of "sufficient" localization. However, for the plus end of microtubule (anterograde) group, it is challenging to quantify the percentage of RNA and dCas13 localized around the plus end of microtubules, because it's difficult to generate an accurate mask for the localized compartment in this case. This is because truncated Kif5b (Kif5b*) has a reported interesting property that its anterograde transport is dependent on cargo loading[39]. Both our results (**Fig. 2h**) and reported studies[39] showed Kif5b* does not localize to the plus end of microtubules without cargo loading. Therefore, in our image analysis, we cannot use the signal of Kif5b* protein from the DMSO group (which does not have a cargo loaded to Kif5b*) to generate the mask for quantifying the % of RNA and dCas13 localized to the plus ends of microtubules in cells. Therefore, we only quantified the percentage of cells with *GAPDH* mRNA and dCas13 enriched at the plus ends of microtubules (**Extended Data Fig. 6k**). We also revised the manuscript to update the new quantification results.

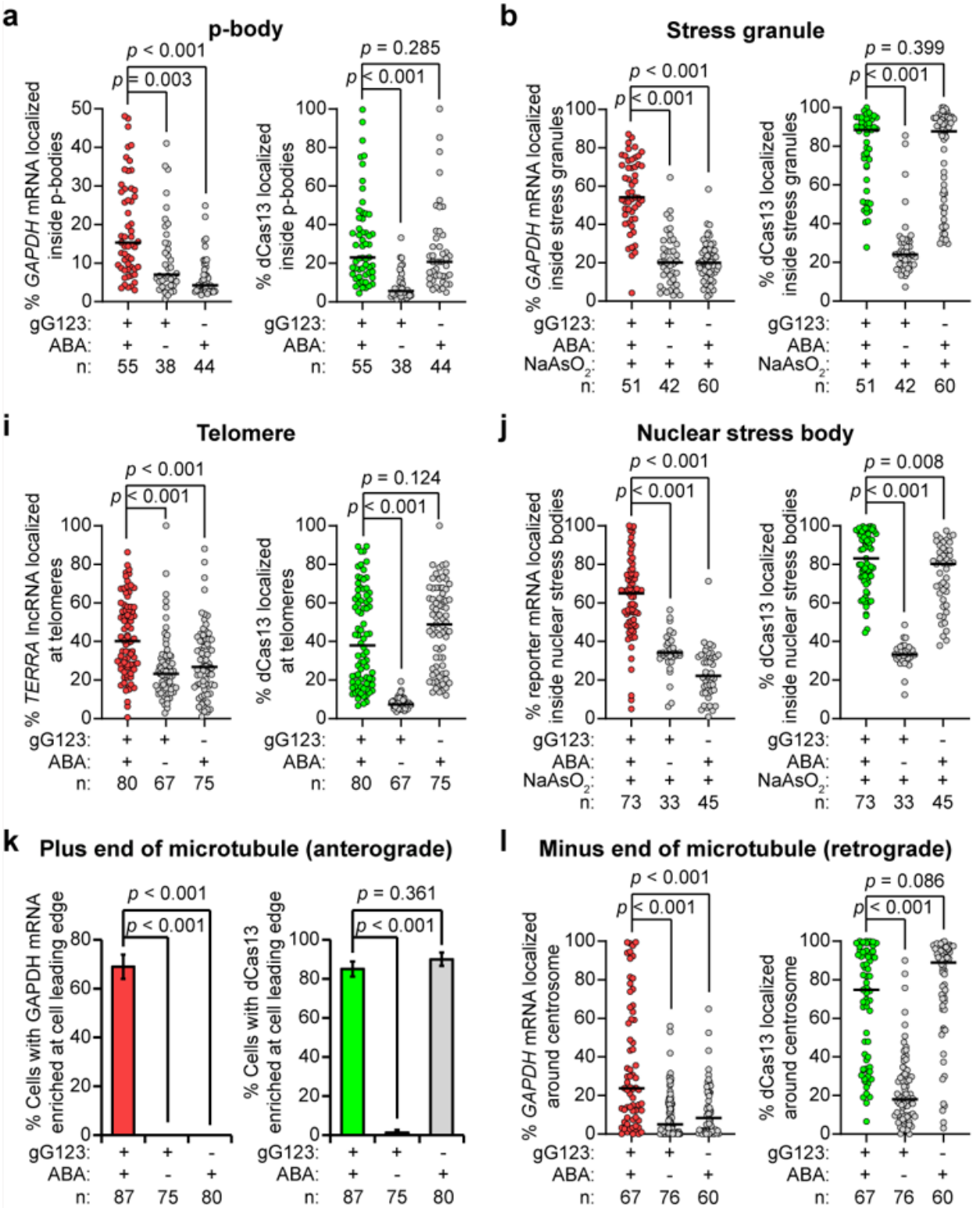

Extended Data Figure 6 | a-b, **i-j**, and **l**, Quantification of the percentage of the target RNA (red) and dCas13 protein (green) localized inside p-bodies (**a**), inside stress granules (**b**), at telomeres (**i**), inside nuclear stress bodies (**j**), and around the centrosome (**l**), related to **Fig. 2b-c**, **e-f**, and **i**. The black bar indicates the median. Unpaired t-test. **k**, Percentage of cells with endogenous

GAPDH mRNA (red) and dCas13 protein (green) enriched at the leading edge of cells, related to **Fig. 2h**. Data was presented as means ± SEM. Two-sided Fisher's exact test. For all figures, only cells co-expressing all the transfected plasmids were analyzed.

6. In figure 3f, it is posited that there are two populations of reporter constructs, one that maintained a constant distance to centrosomes and another that showed potentially directed movement towards centrosomes. How many observed RNA molecules were in each class?

Response:
Single particle tracking of RNA in live cells is challenging due to the fast movement of many RNA molecules (~3 s per frame) and the potential overlap of their trajectories. Therefore, we applied strict filtering conditions to remove overlapping trajectories and collected 60 high-quality trajectories (**Extended Data Fig. 7d**). We sorted these trajectories by their explored distance

$$R = \sqrt{(x(t)_{max} - x(t)_{min})^2 + (y(t)_{max} - y(t)_{min})^2} \quad \text{(Equation 1)}$$

Of these, the first 20 trajectories with low R values (marked in red, **Extended Data Fig. 7d**) were classified as Type I, indicating subdiffucive movement (maintaining a constant distance to centrosomes); the last 20 trajectories with high R values (marked in green, **Extended Data Fig. 7d**) were classified as Type II, which exhibited directed movement toward centrosomes. Although the middle 20 trajectories (marked in yellow, **Extended Data Fig. 7d**) appeared to be a mixture of both types, our rough estimates suggest that overall, approximately 25–30 molecules belong to Type I and 30–35 to Type II. Due to the technical challenges of tracking all rapidly moving mRNA molecules, these numbers are approximate.

7. In figure 3f, The claim that the Type II RNAs are being actively transported to the centrosome could be supported by comparing the velocities of these RNAs to those previously observed for RNA transport to centrosomes (Safieddine et al, Nat Comm, 2021).

Response:
We thank the reviewer for this suggestion and for providing the reference. In Safieddine et al. (2021)[47], the velocity of MS2-tagged *NUMA1* mRNA transport toward centrosomes in HeLa Kyoto cells was reported to be around 0.5-1 μm/s. Our time-lapse microscopy captured individual Type II mRNA particles moving along microtubules over time. The average transport velocity of a r
e
p
Line 287-292:
"Time-lapse microscopy captured individual Type II mRNA particles moving along microtubules over time (**Supplementary Video 2**). The average transport velocity of a representative mRNA particle was 0.57 ± 0.14 μm/s (mean ± std) (**Fig. 3g**), which is consistent with the reported velocity (0.5-1 μm/s) of MS2-tagged *NUMA1* mRNAs naturally transported toward centrosomes in mammalian cells[47], supporting the Type II mRNA particles being actively transported to the centrosome via CRISPR-TO."
t
i
v
e

T

8. In figure 3d, what fraction of the reporter RNA ends up at centrosomes? This is important as the efficiency of CRISPR-TO likely varies widely by subcellular location.

Response:
We quantified the fraction of the reporter mRNA localized around the centrosome over time after ABA addition and found that the fraction of the reporter mRNA localized around the centrosome increased from 0.26% (at 120 seconds) to 3.12% (at 867 seconds) (**Extended Data Figure 7c**). We agree with the reviewer that the efficiency of CRISPR-TO varies widely for different subcellular locations (**Fig. 1c, Extended Data Fig. 6a-b, 6i-j, 6l**). We have included this quantification in **Extended Data Fig. 7**.

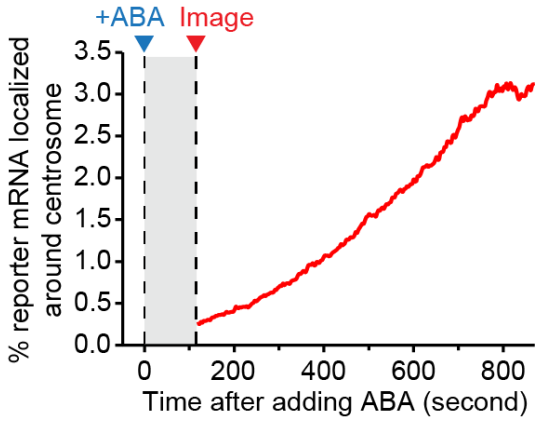

Extended Data Figure 7 | c, Quantification of the fraction of MS2 mRNA located at the minus ends of microtubules in **Fig. 3d** over time after adding ABA.

MINOR COMMENTS

1. Line 118: I believe this refers to extended data 3h-j, not 2h-j.

Response:
We have revised the text to correct this mistake.

2. I think, but am not sure, that the gT indications in figure 5 H and I are incorrect. I believe 5H uses gNT (in which case minus signs for gT would be correct, although slightly confusing) while 5I uses gT (in which case the minus signs for gT should be plus signs).

Response:
We have edited the figure which is **Fig. 5l** now to correct this mistake.

3. Statistics and uncertainties were generally handled appropriately.

Response:
We thank the reviewer for commenting on this.

References

1 Yoon, Y. Sharpening the scissors: mitochondrial fission with aid. *Cell Biochem Biophys* **41**, 193-206, doi:10.1385/CBB:41:2:193 (2004).

2 Khong, A. *et al.* The Stress Granule Transcriptome Reveals Principles of mRNA Accumulation in Stress Granules. *Mol Cell* **68**, 808-820 e805, doi:10.1016/j.molcel.2017.10.015 (2017).

3 Liang, F. S., Ho, W. Q. & Crabtree, G. R. Engineering the ABA plant stress pathway for regulation of induced proximity. *Sci Signal* **4**, rs2, doi:10.1126/scisignal.2001449 (2011).

4 Wu, X. *et al.* Genome-wide binding of the CRISPR endonuclease Cas9 in mammalian cells. *Nat Biotechnol* **32**, 670-676, doi:10.1038/nbt.2889 (2014).

5 Hu, W. *et al.* Single-base tiled screen unveils design principles of PspCas13b for potent and off-target-free RNA silencing. *Nat Struct Mol Biol* **31**, 1702-1716, doi:10.1038/s41594-024-01336-0 (2024).

6 Yang, L. Z. *et al.* Multi-color RNA imaging with CRISPR-Cas13b systems in living cells. *Cell Insight* **1**, 100044, doi:10.1016/j.cellin.2022.100044 (2022).

7 Yang, L. Z. *et al.* Dynamic imaging of RNA in living cells by CRISPR-Cas13 systems. *Mol Cell* **76**, 981-997 e987, doi:10.1016/j.molcel.2019.10.024 (2019).

8 Munoz, P. *et al.* TRF1 controls telomere length and mitotic fidelity in epithelial homeostasis. *Mol Cell Biol* **29**, 1608-1625, doi:10.1128/MCB.01339-08 (2009).

9 Biamonti, G. & Vourc'h, C. Nuclear stress bodies. *Cold Spring Harb Perspect Biol* **2**, a000695, doi:10.1101/cshperspect.a000695 (2010).

10 Park, H. Y., Trcek, T., Wells, A. L., Chao, J. A. & Singer, R. H. An unbiased analysis method to quantify mRNA localization reveals its correlation with cell motility. *Cell Rep* **1**, 179-184, doi:10.1016/j.celrep.2011.12.009 (2012).

11 Wessels, H. H. *et al.* Massively parallel Cas13 screens reveal principles for guide RNA design. *Nat Biotechnol* **38**, 722-727, doi:10.1038/s41587-020-0456-9 (2020).

12 Gumy, L. F. *et al.* Transcriptome analysis of embryonic and adult sensory axons reveals changes in mRNA repertoire localization. *RNA* **17**, 85-98, doi:10.1261/rna.2386111 (2011).

13 Zivraj, K. H. *et al.* Subcellular profiling reveals distinct and developmentally regulated repertoire of growth cone mRNAs. *J Neurosci* **30**, 15464-15478, doi:10.1523/JNEUROSCI.1800-10.2010 (2010).

14 Belmont, L. D. & Mitchison, T. J. Identification of a protein that interacts with tubulin dimers and increases the catastrophe rate of microtubules. *Cell* **84**, 623-631, doi:10.1016/s0092-8674(00)81037-5 (1996).

15 Klim, J. R. *et al.* ALS-implicated protein TDP-43 sustains levels of STMN2, a mediator of motor neuron growth and repair. *Nat Neurosci* **22**, 167-179, doi:10.1038/s41593-018-0300-4 (2019).

16 Melamed, Z. *et al.* Premature polyadenylation-mediated loss of stathmin-2 is a hallmark of TDP-43-dependent neurodegeneration. *Nat Neurosci* **22**, 180-190, doi:10.1038/s41593-018-0293-z (2019).

17 Baughn, M. W. *et al.* Mechanism of STMN2 cryptic splice-polyadenylation and its correction for TDP-43 proteinopathies. *Science* **379**, 1140-1149, doi:10.1126/science.abq5622 (2023).

18 Menge, S., Decker, L. & Freischmidt, A. Restoring expression of Stathmin-2: a novel strategy to treat TDP-43 proteinopathies. *Signal Transduct Target Ther* **8**, 266, doi:10.1038/s41392-023-01533-1 (2023).

19 Cox, D. B. T. *et al.* RNA editing with CRISPR-Cas13. *Science* **358**, 1019-1027, doi:10.1126/science.aaq0180 (2017).

20 Konermann, S. *et al.* Transcriptome engineering with RNA-targeting type VI-D CRISPR effectors. *Cell* **173**, 665-676, doi:10.1016/j.cell.2018.02.033 (2018).
21 Abudayyeh, O. O. *et al.* RNA targeting with CRISPR-Cas13. *Nature* **550**, 280-284, doi:10.1038/nature24049 (2017).
22 Kannan, S. *et al.* Compact RNA editors with small Cas13 proteins. *Nat Biotechnol*, doi:10.1038/s41587-021-01030-2 (2021).
23 Ozcan, A. *et al.* Programmable RNA targeting with the single-protein CRISPR effector Cas7-11. *Nature*, doi:10.1038/s41586-021-03886-5 (2021).
24 Yang, J. *et al.* Engineered LwaCas13a with enhanced collateral activity for nucleic acid detection. *Nat Chem Biol* **19**, 45-54, doi:10.1038/s41589-022-01135-y (2023).
25 Smargon, A. A. *et al.* Cas13b Is a Type VI-B CRISPR-Associated RNA-Guided RNase Differentially Regulated by Accessory Proteins Csx27 and Csx28. *Mol Cell* **65**, 618-630 e617, doi:10.1016/j.molcel.2016.12.023 (2017).
26 Ochs, R. L., Lischwe, M. A., Spohn, W. H. & Busch, H. Fibrillarin: a new protein of the nucleolus identified by autoimmune sera. *Biol Cell* **54**, 123-133, doi:10.1111/j.1768-322x.1985.tb00387.x (1985).
27 Tan, R. *et al.* Nucleolus localization of SpyCas9 affects its stability and interferes with host protein translation in mammalian cells. *Genes Dis* **9**, 731-740, doi:10.1016/j.gendis.2020.09.003 (2022).
28 Chen, B. *et al.* Dynamic imaging of genomic loci in living human cells by an optimized CRISPR/Cas system. *Cell* **155**, 1479-1491, doi:10.1016/j.cell.2013.12.001 (2013).
29 Zeballos, C. M. *et al.* Mitigating a TDP-43 proteinopathy by targeting ataxin-2 using RNA-targeting CRISPR effector proteins. *Nat Commun* **14**, 6492, doi:10.1038/s41467-023-42147-z (2023).
30 Azzolini, F. *et al.* Neuroinflammation Is Associated with GFAP and sTREM2 Levels in Multiple Sclerosis. *Biomolecules* **12**, doi:10.3390/biom12020222 (2022).
31 Afridi, R., Tsuda, M., Ryu, H. & Suk, K. The Function of Glial Cells in the Neuroinflammatory and Neuroimmunological Responses. *Cells* **11**, doi:10.3390/cells11040659 (2022).
32 Luo, B. *et al.* Endoplasmic reticulum stress eIF2alpha-ATF4 pathway-mediated cyclooxygenase-2 induction regulates cadmium-induced autophagy in kidney. *Cell Death Dis* **7**, e2251, doi:10.1038/cddis.2016.78 (2016).
33 Powell, J. E. *et al.* Targeted gene silencing in the nervous system with CRISPR-Cas13. *Sci Adv* **8**, eabk2485, doi:10.1126/sciadv.abk2485 (2022).
34 Xu, K., Zhong, G. & Zhuang, X. Actin, spectrin, and associated proteins form a periodic cytoskeletal structure in axons. *Science* **339**, 452-456, doi:10.1126/science.1232251 (2013).
35 David, A. *et al.* Nuclear translation visualized by ribosome-bound nascent chain puromycylation. *J Cell Biol* **197**, 45-57, doi:10.1083/jcb.201112145 (2012).
36 Apostolopoulos, A. *et al.* dCas13-mediated translational repression for accurate gene silencing in mammalian cells. *Nat Commun* **15**, 2205, doi:10.1038/s41467-024-46412-7 (2024).
37 Das, S., Vera, M., Gandin, V., Singer, R. H. & Tutucci, E. Intracellular mRNA transport and localized translation. *Nat Rev Mol Cell Biol* **22**, 483-504, doi:10.1038/s41580-021-00356-8 (2021).
38 Bassell, G. J. *et al.* Sorting of beta-actin mRNA and protein to neurites and growth cones in culture. *J Neurosci* **18**, 251-265, doi:10.1523/JNEUROSCI.18-01-00251.1998 (1998).
39 Guardia, C. M. *et al.* Reversible association with motor proteins (RAMP): A streptavidin-based method to manipulate organelle positioning. *PLoS Biol* **17**, e3000279, doi:10.1371/journal.pbio.3000279 (2019).

40 Kang, J. ABA Transport Assay in Plant Single-Cell System. *Methods Mol Biol* **2462**, 71-84, doi:10.1007/978-1-0716-2156-1_6 (2022).
41 Turner-Bridger, B. *et al.* Single-molecule analysis of endogenous beta-actin mRNA trafficking reveals a mechanism for compartmentalized mRNA localization in axons. *Proc Natl Acad Sci U S A* **115**, E9697-E9706, doi:10.1073/pnas.1806189115 (2018).
42 Donlin-Asp, P. G., Polisseni, C., Klimek, R., Heckel, A. & Schuman, E. M. Differential regulation of local mRNA dynamics and translation following long-term potentiation and depression. *Proc Natl Acad Sci U S A* **118**, doi:10.1073/pnas.2017578118 (2021).
43 Wang, G. *et al.* Spatial organization of the transcriptome in individual neurons. *bioRxiv*, 2020.2012.2007.414060, doi:10.1101/2020.12.07.414060 (2020).
44 Liao, Y. C. *et al.* RNA Granules Hitchhike on Lysosomes for Long-Distance Transport, Using Annexin A11 as a Molecular Tether. *Cell* **179**, 147-164 e120, doi:10.1016/j.cell.2019.08.050 (2019).
45 Wu, B., Eliscovich, C., Yoon, Y. J. & Singer, R. H. Translation dynamics of single mRNAs in live cells and neurons. *Science* **352**, 1430-1435, doi:10.1126/science.aaf1084 (2016).
46 Pilaz, L. J., Lennox, A. L., Rouanet, J. P. & Silver, D. L. Dynamic mRNA Transport and Local Translation in Radial Glial Progenitors of the Developing Brain. *Curr Biol* **26**, 3383-3392, doi:10.1016/j.cub.2016.10.040 (2016).
47 Safieddine, A. *et al.* A choreography of centrosomal mRNAs reveals a conserved localization mechanism involving active polysome transport. *Nat Commun* **12**, 1352, doi:10.1038/s41467-021-21585-7 (2021).

Referees' comments:

Referee #1 (Remarks to the Author):

The authors have addressed my comments and concerns appropriately, and greatly improved the manuscript overall in response to all reviewers. Some minor comments below.

Minor comments:
1. When referring to binding constant in the main text (Line 252-255: when referring to ED Fig 7a) you define it as ‘Km’, which I still consider the Michaelis constant . Please reword to remove Km and use Kd (apparent) or similar.

Response:

We have now changed K_m to K_d in the manuscript and figures.

Referee #2 (Remarks to the Author):

Han et al., have presented a compelling response to the referee assessment. The authors now provide additional data that this reviewer believes address concerns. Specifically, the authors now include additional experiments assessing transfection efficiency, expression, and cell toxicity and include these data as a Supplementary Note. This is a really important inclusion given the inconsistencies in the field and will make the work more reproducible. The authors also now include representative images of localization for each system tested and provide evidence for localization to the nucleolus. Furthermore, the authors have contextualized the method by highlighting the context-specific applicability of CRISPR-TO and potential broader applicability in bacteria and plant cells. Examining the authors responses to the comments from other reviewers highlights that they have done substantial work to more rigorously assess CRISPR-TO, all of which greatly improve the manuscript. In summary, the manuscript has been greatly improved and still presents a novel contribution to the toolbox that is well described and will be of broad interest to the field.

Referee #3 (Remarks to the Author):

the authors have dealt with my criticisms and suggestions to my satisfaction.

Referee #4 (Remarks to the Author):

The authors have addressed my concerns.

Referees' comments:

Referee #1 (Remarks to the Author):

The authors have addressed my comments and concerns appropriately, and greatly improved the manuscript overall in response to all reviewers. Some minor comments below.

Minor comments:
1. When referring to binding constant in the main text (Line 252-255: when referring to ED Fig 7a) you define it as ‘Km’, which I still consider the Michaelis constant . Please reword to remove Km and use Kd (apparent) or similar.

Response:

We have now changed K_m to K_d in the manuscript and figures.

Referee #2 (Remarks to the Author):

Han et al., have presented a compelling response to the referee assessment. The authors now provide additional data that this reviewer believes address concerns. Specifically, the authors now include additional experiments assessing transfection efficiency, expression, and cell toxicity and include these data as a Supplementary Note. This is a really important inclusion given the inconsistencies in the field and will make the work more reproducible. The authors also now include representative images of localization for each system tested and provide evidence for localization to the nucleolus. Furthermore, the authors have contextualized the method by highlighting the context-specific applicability of CRISPR-TO and potential broader applicability in bacteria and plant cells. Examining the authors responses to the comments from other reviewers highlights that they have done substantial work to more rigorously assess CRISPR-TO, all of which greatly improve the manuscript. In summary, the manuscript has been greatly improved and still presents a novel contribution to the toolbox that is well described and will be of broad interest to the field.

Referee #3 (Remarks to the Author):

the authors have dealt with my criticisms and suggestions to my satisfaction.

Referee #4 (Remarks to the Author):

The authors have addressed my concerns.